Evaluation of Chitosan Stability in Aqueous Systems

By Monica Fee, BSc (Hons) MRPharmS

Thesis submitted to the University of Nottingham for the degree of Doctor of Philosophy,

November 2005

Acknowledgements

I would like to thanks my supervisors Prof. Steve Harding, Prof. Lisbeth Illum and Dr. Alan Smith for their support and guidance during this project. Also Dr. Neil Errington, Dr. Konny Jumel and Prof. Arthur Rowe of the NCMH, University of Nottingham for all their guidance with practical aspects of the project. For financial support I would like to thank the BBSRC and West Pharmaceutical Services.

Most importantly I would like to thank my parents and family for their encouragement and support throughout all my choices in life. I would also like to thanks all the friends I have made during my studies, they make the end of the day more enjoyable and also the coffee breaks!! Thanks to Jamie, Chris, Sarah, Nadine, Fiona, Tracey and all the others.

Abstract

This study considers the molecular weight, conformation, stability and nanoparticle formation of the polysaccharide chitosan in relation to its pharmaceutical applications in the drug delivery. Chitosan has bioadhesive and absorption enhancing properties that augment its use in the delivery of therapeutic proteins and peptides across mucosal membranes.

The molecular weights of a range of chitosans, with degree of aceytlation (DA) ranging form 7 to 30%, were studied using the hydrodynamic techniques of SEC-MALLS (size exclusion chromatography coupled with multi-angle laser light scattering) and analytical ultracentrifugation. It was found that there was reasonable agreement between the two techniques with molecular weights obtained ranging between 42000 and 200000 kDa. These results indicated that the use of SEC-MALLS as a measure of degradation during storage studies would be valid and this technique would be more convenient due to the much shorter time required for each sample.

Conformational studies indicated that in 0.2M acetate buffer, pH 4.3, the chitosan samples studied appeared to have an extended conformation which is in agreement with studies performed by other researchers (e.g. Anthonsen, M. W., K. M. Vårum and O. Smidsrød (1993) *Carbohydrate Polymers* **22**: 193-201 and Dyer, A. M., M. Hinchcliffe, P. Watts, J. Castile, I. Jabbal-Gill, R. Nankervis, A. Smith and L. Illum (2002) *Pharmaceutical Research* **19**(7): 998-1008), non-withstanding complications in interpretation through possible solvent draining effects (Berth, G., Colfen, H., Dautzenberg H (2002) *Prog. Coll. Int. Sci.* **119**, 50-57).

Degradation studies were performed using viscosity measurements and SEC-MALLS to measure molecular weight. The effect of solution parameters such as pH and ionic strength were examined as well as structural parameters, e.g. molecular weight and DA. Degradation was found to increase as the pH of the solution decreased indicating that acid hydrolysis was occurring. The range of ionic strength studied (0.1 – 0.3M) did not have any significant effect on degradation rate. For the samples studied, molecular weight appeared to have little effect on degradation, however, the more deacetylated the polysaccharide, the slower the rate of degradation due to increased charged residues along the chain.

Finally chitosan nanoparticles were then prepared using ionotropic gelation with tripolyphosphate pentasodium. This technique produced nanoparticles in the size range 320 – 380 nm with an insulin loading capacity of 30-50%. Insulin-loaded nanoparticles were prepared and resuspended in acetate buffer at various pHs. The molecular weight and insulin loading was tested at 2-week intervals and results indicated that chitosan degradation was reduced by 30% compared to a control chitosan solution, and the total amount of insulin incorporated remained constant over the storage period.

Contents

List of Figures

List of Tables

Abbreviations

Any abbreviations used in this text are explained upon their first use. Commonly used abbreviations are listed below.

DA - Degree of Acetylation

MTR - Mucociliary transport rate

MCS - Mucociliary clearance system

TMC - *N*-trimethyl chitosan chloride

MHKS - Mark-Houwink-Kuhn-Sakurada

SEC-MALLS – Size Exclusion Chromatography coupled with Multi-Angle Laser Light Scattering

AUC - Analytical Ultracentifuge

TPP - Tripolyphosphate pentasodium

$\bar{v}$ - partial specific volume

p - solution density

f - frictional coefficient

M - molecular weight

η - viscosity

D - translational diffusion coefficient

s - sedimentation coefficient

$s^0_{20,w}$ - infinite dilution sedimentation coefficient

k_s - concentration dependence coefficient

$[\eta]$ - intrinsic viscosity

$M_{w,app}$ - apparent weight average molecular weight

C* - critical overlap concentration

Chapter 1: Introduction

Treatment of various diseases requires the efficient delivery of therapeutic proteins and peptides. Various hormones used in deficiency conditions such as growth hormone, and calcitonin can be delivered subcutaneously for the treatment of dwarfism and osteoporisis. Of particular interest is the treatment of Type I diabetes that requires the administration of insulin. Presently insulin is delivered by subcutaneous injection, which can be inconvenient for the patient. The most convenient method of drug delivery is by the oral route. However, this is not at present possible for insulin due to its degradation in the gastrointestinal tract by enzymatic degradation and the highly acidic conditions in the stomach. However, several drug delivery companies are showing promising results for oral delivery of insulin using novel polymer systems such as Emisphere and Nobex (Angelo *et al.* 2002; Clement *et al.* 2004).

Extensive research also has shown that insulin may be delivered nasally and absorbed in sufficient quantities to obtain a therapeutic response if administered in conjunction with the polysaccharide chitosan (Illum *et al.* 1994; Schipper *et al.* 1996; Schipper *et al.* 1996/9; Hinchcliffe and Illum 1999; Schipper *et al.* 1999; Illum *et al.* 2001). Chitosan is a cationic polysaccharide derived from chitin, which is found in the shells of crustaceans (Anthonsen *et al.* 1993; Sugimoto *et al.* 1998). Chitosan enables insulin to be delivered intranasally by two important mechanisms. Firstly, chitosan is mucoadhesive due to its cationic nature (Lehr *et al.* 1992; He *et al.* 1998), and secondly, it is believed to cause a transient opening of the tight junctions between the mucosal epithelium cells allowing the protein insulin to be

absorbed through the nasal membrane (Artursson *et al.* 1994; Borchard *et al.* 1996; Schipper *et al.* 1997). These properties of chitosan are discussed in more detail in sections 1.1 and 1.2.

In a nasal insulin formulation, chitosan acts as an absorption enhancer and is therefore an essential excipient in the formulation. Changes in the molecular weight and structure of chitosan due to degradation processes during storage of the formulation, may affect its mucoadhesive properties and its ability to function as an absorption enhancer. In this project, the degradation of chitosan was investigated under various solvent conditions and evaluated by measurement of the molecular weight using various hydrodynamic techniques (described in Chapter 4 and 5).

Further research on the formulation used to deliver insulin nasally has lead to the development of chitosan nanoparticles (Illum *et al.* 1987; Calvo *et al.* 1997; Fernández-Urrusuno *et al.* 1999; Janes *et al.* 2001; Dyer *et al.* 2002). The second part of this project was focused on the optimisation of nanoparticle formation, methods for measuring insulin loading and the stability of chitosan within a nanoparticle preparation (Chapters 6 and 7).

Firstly, we will look at the use of chitosan in drug delivery and the physicochemical properties of chitosan.

1.1 Use of Chitosan in Drug Delivery

The development of new routes for administering therapeutic proteins and peptides is of considerable interest to the pharmaceutical industry. Today, most of these compounds are delivered parenterally due to problems with the use of other routes of delivery such as degradation in the stomach and in the gastrointestinal tract and poor permeation of the mucosa associated with oral delivery. The use of parenteral delivery is inconvenient for the patient and can lead to reduced compliance.

Extensive research has been carried out on alternative ways of delivering macromolecular compounds to the body. As such, chitosan as a drug delivery system for nasal and oral delivery has been intensively investigated (Illum *et al.* 1994; Davis 1999; Fernández-Urrusuno *et al.* 1999; Hinchcliffe and Illum 1999; Bernkop-Schnurch 2000; Janes *et al.* 2001). Chitosan possesses two important properties, which makes it an exciting polymer in drug delivery. These are bioadhesion and absorption enhancement. We shall now consider these properties in detail.

1.1.1 Bioadhesion

There are a number of characteristics necessary for a polymer to exhibit mucoadhesion (Lehr *et al.* 1992). These include:

1) strong hydrogen-bonding groups (-OH, -COOH)
2) high molecular weight
3) sufficient chain flexibility
4) surface energy properties favouring spreading onto mucus.

Chitosan possesses all of these properties (Lehr *et al.* 1992) and therefore should be mucoadhesive. Chitosan is a cationic polysaccharide, and it has

been suggested that positively charged polymeric hydrogels could develop additional molecular attraction forces by electrostatic interactions with negatively charged mucosal surfaces.

Mucus is a viscoelastic substance with a characteristic stickiness which lines the gastrointestinal tract and other routes in the body such as the nasal cavity. By weight, mucus is mostly water (95.0 – 99.5%) with electrolytes, serum proteins, immunoglobulins and lipids. Its most important polymeric, gel-forming component is the mucus glycoprotein or mucin (0.5 – 5.0%). Mucins are large molecules with molecular weights ranging from 0.5 x 10^6 to over 20 x 10^6 g/mol and contain a large amount of carbohydrates. These carbohydrates are made up of several different monosaccharides, of which sialic acid is the most important in terms of mucoadhesion (Harding *et al.* 1999). In nasal delivery, the mucociliary clearance may greatly affect the absorption especially of hydrophilic drugs. The importance of the continual clearance of the mucus layer in the GI tract for absorption is less certain. The addition of a mucoadhesive agent to a drug formulation will increase the time that the drug is in contact with the mucosal surface, and hence increase absorption.

It is the electrostatic attraction between the positively charged amino groups on chitosan and the negatively charged sialic acid residues in mucin that is believed to account for chitosan's mucoadhesive nature. This has been demonstrated by He *et al.* (1998) who studied the mucoadhesive properties of chitosan and poly(vinyl alcohol) by turbidimetric measurements. The results suggested a strong interaction between chitosan and mucin, whilst there was little interaction between PVA and mucin due to PVA being negatively

charged. The attraction between chitosan and sialic acid was also confirmed by the observation of greater adsorption the greater the sialic acid content of the mucin.

Fiebrig *et al.* (1994) also demonstrated the interaction of chitosan and mucin using the analytical ultracentrifuge. When chitosan and mucin where mixed, large complexes where formed with a s_{mix}/s_{mucin} ratio of approximately 15-38. This complexation was pH dependent (see below). Also, no mucin was found to be unreacted and the results were consistent with a strong electrostatic interaction.

1.1.1.1 Effect of pH on Bioadhesion

Several groups have observed differences in the bioadhesion of chitosan at different pHs (Lehr *et al.* 1992; He *et al.* 1998; Rossi *et al.* 2000).

Most studies on the bioadhesive properties of chitosan have looked at the effects in the gastrointestinal tract. The pH in the GI tract varies from pH 1.2 in the stomach to pH 7.5 in the large intestine. This will affect the ionisation of both chitosan (pKa ~ 6.5) and sialic acid (pKa = 2.6).

In an acidic environment (pH<5.5), approximately 90% of the amino residues on chitosan exist in the ionic form. Further decreases in pH will have little further effect on ionisation. On the other hand, sialic acid is highly sensitive to pH changes in an acidic environment. He *et al.* (1998) observed a decrease in the number of ionised sialic acid residues when the pH changed from pH 5.5 to pH 3.5, and furthermore, when the pH changed to pH 1.2, the zeta potential of mucin reversed from negative to positive. The electrostatic interaction between chitosan and mucin will therefore be strongest at ~pH5.5 due to the increased number of charged sialic acid residues.

Fiebrig *et al.* (1994) also studied the effect of pH on chitosan-mucin interaction using the analytical ultracentrifuge. The results showed that as the pH was lowered below pH 6.5 to below the pKa of sialic acid, the size of the complex reduced (~12-22) but the interaction was still significant.

1.1.2 Absorption Enhancement

Bioadhesion can account for some of the absorption enhancement abilities of chitosan since it will allow a drug to stay longer in contact with the mucosal surface, increasing the available time for absorption.

Further absorption enhancement has been attributed to chitosan's ability to cause a transient opening of the tight junctions in the epithelial membrane (Artursson *et al.* 1994; Borchard *et al.* 1996; Schipper *et al.* 1997). This function is very important for the delivery of proteins and peptides, which are excluded from transcellular transport due to their size and hydrophilic nature. The paracellular absorption pathway is also limited, due to the entry of large molecules being restricted by the tight junctions (Artursson *et al.* 1994; Kotzé *et al.* 1997).

1.1.2.1 Structure and Function of Tight Junctions

One of the functions of the epithelial cells is to provide a permeability barrier between the different environments on either side of the cell and to allow transport across the cell layer. In order to perform these functions, the epithelial cells contain a highly specialised cellular component: the junctional complex. The junctional complex contains several well defined structures of which the tight junction is the most relevant here.

The tight junction separates the apical and basolateral domains and is the major paracellular barrier to the absorption of proteins and other compounds

(Denker and Nigam 1998). Several proteins are associated with the tight junctions; membrane bound proteins such as occludin and cytoplasmic proteins such as zona occludens 1 (ZO-1). Occludin is believed to control the paracellular permeability of the tight junction while ZO-1 may function as part of a signal pathway within the cytoskeleton in controlling membrane permeability. In intact tight junctions these proteins are strongly associated with the plasma membrane, however, when tight junction formation is prevented e.g. ATP depletion, these proteins are relocated from the membrane to other cellular compartments (Smith *et al.* 2004).

1.1.2.2 Effect of Chitosan on Tight Junctions

Dodane *et al.* (1999) and Kotzé *et al.* (1999) studied the effect of chitosan on caco-2 cell monolayers. It was found that chitosan hydrochloride and chitosan glutamate decreased the transepithelial electrical resistance (TEER) of caco-2 monolayers, which indicates a decrease in the tightness of the junctions between cells. Chitosan hydrochloride was found to be more effective than chitosan glutamate, however, this could be explained by differences in the amount of free chitosan base in each salt. About 50% of chitosan glutamate by weight is the glutamate salt whereas only a small fraction (5-10%) of chitosan hydrochloride is the chloride salt.

Dodane and Vilivalam (1998) and Smith *et al.* (2004) found that chitosan affected the location of ZO-1 and occludin. These membrane bound proteins were found to have relocated to the cytoskeleton after chitosan treatment. It was thought that chitosan may affect the intracellular ATP levels, since a similar pattern of protein relocation is seen during the formation of tight

junctions following ATP depletion, however, measurement of ATP levels showed no depletion in ATP.

Artursson *et al.* (1994) and Dodane and Vilivalam (1998) also found a change in the F-actin distribution, which is known to increase paracellular permeability (Meza *et al.* 1982). However, this effect was not observed by Smith *et al.* (2004). In conclusion it would appear that the effects of chitosan on membrane permeability are due to relocation of the tight junction proteins resulting in their transient opening.

Many other compounds have been studied as absorption enhancers for proteins and peptides, however, many of them cause damage to the epithelial membrane (Thanou *et al.* 2001). Chitosan does not cause irreversible damage to the epithelia as has been demonstrated by several authors. Kotzé *et al.* (1997) stained caco-2 cell monolayers with trypan blue after prolonged incubation with chitosan. No visible intracellular uptake of this marker was observed indicating that the monolayers remained undamaged and functionally intact. Also, after removal of the polymer, the TEER of the caco-2 cells recovered, again showing that the cells were undamaged and functionally intact (Borchard *et al.* 1996; Dodane *et al.* 1999). Aspden *et al.* (1996) studied the effects of chitosan on nasal epithelia membranes and found only slightly more protein and enzyme release than occurred after perfusing with normal saline. The increased protein release was attributed to increased mucus production by the goblet cells, and it was concluded that chitosan would be safe to use as a nasal drug enhancer.

The influence of chitosan's degree of acetylation and molecular weight on the permeability of caco-2 cell intestinal monolayers was studied by Schipper *et*

al. (1996) using chitosan solution at pH 5.5 and the non-absorbable paracellular marker [^{14}C] mannitol. It was found that chitosans with a low degree of acetylation (DA) were effective as permeation enhancers at low and high molecular weight, whereas chitosans of high DA were effective at only high molecular weight. The effects of chitosans of both high and low molecular weight and degree of acetylation were further investigated as regard to the ability of these compounds to bind with epithelial caco-2 cell monolayers (Schipper *et al.* 1997). Both chitosans appeared to bind tightly to the epithelium, inducing a redistribution of F-actin and the tight junction protein ZO-1. No intracellular uptake of chitosan could be observed. It was also shown that these effects were mediated by cationic charges of chitosan, since the addition of the highly anionic heparin in the test solutions inhibited the permeation enhancing effects.

Chitosan also has other characteristics that are considered necessary for an absorption enhancer (Behl *et al.* 1998), for example:

- pharmacologically inert at concentrations used,
- non-irritating, non-toxic and non-allergenic,
- any effect on the mucosa is completely reversible,
- remains in contact with the mucosa long enough to achieve a maximal effect,
- no offensive odour or taste,
- relatively inexpensive and readily available.

1.1.3 Oral Delivery of Polypeptides

At present, most protein and peptide drugs are administered parenterally. This can be inconvenient for the patient and lead to reduced compliance. Oral

delivery is the most convenient method of drug delivery; however, this poses problems for polypeptides.

Most protein and peptide drugs are poorly absorbed following oral administration due to substantial degradation in the GI tract and/or poor permeability of the intestinal epithelial barrier. It is known for instance that dietary proteins do not normally cross the intestinal epithelium intact, but must first be broken down to their constituent free amino acids, which are then absorbed. Such degradation and consequent absorption destroys all physiological activity of the protein and can explain why typical oral bioavailabilities of proteins are usually less than 1-2% (Carino and Mathiowitz 1999). Furthermore drugs delivered orally are susceptible to first pass metabolism in the liver.

The addition of chitosan to an oral formulation can reduce permeability problems, as it possesses bioadhesive and absorption enhancement properties, however, this does not solve the problems of degradation that occurs in the GI tract. Also, the changes in pH along the GI tract from pH 1.2 in the stomach to pH 7.5 in the large intestine affect the solubility and protonation of chitosan.

1.1.3.1 Chitosan for Oral Absorption Enhancement

The oral delivery of proteins is hindered by low bioavailability, poor residence time at site of absorption, and poor drug stability due to proteolytic enzymes. Chitosan may improve absorption and residence times through its absorption enhancing properties and mucoadhesion, however, there is still a low bioavailability due to degradation of the drug both in the acidic conditions of the stomach and by proteolytic enzymes. It is known that chitosan does not

exhibit any inhibitory action on proteolytic enzymes as demonstrated by Lueßen *et al.* (1996) following oral administration of a synthetic peptide in rats. A potential method to overcome the acidic conditions in the stomach are to use a controlled delivery matrix such as hydroxypropyl methylcellulose (HPMC), which swells on contact with water to form a hydrated gel that remains sufficiently intact through the gastrointestinal tract to protect the incorporated drug. Unfortunately, chitosan is unable to act as an absorption enhancer in the small intestine due to the neutral pH at which it is insoluble (Hejazi and Amiji 2003). Borchard *et al.* (1996) investigated chitosan glutamate solutions at pH 7.4 for their effect in increasing the paracellular permeability of [^{14}C] mannitol and fluorescently labelled dextran (MW 4400Da) in vitro in caco-2 cells. No effect on the permeability of the monolayers could be observed, indicating that at neutral pH chitosan is not effective as permeation enhancer. The pH dependency of chitosan's effect on epithelial permeability was further studied by Kotzé *et al.* (1998). Two chitosan salts (hydrochloride and glutamate) were evaluated for their ability to enhance the transport of [^{14}C] mannitol across caco-2 cell monolayers at two pH values, 6.2 and 7.4. At low pH both chitosans showed a pronounced effect on the permeability of the marker, leading to 25-fold (glutamate salt) and 36-fold (hydrochloride salt) enhancement. However, at pH 7.4 both chitosans failed to increase the permeability, due to solubility problems. Chitosan and chitosan salts have poor solubility at neutral pH values since aggregation occurs in solutions at pH values above 6.5, and only protonated chitosan (i.e. in its uncoiled configuration) can trigger the opening of the tight junctions (Artursson *et al.* 1994), thereby facilitating the paracellular transport of

hydrophilic compounds. Chitosan can only be effective as an absorption enhancer in a limited area of the intestinal lumen where the pH values are close to its pKa. For intestinal absorption the use of a chitosan derivative is necessary and these are discussed in section 1.1.3.2.

An alternative delivery site of peptides and proteins is the colon, where there is lower proteolytic enzyme activity and a longer residence time. Tozaki *et al.* (1997) studied the use of HPMC coated chitosan capsules for the colonic delivery of insulin in rats. It was found that after 6 hrs, when the capsules reached the colon, a hypoglycaemic effect was observed that lasted for 24 hrs. The HPMC outer coating protected the insulin from the acidic conditions in the stomach. It then dissolves in the small intestine and the inner chitosan capsule layer protects the insulin until it reaches the colon where the microflora biodegrade the chitosan capsule and the insulin is released. Tominaga *et al.* (1998) demonstrated a similar delivery system using an inner coating of chitosan and an outer coating of phytin, a gastric acid resistant material.

1.1.3.2 Chitosan derivatives for oral absorption enhancement

N-trimethyl chitosan chloride (TMC), a partially quaternised derivative of chitosan, shows much higher aqueous solubility than chitosan in a much broader pH and concentration range. The reason for this improved solubility is the substitution of the primary amine with methyl groups and the prevention of hydrogen bond formation between the amine and the hydroxylic groups of the chitosan backbone. Thanou *et al.* (2001) and Kotzé *et al.* (1999) studied the effects of TMC on intestinal absorption. Chitosan HCl and TMCs of different degrees of trimethylation were tested for enhancing the permeability of the

radiolabelled marker [^{14}C] mannitol in caco-2 intestinal epithelia at neutral pH values (pH 7.2). Chitosan HCl failed to increase the permeation of these monolayers and so did TMC with a degree of methylation of 12.8%. However, TMC with a degree of trimethylation of 60% increased significantly the [^{14}C] mannitol permeability across caco-2 intestinal monolayers, indicating that a threshold value at the charge density of the polymer is necessary to trigger the opening of the tight junctions at neutral pH values. Visualisation studies using confocal laser scanning microscopy showed that TMC polymers widened the paracellular pathways in a similar way to protonated chitosan without causing cell membrane damage. The effect of TMC60 was studied in vivo in rats using the peptide drug buserelin. Buserelin formulations with or without TMC60 (pH 7.2) were compared with chitosan dispersions at neutral pH values after intraduodenal administration in rats. A remarkable increase in buserelin serum concentrations was observed after co-administration with TMC60, whereas buserelin alone was poorly absorbed.

1.1.3.3 Chitosan nanoparticles for oral delivery

An alternative approach for the oral delivery of proteins is using microspheres/capsules. There are three major mechanisms by which microspheres can improve oral delivery of proteins (Carino *et al.* 2000):

1. the spheres can protect the protein from proteolysis
2. the spheres can cross over the intestinal mucosa
3. the spheres can change the inter-tissue distribution of the protein.

Damge *et al.* (1990) studied the oral delivery of insulin in rats using isobutyl 2-cyanoacrylate microspheres. A significant reduction in blood glucose levels was observed that lasted for 20 days demonstrating that the microspheres

protected the insulin from proteolysis and was able to change the distribution of insulin so that a slow and prolonged release occurred. However, similar studies showed no therapeutic response and possible degradation of the insulin (Couvreur *et al.* 1980), and ineffectiveness when administered to fed rats (Damge *et al.* 1988). For intestinal uptake of microspheres an upper size limit of about 10μm has been observed (Ermak *et al.* 1995). Since it is difficult to control the size distribution of microspheres/nanoparticles produced, and hence their uptake across the intestinal mucosa, an alternative use of microspheres is to provide the delivery of the protein to the site of absorption at a high concentration. However, for this to be advantageous the addition of mucoadhesives and absorption enhancers is necessary and as such chitosan nanoparticles can provide both of these characteristics.

Chitosan nanoparticles can be formed using several techniques. For example, Ohya *et al.* (1994) prepared nanospheres using a water-in-oil emulsion method followed by crosslinking with glutaraldehyde. However, the glutaraldehyde not only interacted with the chitosan but also with the active drug, causing drug immobilization rather than encapsulation. Since proteins can easily denatured by production methods that require harsh conditions such as high temperatures or crosslinking agents, the use of an ionic gelation technique has proved highly favourable. Chitosan nanoparticles can be formed by a mild ionotropic gelation method using the anionic counter-ion tripolyphosphate pentasodium (TPP). These nanoparticles have been studied by several researchers (Bodmeier *et al.* 1989; Fernández-Urrusuno *et al.* 1999; Shu and Zhu 2000; Dyer *et al.* 2002). These nanoparticles show high protein loading (up to 50mg per 100mg of nanoparticles) and along with the absorption

enhancing properties of chitosan offer a very promising delivery system for proteins and peptides.

1.1.4 Nasal Delivery of Polypeptides

Oral delivery of proteins and peptides requires further research, especially if an oral formulation for the delivery of insulin is to be considered. An alternative delivery route is via the nose. The nasal cavity possesses many advantages for drug delivery (Behl *et al.* 1998; Soane *et al.* 1999):

- relatively large surface area for absorption with subepithelial layer that is highly vascularised (only two cell layers separate the nasal lumen from the dense blood vessel network in the lamina proporia),
- blood drains directly into the systemic circulation, avoiding first pass metabolism by the liver,
- fast onset of therapeutic action,
- non-invasive, therefore, reduced risk of infection,
- ease of convenience and self-medication, and improved patient compliance.

Despite these structural advantages for drug delivery, the bioavailability of most polypeptide drugs is less than 1% since the molecules are polar and too large to easily pass the tight junctions in the membrane. Furthermore, the time available for absorption is limited due to mucociliary clearance. Chitosan can increase the nasal bioavailability of poorly absorbed drugs by increasing nasal membrane permeability and increasing the contact time for absorption by reducing the mucociliary clearance rate.

1.1.4.1 Structure of Nasal Cavity

The nasal cavity, located mainly within the skull, is divided into two approximately equal halves by the nasal septum with each half beginning anteriorly at the nares/nostrils of the external nose and extending posteriorly to the nasopharynx where the two halves of the airway join together. It has a total volume of 15-20ml and a total surface area of about 150cm^2 which can be divided into three functional regions:

- the vestibular region (the anterior 10-20cm^2),
- the olfactory region (occupying 10-20cm^2 in the roof of the nasal cavity),
- the respiratory region (about 130cm^2), which occupies the majority of the main part of the nasal cavity and is important for the absorption of drugs into the systemic circulation.

The respiratory region contains bony "scroll-like" turbinates (inferior, middle and superior), which are attached to the lateral wall and project downwards into the main part of the nasal cavity, considerably increasing the surface area. In this region, the epithelium is composed of ciliated and non-ciliated cells (Mygind and Dahl 1998). Cilia play an important role in mucociliary clearance which is discussed in more detail in section 1.1.4.2.1. The lamina propria (a loose type of connective tissue which anchors the mucosa to the underlying skeletal structure) contains many blood vessels, nerves and glands. Blood is supplied to the nose posteriorly by a large branch of the sphenopalatine artery, superiorly by a branch from the anterior ethmoid artery and antero-inferiorly by a branch from the superior labial branch of the facial artery (Jones 2001).

The respiratory epithelium, in addition to cilia, is covered by a mucus layer consisting of two distinctive layers, the aqueous periciliary layer that surrounds the cilia and a more gellous upper layer on top of the cilia. Both cilia and the mucus layer play an important role in mucociliary clearance which is a major barrier to nasal drug absorption.

1.1.4.2 Factors affecting nasal absorption

1.1.4.2.1 Mucociliary clearance

The function of the mucociliary clearance system (MCS) is to remove foreign substances and particles from the nasal cavity, preventing them reaching the lower airways. Normal mucociliary transit time in humans has been reported to be 12 to 15 minutes, with the average rate of nasal clearance being 8mm/min (Marttin *et al.* 1998).

Cilia range in length between 5 and 10 μm and in width from 0.1 to 0.3 μm. The number of cilia per cell is approximately 200, with a density of 6 – 8 cilia per μm^2. The beating of a cilium has three phases; an effective stroke, during which the cilium is extended maximally; the rest phase, in which it is parallel to the cell surface; and the recovery stroke. The average ciliary beat frequency in humans is 10 Hz and is regulated by several factors: temperature, intracellular Ca^{2+} and cAMP levels, and by extracellular ATP. An increase in temperature of between 5 and 20°C increases ciliary beat frequency (Marttin *et al.* 1998) and the optimum working temperature is 35-40°C (Jones 2001).

Mucus forms the other part of the MCS. This consists of two distinct layers: the aqueous periciliary layer and a more gellous upper layer. The periciliary layer is a low viscosity fluid, probably formed by epithelial cell exudates, with a thickness that is slightly less than the length of an extended cilium. This is

covered by a more viscous upper layer of about 0.5-5.0 μm deep, which is secreted by the goblet cells (Marttin *et al.* 1998). Mucus exhibits non-Newtonian behaviour, i.e., it possesses both viscous and elastic properties. This enables the mucus to efficiently accept the energy transfered from the cilia, while its elastic properties enable it to relax sufficiently to be propelled towards the nasopharynx, where it is swallowed.

The MCS is particularly susceptible to damage. This can be potentially harmful to the patient since impaired mucociliary clearance causes longer contact times of the airway mucosa with bacteria and viruses, which could lead to infections of the respiratory tract. The efficiency of the MCS depends on three factors (Marttin *et al.* 1998):

1) the amount of ciliary input, determined by the length and density of the cilia and their beating frequency,
2) the amount of mucus and the depth of the periciliary layer
3) the viscoelastic properties of the mucus.

The effect of chitosan on these factors has been studied. Aspden *et al.* (1995 and 1997) for example looked at the effect of chitosan on mucociliary transport rates (MTR) in the frog palate model, human turbinates and human volunteers. They found that chitosan had an inhibitory effect on MTR which was greater and more prolonged with higher molecular weight chitosans. Studies on turbinates indicated that cilia continued to beat and that the effect of chitosans on MTR was predominantly physical. Chitosan and mucus interact to form a viscous and adhesive complex (result of interaction between negatively charged sialic residues of mucus and cationic chitosan molecules), which prevents cilia transporting particles over the surface of the mucus layer.

In human volunteers, no significant difference was observed in saccharin clearance times recorded before and after 7 days of a daily chitosan application, indicating that the inhibitory effect of chitosan on MTR is transient and results in no permanent damage.

It is also important to study the effect of the drugs and other components of the nasal formulation, e.g. preservatives, on the MCS. Marttin *et al.* (1998) reviewed the effect of drugs and preservatives on the MCS. Studies on insulin and salmon calcitonin showed little to no effect on MTR in the frog palate model and any cilio-inhibition observed in vitro was reversible. The preservative benzalkonium chloride did not alter MTR in humans, though cilio-inhibition and ciliostasis were observed in vitro in chicken embryo tracheas.

1.1.4.2.2 Physicochemical Properties of Drugs

1.1.4.2.2.1 Molecular Weight

The effect of physicochemical properties of drug molecules on nasal absorption has been studied by several researchers (Fisher *et al.* 1987; McMartin *et al.* 1987; Donovan *et al.* 1990; Fisher *et al.* 1991). They found that whilst there was some correlation between charge and degree of hydrophobicity of a molecule on absorption, the predominant factor for absorption was the molecular weight of the compounds. Studies on groups of dextrans and polyethylene glycols of varying molecular weight demonstrated that absorption decreased as molecular weight increased. For example, dextrans of (weight average) molecular weight 1,260 and 45,500 Da had bioavailabilities of 52.7% and 0.6% respectively. In general compounds with a molecular weight greater than 1,000 Da are not likely to result in

bioavailabilities greater than 10% regardless of physicochemical properties. Nasal absorption fell off sharply at molecular weight >1,000 Da, while oral absorption declined even more steeply at molecular weights >200 Da. Rapid peaking occurred even when total nasal absorption was low, indicating that a substantial portion of the poorly absorbed compounds are eliminated from the site of absorption either mechanically (mucociliary clearance) or by degradation.

1.1.4.2.2.2 Solubility and Dissolution Rate

Drug solubility can limit absorption and can also affect the formulation. For particulate nasal products, administered as either powder inhalation or in the form of suspensions, the dissolution rate of a drug and saturation solubility becomes important. Particles deposited in the nostrils need to be dissolved prior to absorption. If the drug remains as particles, they may be cleared from the nasal cavity and absorption will not occur (Behl *et al.* 1998).

1.1.4.2.3 Drug Formulation – pH and osmolarity

Ohwaki *et al.* (1985), Pujara *et al.* (1995) and Behl *et al.* (1998) studied the effect of formulation variables on the nasal mucosa. The pH of the rat nasal mucosa is 7.39 and the pH of the human nasal mucosa is in the range of 5.5 – 6.5. The nasal cavity of rats was perfused with solutions of various pHs and the perfusate examined. Protein release from the nasal mucosa was maximal at pH 12 and 2 indicating membrane and intracellular damage (both lactate dehydrogenase-LDH, an intracellular enzyme and 5'nucleotidase-5'ND, a membrane-bound enzyme were released). Buffers within pH values of 3 and 10 caused very low and similar amounts of total protein release. It was concluded that these pH effects were due to structural changes in the epithelial

cells, and to avoid nasal irritation, the formulation pH should be adjusted between 4.5 and 6.5.

Drug absorption through the nasal mucosa can be substantially affected by formulation tonicity. It was found that the absorption of secretin in rats was affected by the concentration of sodium chloride and absorption reached a maximum at a 0.462M sodium chloride concentration (hypertonic) probably due to the observed shrinkage of epithelial cells. The effect of osmolarity on the nasal epithelium was studied and it was found that pure water of zero osmolarity caused the most mucosal marker leakage due to swelling of the epithelial cells. Isotonic and hypertonic solutions demonstrated very little effect on the LDH release from the nasal epithelium, leading to the conclusion that isotonic and hypertonic solutions are less damaging than hypotonic solutions. In general, an isotonic formulation (0.9% NaCl) is preferable.

1.1.4.2.4 Deposition of drug

The clearance of a drug formulation from the nasal cavity is influenced by its site of deposition (Kublik and Vidgren 1998). The turbinates, which are covered by respiratory epithelia, are the primary sites for systemic absorption of nasally administered drugs. Ciliated epithelia are present in the middle and posterior parts of the turbinates, but are almost absent in the anterior regions. A drug deposited posteriorly in the nose is cleared more rapidly than a drug deposited anteriorly, because mucociliary clearance is slower in the anterior part of the nose. Three different clearance phases following nasal delivery have been distinguished. The first phase within the first minute after application, mainly applicable for liquid formulations and large application volumes, is a very rapid clearance due to swallowing or run-through of the

formulation into the pharynx. The following second phase occurring 15-30 minutes after application results from progressive clearance of the material deposited in the ciliated area of the main nasal passages. The part of the dose distributed in the non-ciliated for anterior part of the nose disappears very slowly, this clearance phase lasts over several hours. The second and third phases are claimed to be responsible for the biphasic clearance pattern observed in nearly every deposition study.

1.1.4.3 Formulations for nasal administration

Developing an appropriate formulation for a given drug is vitally important. A good drug can be rendered useless, ineffective or mediocre by the choice of an inappropriate formulation. The choice of dosage form depends on the drug being developed, indication being pursed, and patient population. Behl *et al.* (1998), Kublik and Vidgren (1998), and Hinchcliffe and Illum (1999) reviewed various formulations for nasal drug delivery.

1.1.4.3.1 Solutions and Suspensions

Nasal solutions can be administered by simple drops or using sprays. Nasal drops are very simple and represent a convenient form of administering drugs. The development of metered dose nasal actuators enabled the delivery of accurate actuation volumes as low as 25 µl. Suspensions can also be administered using metered dose actuators that have been designed to account for the specific particle size and morphology of the drug particles.

1.1.4.3.2 Powders

If a suitable solution or suspension of the drug cannot be developed, a dry powder form may be used. Powders are not favourable products since they can cause irritation on the nasal mucosa, and are also more expensive to

manufacture because of the particle size/morphology considerations. Administration of nasal powders may evidently increase patient compliance, especially for children if the smell and taste of the delivered drug is unacceptable. The powder facilitates the delivery of the highest mass of active ingredient without the necessity of a vehicle.

1.1.4.3.3 Gels

Gels are either thickened/gelled solutions or suspensions of drugs. They can offer several advantages over other dosage systems (Behl *et al.* 1998). For example, a gel can localise the formulation on the mucosa thereby providing a better chance of absorption of the drug.

1.1.4.3.4 Microspheres

Current trends in nasal drug delivery methods appear to be focused on the use of microsphere technology (Hussain 1998). By using microspheres formulated using biocompatible materials, e.g. starch, gelation and chitosan (Illum *et al.* 1988; Illum *et al.* 2001; Janes *et al.* 2001) a more intimate and prolonged contact between the drug and the mucosal membrane can be achieved allowing increased absorption of the drug.

(Illum *et al.* 1987 and 1988) have studied nasal delivery using starch microspheres in rats and sheep. Reduced clearance and increased drug absorption occurred due to absorption of water from the epithelial mucosa during the gelling process and resulted in a reversible shrinkage of the epithelial cells. This shrinkage could lead to the physical separation of the intracellular junctions and enhance paracellular absorption. Soane *et al.* (1999) compared the clearance of chitosan solution, starch microspheres and chitosan microspheres to a control solution of 99m Tc-DTPA solution (99m-

Technetium labelled diethylenetriaminepentaacetic acid). The time taken for 50% clearance of the chitosan solution almost doubled (compared to the control solution) to 41 minutes, whilst the half-life of clearance for the starch microspheres more than tripled to 68 minutes and of chitosan microspheres half-life of clearance quadrupled to 84 minutes. The slow clearance of the chitosan and starch systems can be explained by their bioadhesive properties, and additional dehydration of the mucus layer causing an increase in its viscosity and increasing cilia resistance. The chitosan solution will also interact rapidly with mucins due to its cationic nature, possibly explaining its increased residence time.

The effects of various microsphere systems on the bioavailability of the peptide insulin have been studied. Starch and dextrin microspheres cross-linked with epichlorohydrin were studied in rats (Edman *et al.* 1992). Both systems caused a rapid reduction in glucose levels after nasal administration with a maximal reduction observed within 30-40 minutes. Starch microspheres were more effective than dextrin microspheres in reducing blood sugar levels. A study by Farraj *et al.* (1990) using starch microspheres in sheep appeared to show that the absolute bioavailability of insulin from the starch microspheres was 4.5% compared to about 1% for a solution of insulin without absorption enhancers. Illum *et al.* (1994) studied the use of hyaluronic acid ester microspheres as a nasal delivery system for insulin in sheep. The microsphere system evidently produced large and significant increases in nasal absorption similar to those obtained for bioadhesive starch microspheres. The mean relative bioavailability was claimed to be 11% when compared with insulin administered by the subcutaneous route.

1.1.4.3.5 Nanoparticles

It has been considered that chitosan nanoparticles, like microspheres, would intensify the contact between the protein and nasal absorptive mucosa, leading to increased protein concentration at the absorption site (Fernández-Urrusuno *et al.* 1999).

Studies *in vivo* showed that administration of insulin loaded chitosan nanoparticles prepared using ionotropic gelation with TPP resulted in a fall in glucose levels after nasal administration (Fernández-Urrusuno *et al.* 1999). For this effect to be observed the insulin released from the nanoparticles has to be in its active form indicating that the preparation method was not harmful to the protein. Further studies by Dyer *et al.* (2002) in rat and sheep models also appeared to show a fall in glucose levels after nasal administration of chitosan nanoparticles loaded with insulin.

In vitro release of insulin from chitosan nanoparticles appears to be dependent on the pH of the surrounding medium. Release is evidently rapid at pH 7.4 and pH 4, but slightly slower at pH 6.4. (Fernández-Urrusuno *et al.* 1999). This could be attributed to the lower solubility of insulin at pH 6.4 (9.4 μg/ml) compared to at pH 7.4 (834 μg/ml) and pH 4 (>1 mg/ml). Release of insulin in water was claimed by these researchers to be much slower than in a buffered medium suggesting that the interaction forces between insulin and chitosan are reversible and very weak, and that insulin releases from the nanoparticles by a simple dissolution mechanism (Fernández-Urrusuno *et al.* 1999; Janes *et al.* 2001).

In conclusion, chitosan nanoparticles display several attractive features for the delivery of therapeutic proteins and peptides:

- formation under extremely mild conditions
- great capacity for association of proteins
- release rates of different rates depending on composition
- increased absorption due to bioadhesive and absorption enhancing nature of chitosan.

1.2 Chitosan and Degradation

1.2.1 Chitosan

Chitosan is a derivative of chitin, the second most abundant polysaccharide after cellulose ((Paradossi *et al.* 1992; Ottøy *et al.* 1996; Boryniec *et al.* 1997)). Chitin is a linear polysaccharide consisting of *N*-acetyl-D-glucosamine units (Glc-NAc), and the term chitosan refers to a series of deacetylated chitins containing *N*-acetyl-D-glucosamine units and D-glucosamine units (Glc-N) in varying proportions. The structure of chitosan is shown in Figure 1-1.

1.2.1.1 Production of Chitosan

Chitin is an abundant biopolymer like cellulose and is distributed in the shells of crustacea, e.g. crab and shrimp, the cuticle of insects and also in the cell wall of some fungi and micro-organisms (Anthonsen *et al.* 1993; Sugimoto *et al.* 1998).

Chitosan can be obtained by commercial *N*-deacetylation of chitin, after its isolation from, for example, the shells of crabs (Anthonsen *et al.* 1993; Vårum *et al.* 1994). Demineralisation is carried out at room temperature in hydrochloric acid, followed by deproteination using alkaline treatment in sodium hydroxide at 80-85°C (Tolaimate *et al.* 2000). Deacetylation is then carried out using strong alkaline solution (~40% w/w) at high temperatures

(~80°C). The influence of alkaline concentration and temperature have been investigated by Chang *et al.* (1997), who found that the kinetics of homogeneous and heterogeneous alkaline *N*-deacetylation was first order, i.e. the rate of deacetylation was directly proportional to the alkaline concentration and the reaction temperature. Temperature and alkaline concentration dramatically affected the rate of deacetylation, which increased with increasing temperature and alkaline concentration. The resulting degree of acetylation was found to be proportional to the reaction time (Rege and Block 1999; Tolaimate *et al.* 2000).

As well as the occurrence deacetylation, degradation of chitin also takes place during the deacetylation process due to the high concentration of alkaline solution and the prolonged reaction times required to obtain significant deacetylation (Tolaimate *et al.* 2000). Under the most drastic conditions, the molecular weight can decrease by a factor of about 5-10. To achieve a desired degree of acetylation, the process may normally have to be repeated several times. However, Tolaimate *et al.* (2000) found that after two repeated alkaline steps the desired degree of acetylation can be obtained and that further reaction steps only lead to depolymerisation.

Figure 1-1: Schematic Structure of Chitosan; R=acetyl or H, depending on the degree of acetylation

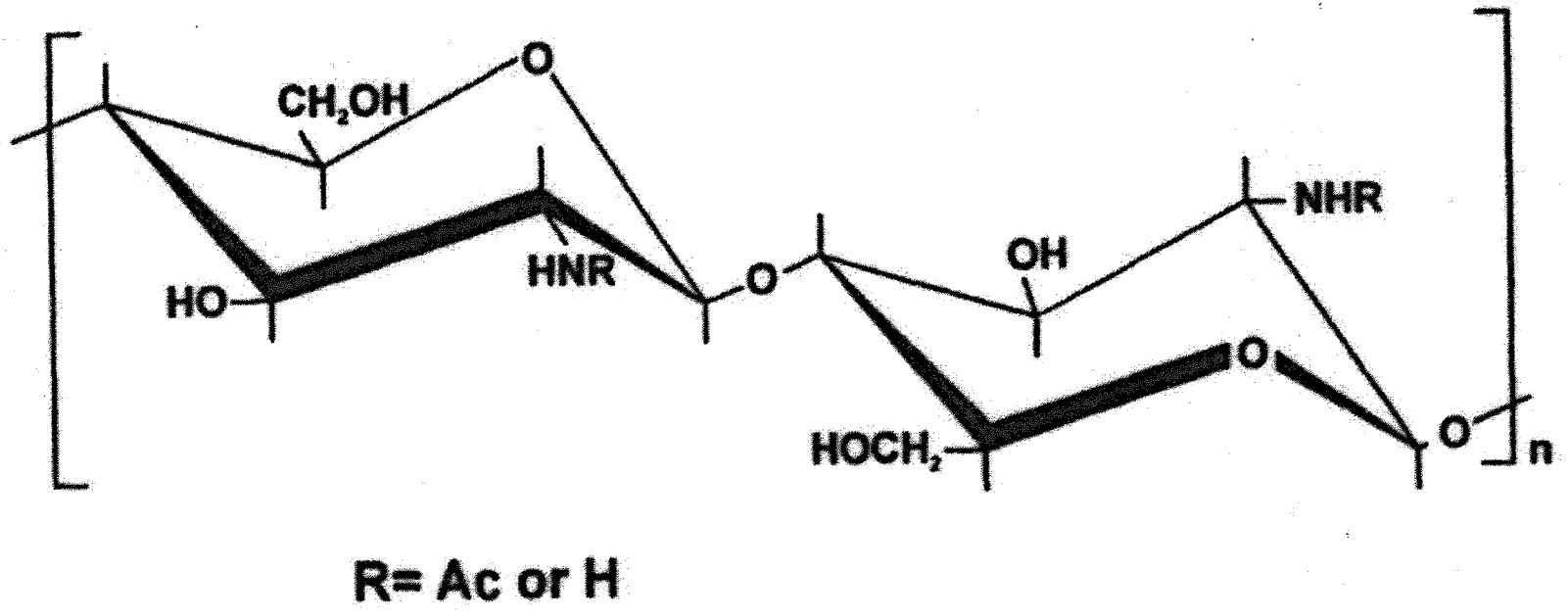

1.2.1.2 Physico-chemical characterisation of chitosan

Chitosan is insoluble in water at neutral and basic pH-values (Vårum *et al.* 1994), however it is soluble in aqueous acidic solution. When dissolved in acidic media it becomes a polyelectrolyte due to the protonation of the $-NH_2$ groups, and the following equilibrium reaction occurs (Rinaudo *et al.* 1999):

$$\text{Chit-NH}_2 + H_3O^+ \leftrightarrow \text{Chit-NH}_3^+ + H_2O \qquad \textbf{(1 - 1)}$$

Chitosan differs from other polysaccharides in two main ways:

- The term chitosan does not refer to a defined structure but to a group of polysaccharides, whose structures differ depending on the DA. The DA describes the ratio of *N*-acetylated to deacetylated subunits. A structure consisting of only *N*-acetyl-D-glucosamine units would be described as having a DA of 100%, while a structure consisting of only D-glucosamine units has a DA of 0%.
- In aqueous acidic media chitosan is a cationic polyelectrolyte and the conformation of the chitosan molecule depends on the composition of the solvent (especially the ionic strength). An uncharged flexible polymer molecule may take on any configuration compatible with its bond length and angles and other steric restrictions. This is also possible for charged polymer molecules, however, each configuration will have different free energies, with a relatively high free energy for compact configurations and a relatively low free energy for expanded ones. The lower the free energy of a molecule, the more stable it is, therefore polyelectrolytes tend to have an expanded configuration.

Changing the composition of the solvent, mainly the ionic strength, may alter the configuration of a charged molecule. At low ionic strength the polymer molecule has a more extended conformation. As the ionic strength is increased, the molecule will become less extended. This is due to shielding of the charges on the molecule as the ionic strength increases and thus less expansion is required to reduce the free energy of the molecule (Tanford 1961).

Chitosan can also be characterised by its molecular weight. In Chapter 3 the molecular weight of several chitosans are determined using several hydrodynamic techniques, the details of which are found in Chapter 2. These techniques include analytical ultracentrifugation and light scattering. Chitosan is also a polydisperse material, that is, the sample will contain a range of different molecular weights. The techniques therefore measure an average molecular weight and this is discussed in more details in Chapter 2.

1.2.1.3 Conformation

The gross conformation and chain flexibility of chitosan in solution may be affected by solvent conditions, namely ionic strength, pH and temperature of the solution, as well as the molecular weight and degree of acetylation of the chitosan used (Tsaih and Chen 1997). The conformation of chitosan in solution may be affected by the DA of the chitosan in two possible ways:

- By the presence of bulky acetyl groups – due to steric hindrance, chitosan with the highest DA should therefore hold the most expanded conformation
- By the number of positive charge from free amino groups in acidic solutions. Positive charges in solution will repel each other. The

chitosan with lowest DA will have the highest amount of amino groups and hence the highest charge effect. The repulsive effect will be highest and the chitosan will have the most expanded conformation. This effect is most important at very low ionic strengths. At high ionic strengths, repulsion is largely suppressed due to screening effects of the added salt: the electrostatic contribution to chain stiffness becomes small.

For chitosan to be soluble, it needs to have a DA of less than 50%. Below this DA, half of the residues will possess a charged group in acidic solution, and it may be expected that the charge effects will determine the conformation.

Ellipsoid modelling and bead modelling can be used to represent the conformation of quasi-rigid systems such as proteins. However, the stringent assumptions that are used make these modelling techniques unsuitable for flexible systems such as many polysaccharides: their polydispersity also adds to the complications.

For polysaccharides, the Mark-Houwink-Kuhn-Sakurada exponents can be used to distinguish between classes of conformation (compact sphere, rigid rod and random coil). The MHKS equation relates intrinsic viscosity to molecular weight as shown:

$$[\eta] = kM^a \qquad \textbf{(1 - 2)}$$

where $[\eta]$ is the intrinsic viscosity, M the molecular weight, a the MHKS exponent and k the MHKS constant (see for example Harding 1997).

Table 1-1 shows the values for the MHKS exponent that relate to different conformations.

Table 1-1: Relationship between polymer conformation and MHKS exponent

Value of *a*	Conformation
0	Sphere
0.5 ~ 0.8	Random coil
1.8	Rod shape

Anthonsen *et al.* (1993) found that for chitosans dissolved in a 0.1M ionic strength solution, as the DA increases the value of the Mark-Houwink-Kuhn-Sakurada exponent *a* increases.As DA increases the number of NH_3^+ groups will decrease, therefore the electrostatic repulsion will decrease. It would be expected that the chitosan molecule would become more compact, however the opposite occurs. This indicates that at an ionic strength of 0.1M, it is the influence of the *N*-acetyl groups rather than the electrostatic effects of charged amino groups that determine the extension of the chitosan chain. Similar results from viscosity and light scattering measurements have been obtained (Wang *et al.* 1991). Draining effects may also have a significant effect on the value of *a* (see for example Berth et al, 2002).

The Haug triangle is a graphical way of representing the relation between the three conformation extremes – sphere, rod and coil (Smidsrød and Andresen 1979). The extremes of conformation are placed at the corners of the triangle and the conformation of a given macromolecule can then be represented by a locus along the perimeter of the triangle. For example, a globular protein would be represented by a locus somewhere between the extremes of sphere

and rod (side A), a polysaccharide, DNA or a mucus glycoprotein between rod and coil (side B) and a denatured protein between coil and sphere (side C).

Figure 1-2: Haug triangle representation of the gross conformation of macromolecules

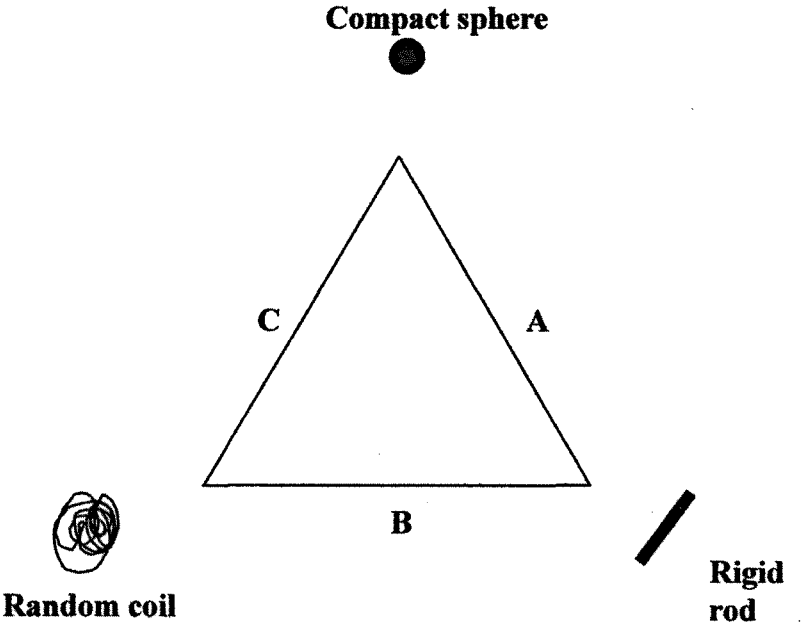

Polysaccharides are best represented by the worm-like chain model that allows for continuous flexibility throughout the polymer chain. Generally the more charged a polysaccharide is, the more rod-like its conformation. Highly charged polyanions such as pectin and polycations like chitosan have behaviour approaching that of stiff rods, whereas those of low or no charge behave more like random coils e.g. pullalan. The flexibility of these worm-like chains can be represented by various parameters such as the ratio L_p/L_c, the ratio of the contour length of the chain to its persistence length. In the limits $L_p/L_c \rightarrow 0$ and $L_p/L_c \rightarrow \infty$ the conformation is rod-like and random coil respectively.

Figure 1-3: The persistence length L_p and contour length L_c of a linear macromolecule (Harding 1997)

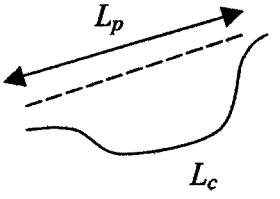

Further information on the stiffness/flexibility of a polysaccharide can be determined from relations between intrinsic viscosity and ionic strength. The simplest is the "Smidsrød" stiffness parameter B, which is defined by:

$$S = B.([\eta]_{I=0.1})^{v} \qquad \textbf{(1-3)}$$

where the exponent v equals 1.3, and S is measured from a plot of [η] versus I and the equation $[\eta] = [\eta]_{\infty} + \left(S.I^{-1/2}\right)$.

Flory and co-workers also estimated the stiffness of a macromolecule using the characteristic ratio C_{∞}:

$$C_{\infty} = < h^2 > / nl^2 \qquad \textbf{(1-4)}$$

where $<h^2>$ is the mean square end to end distance, n is the number of segments in the chain and l is the length of each segment. $C_{\infty} \geq 1$ holds only for a perfectly flexible chain. In practical terms, flexible coils appear to have values of $C_{\infty} \sim$ 1-10 whereas very stiff polymers have $C_{\infty} > \sim$ 25-400. C_{∞} can be estimated from the intercept of a plot of $[\eta]/M^{1/2}$ versus $M^{1/2}$ together with knowledge of the residue length l and residue molecular weight.

1.2.2 Degradation

Chitosan, like all polysaccharides, will degrade over time, mainly due to hydrolysis of the β(1→4) linkage between the monomers (BeMiller 1967). This normally happens faster with chitosan in solution than in the solid state

(Holme *et al.* 2001). In order to market a drug formulation it is necessary to ensure that the bioavailability and pharmacological effectiveness of the drug are not compromised over a specified shelf life, e.g. three years (Aulton 2002). Various factors will affect the rate of degradation of chitosan, including temperature, pH, and ionic strength (BeMiller 1967).

Looking at the kinetics of polymer degradation, the simplest model assumes that all the bonds of the macromolecular chain are equally susceptible to rupture, and that rate of rupture is proportional to the number of bonds remaining. The degradation process is non-specific and can be describe as "random scission degradation" (Tanford 1961).

In random scission degradation the rate at which bonds are broken is proportional to the total number of intact bonds:

$$p = p_0 e^{-kt} \qquad \textbf{(1-5)}$$

where p_0 is the initial number of bonds and p is the number of bonds at time t.

The degradation of a polymer can often be measured experimentally by change in molecular weight as a function of time, using light scattering or viscosity as a measure of molecular weight. These techniques can only be applied if the molecular weight remains large throughout the course of the experiment. In this case, p will remain close to unity and so will e^{-kt}. Therefore equation (1-5) can be rewritten as:

$$p = p_0(1 - kt) \qquad \textbf{(1-6)}$$

and the change in the degree of polymerisation will be a linear function of time:

$$1/\bar{x}_n = 1/(x_n)_0 + kt \qquad \textbf{(1-7)}$$

This method of determining the rate of degradation can be applied to polysaccharides as has been demonstrated using cellulose. The degradation of cellulose was studied using hydrolysis by phosphoric acid and the rate constant increased with increasing concentration of phosphoric acid (Tanford 1961).

1.2.2.1 Acid Hydrolysis

The rate of acid hydrolysis of the glycosidic linkages in model compounds such as methyl-2-acetamido-2-deoxy-β-D-glucopyranose and methyl-2-amino-2-deoxy-β-D-glucopyranose has been determined, and it was shown that the *N*-acetylated methyl-glucosaminide was hydrolysed much faster than the corresponding de-*N*-acetylated sugar (Vårum *et al.* 2001).

Vårum *et al.* (2001) also measured the degradation rate constants for chitosan as a function of acid concentration. It was found that the degradation rate increased in direct proportion to the acid concentration (0.01M < [HCl] < 0.8M), which indicated that acid hydrolysis was the mechanism by which chitosan was degraded. Degradation was also measured as a function of degree of acetylation. Degradation increased with increasing degree of acetylation. Degradation of a less acetylated chitosan is believed to be slower due the protonation of the amine group in acidic conditions. The protonated amine group shields the glycosidic oxygen from protonation, which is the first step in the acid hydrolysis reaction (Roberts 1992).

Acid hydrolysis causes depolymerisation by hydrolysis of the O-glycosidic linkage, however, at the same time deacetylation occurs by hydrolysis of the *N*-acetyl linkage. In dilute acid (0.1M HCl), the rate of deacetylation and depolymerisation have been shown to be similar (Vårum *et al.* 2001), whereas

in concentrated acid (12.08M HCl) the rate of hydrolysis was more than ten times higher than the rate of deacetylation. There was also a high specificity observed for the hydrolysis reaction in concentrated acid, such that the linkages between two acetylated units (**A-A**) and between an acetylated and a deacetylated unit (**A-D**) were cleaved with about equal rate and three orders of magnitude faster than the other two linkages (**D-A** and **D-D**). These studies were undertaken at high temperatures (60-80°C) which would not be encountered under normal storage conditions for a pharmaceutical formulation. The effects of acidic conditions under normal storage conditions are investigated in Chapter 4.

Figure 1-4: Schematic illustration of mechanism for acid hydrolysis of glycosidic linkage in chitosan (from Vårum *et al.* 2001)

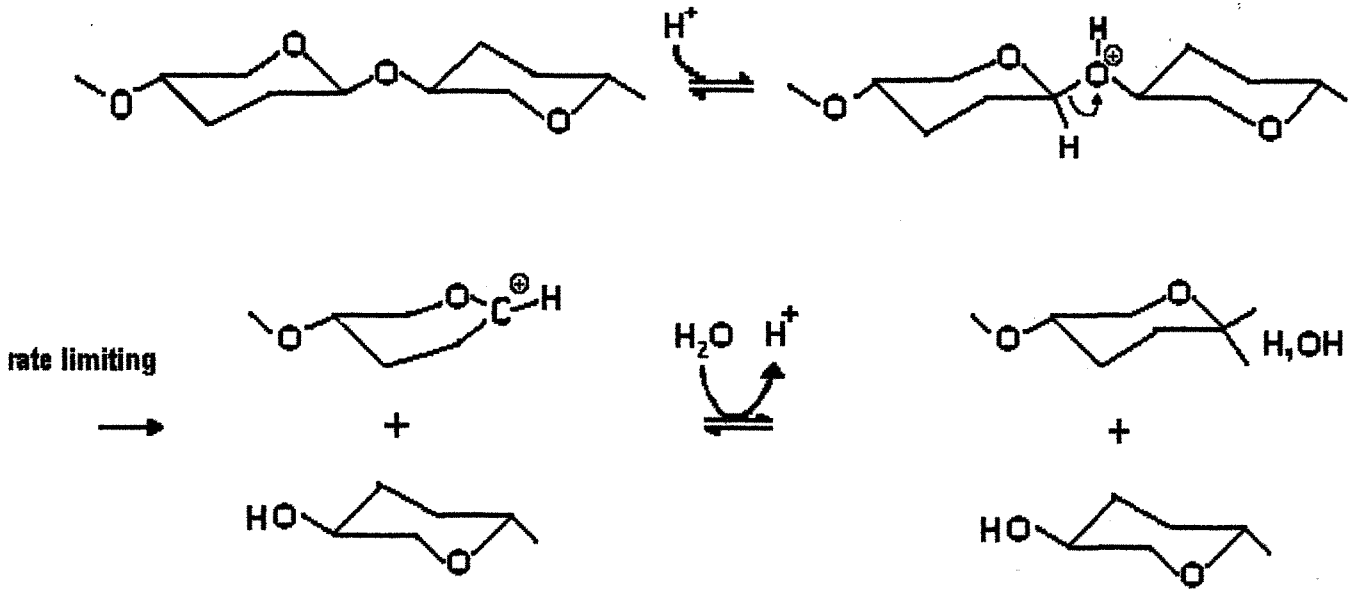

1.2.2.2 Oxidative Reductive Degradation (ORD)

Chitosan can also be degraded in the presence of molecular oxygen. ORD involves a series of free radical reactions that ultimately lead to chain scission. Reducing compounds are oxidised yielding peroxide. The decomposition of peroxide is catalysed by transition metals and leads to the formation of free radicals. The free radicals will be involved in a series of chain reactions, some of which result in the attack on the polymer chain. The "Polymer radical" is unstable, and further reactions of unknown mechanisms result in cleavage of glycosidic bonds (Pettersen *et al.* 1997).

Free radical degradation of chitosan using hydrogen peroxide has been extensively studied (Chang *et al.* 1999; Qin *et al.* 2002). When peroxide is dissolved in water it can dissociate into hydrogen ions and perhydroxyl ions (equation 1-8). The perhydroxyl anion further reacts with H_2O_2 to form the highly reactive hydroxyl radical (HO·) (equation 1-10).

$$H_2O_2 \rightarrow H^+ + HOO^- \qquad \textbf{(1 - 8)}$$

$$H_2O_2 + HOO^- \rightarrow HO\cdot + O_2 + H_2O \qquad \textbf{(1 - 9)}$$

Like other natural polysaccharides, chitosan also contains measurable traces of metal ions, e.g. iron and copper. These metal ions can catalyse the decomposition of H_2O_2, and Fenton type reactions would be feasible. These reactions may also occur in a pharmaceutical formulation since the trace metal ions will be present.

$$Fe^{2+} + H_2O_2 \rightarrow Fe^{3+} + OH^- + OH\cdot \qquad \textbf{(1 - 10)}$$

The hydroxyl radical reacts with carbohydrates exceedingly rapidly abstracting a C-bonded H atom (hydrogen abstraction) according to the general equation (1-11):

$$RH + HO\cdot \rightarrow R\cdot + H_2O \qquad \textbf{(1 - 11)}$$

Chang *et al.* studied the effect of adding different free radical scavengers and metal chelators to the degradation of chitosan by hydrogen peroxide. It was found that EDTA slightly decreased the chitosan degradation as measured by a decrease in the extent of viscosity reduction, which indicated that when some of the metal ions were chelated, the reaction rate decreased. However, the reaction was not completely blocked suggesting that the EDTA-metal ion complex could still participate in chitosan degradation. Some metal ions may also form complexes with chitosan and these were not inhibited by EDTA. Tanioka *et al.* (1996) also studied the effect of EDTA on depolymerisation using copper ions. It was found that EDTA only inhibited depolymerisation when added before initiation of the reaction. Cu(II) coordinates to three –NH2 and one –OH groups to form intramolecular twisted chelate. EDTA showed no protection when added during the reaction possibility due to its low ability to withdraw Cu(II) from the chitosan-Cu(II) complex. It was also found that chitin was not depolymerised by the Cu(II)-ascorbate system, suggesting that the free amino group of glucosamine is important in the depolymerisation of chitosan (Tanioka *et al.* 1996).

Interestingly, when chitosan was degraded by H_2O_2 in HCl solution, the rate of degradation was not proportional to the concentration of HCl as described in section 1.2.2.1. In 0.23% HCl (pH 5.5), chitosan degraded more rapidly and its molecular weight dropped to 2.64×10^3 in two hours, whereas, in 9% HCl, the molecular weight only declined to 21.2×10^4 (Qin *et al.* 2002). At too low a concentration of HCl, chitosan was not dissolved completely, and the strong acidity of 9% HCl inhibited the degradation. This may be due to the protonation of the amino group as suggested by Roberts (1992), and in that study the reduction in molecular weight was due to oxidative cleavage of the chitosan chain.

1.2.2.3 Ultrasonic degradation and radiation

Chitosans can also be degraded by ultrasonic treatment and radiation. The principle behind these physical means of degradation is that the added energy needed to break chemical bonds is provided by the energy source. Chen *et al.* (1997) studied the effect of ultrasonic treatment on the degradation of chitosan under various conditions. It was found that chitosan was degraded faster in dilute solutions, possibly due the increased available energy per unit length of molecule. Raising the reaction temperature resulted in a lower degradation rate, suggesting that elevating the solution temperature is detrimental to the degradation process by ultrasonics. Degradation increased with prolonged ultrasonic time, and chitosan was degraded during storage in an acidic solution at ambient temperatures. Boryniec *et al.* (1997) studied the effect of γ-radiation from a ^{60}Co source on chitosan degradation. The results suggested that the degradation was random and independent of the macromolecular structure and chemical composition of the polymer chains.

1.2.2.4 Enzymatic Degradation

Chitosan can be enzymatically degraded by, for example, chitinases, chitosanases, and lysozymes (Shigemasa *et al.* 1994). Chitosanase type enzyme can catalyse the cleavage of the D-Glucosamine reducing end, while chitinase type enzymes can catalyse the cleavage of the N-acetyl-D-glucosamine reducing ends. The DA of chitosan plays an important role in the activity of these enzymes (Shin-ya *et al.* 2001). Chitinase showed increased activity with increasing DA, while chitosanase showed decreased activity with increasing DA. Degradation using pectinase increased with increasing DA (Shin-ya *et al.* 2001).

The hydrolysis of chitosan by lysozyme is reported to be the most important depolymerisation mechanism in human serum (Vårum *et al.* 1997). The degradation rate in human serum increased as the degree of acetylation increased. The same increase was also observed with hen egg white and human lysozyme (Vårum *et al.* 1997). This will be important for oral delivery formulations since there is a large amount of proteolytic enzymes present in the stomach and in the small intestine.

The specificity of chitosan degradation using lysozyme was studied by Vårum *et al.* (1996). Using NMR spectroscopy the identity of the new reducing ends could be determined. In the study these were found to be exclusively *N*-acetyl-D-glucosamine subunits. This shows that the active cleft of lysozyme has a much higher affinity for *N*-acetyl-D-glucosamine units than for D-glucosamine units.

1.3 Aims and Objectives

The objectives of this thesis were as follows:

- to characterise the hydrodynamic behaviour of a range of chitosans (varying in molecular weight and degree of acetylation). Of particular interest was the use of a combination of hydrodynamic techniques, namely analytical ultracentrifugation, SEC-MALLS and viscometry, to determine the influence of DA on chain conformation. The validity of molecular weight measurements using SEC-MALLS was investigated and results compared to those obtained using sedimentation equilibrium experiment on the AUC.
- to obtain information on the degradation mechanisms and rate of degradation of chitosan under various storage conditions. The degradation was monitored using viscosity and molecular weight measurements (SEC-MALLS and AUC) to obtain quantitative measures of degradation rates.
- to prepare chitosan nanoparticles using the counterion tripolyphosphate pentasodium (TPP) which could be used to deliver insulin or other therapeutics proteins/peptides across the nasal mucosa. The encapsulation efficiency and loading capacity of nanoparticles prepared using different ratios of TPP and chitosan was studied and the effect of complexation on the degradation rate of chitosan was also investigated.

Chapter 2: Materials and Methods

2.1 Materials

2.1.1 Solvents

The main solvent used in this work was a 0.2M acetate buffer (pH 4.3). This was prepared by dissolving 12.01g/l acetic acid and 7.994g/l NaCl in pure water and adjusting to pH 4.29 with monovalent strong base or acid as needed. Acetate buffers of different ionic strengths and pH were prepared by altering the quantities of acid and NaCl accordingly and adjusted to the desired pH using monovalent strong acid or base.

2.1.2 Chitosan

Chitosan samples were kindly supplied by Pronova Ltd., Drammen, Norway. These highly purified samples were used as supplied, and the physicochemical details for each sample can be found in Table 3.1, Chapter 3.

2.1.3 Insulin

Human zinc insulin (26.3 IU/mg) was obtained from Eli Lilly (Indianapolis, USA).

2.1.4 Other Materials

All other materials were of analytical grade and supplied by Sigma, UK.

2.2 Methods

2.2.1 Analytical Ultracentrifugation

The Analytical Ultracentrifuge (AUC) was invented by Thé Svedberg in 1923 (Schachman 1992) and can be used to determine the molecular weight, and assess the size, shape and homogeneity/heterogeneity of macromolecular samples e.g. proteins and polysaccharides. Although the basic principles of sedimentation velocity and sedimentation equilibrium were established over

50 years ago, the modern delivery (instrumentation, data capture and analysis software) makes it a very attractive tool for macromolecular characterisation in solution.

2.2.1.1 Optical Systems

Three different optical systems can be used to collect data from the AUC (Lloyd 1974):

1. Absorption Optics
2. Interference Optics
3. Schlieren Optics

Absorption optics depends on the macromolecule of interest containing a chromophore. Chitosan does not possess a chromophore in the useable part of the UV spectrum unless chemically modified and hence this optical system has not been used in this project and will not be discussed here. Both Interference optics and Schlieren optics depend on the refractive index of the sample.

2.2.1.1.1 Interference Optics

An interference pattern is produced by splitting a beam of coherent light and passing it through paired sectors of a cell in a spinning rotor (Lloyd 1974). The speed of light will be altered as it passes through these sectors, to an extent dependent upon the refractive index. When the beams are merged after passage through the sectors, the waves combine to form an interference pattern. If both sectors are identical in length and contain identical solutions, a pattern of straight (i.e. undeviated) interferences fringes will be produced when the beams are recombined. However, if one sector contains a reference solvent and the other contains the same solvent but containing also the dissolved sample of interest, the greater concentration in the sample sector will

alter the light vector as it passes through that solution more than will be the case in the reference sector. When these beams are recombined, the fringe pattern will be shifted to an extent that corresponds to the concentration difference between the sectors. The fringe shift is related to the concentration by the classical relationship:

$$J = a(\Delta n)/\lambda \qquad (2-1)$$

where J is the fringe shift, equivalent to the differential number of wavelengths between the solvent and the solution, a is the length of the light path through the sample or solvents compartments, λ is the wavelength of the light, and Δn is the refractive index difference between the solvent and solution. Since the refractive index is generally proportional to concentration, the fringe shift can be used to follow the redistribution of sample as a function of radius in the sample sector (Furst 1997).

2.2.1.1.2 Schlieren Optics on the Model E ultracentrifuge

Schlieren optics, like interference optics, is based on the refractive index of the solution (Clewlow *et al.* 1997). Light passing through a region in the cell where concentration (and hence refractive index) is changing will be deviated radially, as light passing through a prism is deviated towards the direction normal to the surface. The schlieren optical system converts the radial deviation of light into a vertical displacement of an image at the camera. This displacement is proportional to the concentration gradient. Light passing through either pure solvent or a uniform concentration will not be deviated radially, and the image will not be vertically displaced in those regions. The

schlieren image is thus a measure of the concentration gradient, *dc/dr*, as a function of radial distance, *r*.

2.2.1.2 Sedimentation Velocity

In sedimentation velocity, a sample is spun at high speed (usually 40-60 K rpm) in the analytical ultracentrifuge until the macromolecule has sedimented to the base of the cell. Here follows a summary of the technique (Ralston 1993).

Figure 2-1: Forces acting on a solute particle in a gravitational field (from Ralston 1993)

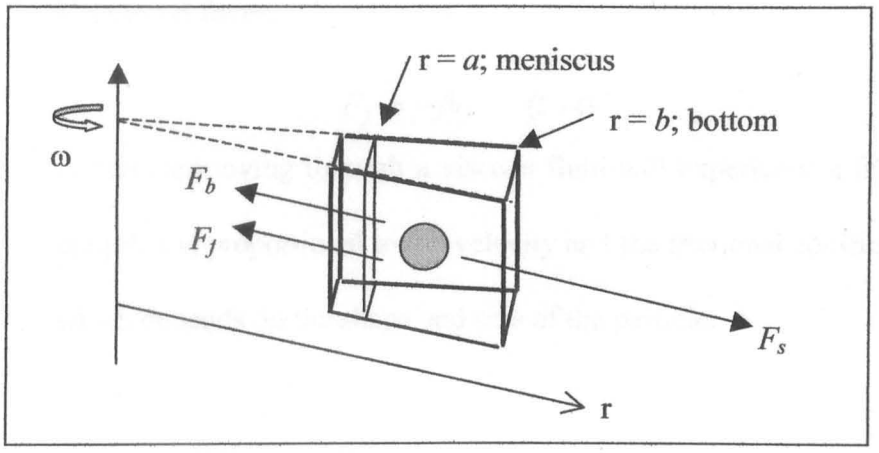

When a solute particle suspended in a solvent is placed in a gravitational field, it is subject to three forces acting on it (Figure 2-1). These are:

1. **Sedimenting or gravitational force.**

$$F_s = m\omega^2 r = \frac{M}{N_A}\omega^2 r \qquad (2-2)$$

In a spinning rotor, the acceleration of a particle is determined by the product of its distance from the axis of rotation, *r*, and, the square of the angular velocity, ω (in radians per second). The gravitational force is the product of the mass, *m*, of a single particle and the accelaration.

M is the molar mass ("molecular weight") of the solute in g/mol and N_A is Avogadro's number.

2. **Buoyant force.**

$$F_b = -m_0\omega^2 r = -m\bar{v}\rho\omega^2 r \qquad (2-3)$$

The buoyant force is related to the weight of fluid displaced, where m_0 is the mass of fluid displaced by the particle, $\bar{v}$ the partial specific volume and ρ the solution density.

3. **Frictional force.**

$$F_f = -fu \qquad (2-4)$$

A particle moving through a viscous fluid will experience a frictional drag that is proportional to the velocity and the frictional coefficient, f, which depends on the shape and size of the particle.

When a high centrifugal force is applied, the solute particles initially accelerate, but quickly reach a terminal velocity, u. At this point the three forces come into balance:

$$F_s + F_b + F_f = 0 \qquad (2-5)$$

$$\frac{M}{N_A}(1-\bar{v}\rho)\omega^2 r - fu = 0 \qquad (2-6)$$

The particles rapidly deplete from the region nearest the centre of the rotor (the meniscus region at the air/solution interface), forming a boundary which moves toward the outside of the rotor with time until finally all the macromolecules form a pellet at the base of the cell (Figure 2-2).

Figure 2-2: Position of solvent and sample menisci in a double sector centrepiece and boundary formed by sedimenting particles (from Ralston 1993)).

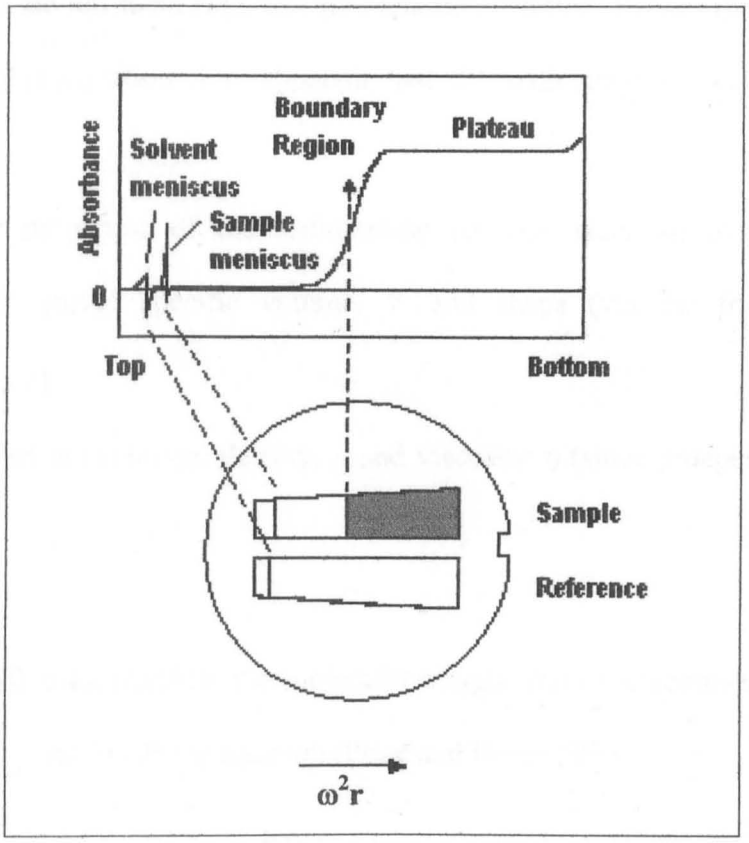

The sedimentation coefficient, s, is essentially based on the measurement of the velocity of movement, u, of this boundary and is defined by:

$$s = \frac{M(1-\bar{v}\rho)}{N_A f} = \frac{u}{\omega^2 r} \qquad (2-7)$$

Equation (2-7) expresses the sedimentation coefficient in terms of molecular parameters on the left hand side, and measurable quantities on the right hand side. From this equation it is apparent that the sedimentation coefficient depends on:

- Molecular properties of the sedimenting particle, such as: molecular weight, M, partial specific volume, $\bar{v}$ and shape (via the frictional coefficient, f).
- Properties of the solution: density, ρ and viscosity η (since f depends on this).

It is also possible to calculate the molecular weight from the sedimentation coefficient using the Svedberg equation (Price and Dwek 1979):

$$M = \frac{RTs}{D(1-\bar{v}\rho)} \qquad (2-8)$$

where R is the gas constant, T the absolute temperature, and D is the translational diffusion coefficient which can be determined from the rate of spreading of the sedimenting boundary. However, sedimentation velocity is ineffective for polydisperse samples such as chitosan, since boundary spreading measurements are masked by polydispersity. For these systems dynamic light scattering is probably the method of choice (Ralston 1993).

2.2.1.2.1 Analysis of data using DCDT+ software

At set time intervals during a sedimentation velocity experiment, scans are taken of the solute concentration across the centrifuge cell. Using the DCDT+ software (Philo 2000), a series of approximately ten consecutive scans are selected after the sedimenting boundary has travelled approximately 2/3 across the cell length. The sedimentation coefficient distribution function, $\hat{g}(s^*)$, can then be derived. This represents the change in concentration distribution across the cell with time, when different components will have undergone radial dilution to a different extent. This is normally corrected to $g(s^*)$, the apparent distribution when the sample was loaded. It is possible to fit individual peaks in the $g(s^*)$ distribution to Gaussian functions and determine both the sedimentation coefficient (from the centre position) for individual species and for monodisperse systems the diffusion coefficient (from the width of the Gaussian peak).

The sedimentation coefficient is converted to standard conditions (solvent – water; temperature - 20°C) to account for differences in density and viscosity of the solvent using the equation:

$$s_{20,w} = s_{obs}\left(\frac{\eta_{T,w}}{\eta_{20,w}}\right)\left(\frac{\eta_s}{\eta_w}\right)\left(\frac{1-\bar{v}\rho_{20,w}}{1-\bar{v}\rho_{T,s}}\right) \quad \textbf{(2 - 9)}$$

where $s_{20,w}$ is the sedimentation coefficient in terms of the standard solvent water at 20°C; s_{obs} is the measured sedimentation coefficient in the experimental solvent at temperature T; $\eta_{T,w}$ and $\eta_{20,w}$ are the viscosities of water at the temperature of the experiment and at 20°respectively; η_s and η_w are the viscosities of the solvent and water at a common temperature; $\rho_{20,w}$ is the density of water at 20°C and $\rho_{T,s}$ the density of the solvent at the temperature of the solvent.

2.2.1.2.2 Dependence of Sedimentation Coefficient on Concentration

Sedimentation coefficients measured at a finite concentration will be apparent ones because of the effects of non-ideality. Apparent sedimentation coefficients are therefore concentration dependent (Wales and Holde 1954), the measured apparent sedimentation coefficient decreases with increasing concentration. By measuring the apparent sedimentation coefficient at a series of concentration and extrapolated to zero concentration, the infinite dilution sedimentation coefficient ($s^0_{20,w}$) can be determined using the equation:

$$s_{20,w} = (1/s^0_{20,w}).(1 + k_s c) \qquad \textbf{(2 - 10)}$$

The concentration dependence arises from the increased viscosity of the solution at higher concentrations, and from the fact that sedimenting solute particles must displace solvent backwards as they sediment. Both effects become extremely small as concentration is decreased.

The concentration-dependence coefficient, k_s, is a useful property for indicating molecular shape. It has been shown that the relationship "$k_s/[\eta]$" ~ 1.6 for spherical particles and random coils, and tends towards ~0.2 for rod-like particles (independent of particle size) (Harding 1995).

2.2.1.3 Sedimentation Equilibrium

In sedimentation equilibrium the sample is spun in an analytical ultracentrifuge at a low speed, which causes the macromolecule to move towards the outside of the rotor. As the macromolecule sediments towards the base of the cell, diffusion acts to oppose the sedimentation process. After a period of time, usually 2-3 days, a balance is reached between the sedimentation and diffusion processes, and a concentration distribution is

formed that increases exponentially towards the cell base. This distribution depends only on molecular mass of the macromolecule and is entirely independent of the shape of the molecule. By measurement of concentration at different points in this distribution, the molecular weight can be determined. For a single, ideal, non-associating solute, the molecular weight can be calculated from the following equation:

$$M_w = \frac{2RT}{(1-\bar{v}\rho)\omega^2}\frac{d\ln c}{dr^2} \qquad \textbf{(2- 11)}$$

However, due to non-ideality, an apparent weight-average molecular weight is obtained from sedimentation equilibrium that will tend to be lower than the true molecular weight. By extrapolation of the reciprocal of the apparent weight average molecular weight to zero concentration the true molecular weight can be obtained:

$$1/M_{w,app} = (1/M_w)(1+2BM_w c) \qquad \textbf{(2 - 12)}$$

where B is the thermodynamic or "osmotic pressure" second virial coefficient.

2.2.1.3.1 MSTAR

The data set (concentration of solute vs. radius/distance from meniscus) obtained from sedimentation equilibrium experiment can be analysed using MSTAR program (Cölfen and Harding 1997) to obtain a value for $M_{w,app}$.

Using the MSTAR program, an operational point average (i.e. a function of radial distance at a point in the ultracentrifuge cell from the axis of rotation) molecular weight (M*) is calculated. This is defined by (Creeth and Harding 1982):

$$M^*(r) - \frac{c(r) - c_a}{kc_a(r^2 - r_a^2) + 2k\int_{r_a}^{r} r[c(r) - c_a]dr} \quad \textbf{(2 - 13)}$$

where $k = \frac{(1-\bar{v}\rho)\omega^2}{2RT}$, c is the polymer concentration at r (radial distance from centre of rotation) or a, the meniscus. $M_{w,app}$ is calculated by extrapolation of M* to the base of the cell.

2.2.1.3.2 Lamm Equation

Data obtained using the Schlieren optical system on the model E differs from that obtained on the XLI AUC. The data obtained here is in the form of concentration difference vs. distance from centre of rotation and can be analysed by fitting to the Lamm equation (Clewlow *et al.* 1997) to obtain M_z.

$$d\ln\left(\frac{1}{r}\frac{dn}{dr}\right) / d(r^2) = M_{z,app}(1-\bar{v}\rho)\omega^2 / 2RT \quad \textbf{(2 - 14)}$$

where n is the refractive index, r the radial position from the centre of the rotor, ρ is the density of solvent, $M_{z,app}$ the z-average apparent molecular weight, ω the angular velocity of the rotor, R the gas constant and T the absolute temperature. A graph of $\ln\left(\frac{1}{r}\frac{dn}{dr}\right)$ versus r^2 has a slope proportional to the z-average molecular weight ($M_{z,app}$).

The data set can be transformed by integrating with respect to r, distance from meniscus, and analysed using MSTAR program to obtain $M_{w,app}$ (Cölfen and Harding 1997).

2.2.2 Viscometry

The viscosity of a solution is a measure of its resistance to flow. By adding a substance to a solvent, its viscosity will increase since the frictional forces

associated with the system increase. Herein follows a summary of the technique (Harding 1997).

The effect of this added macromolecule on the viscosity of the solvent can be described by the relative viscosity, η_{rel} or the reduced viscosity, η_{red}:

$$\eta_{rel} = \eta / \eta_0 \qquad (2\text{-}15)$$

$$\eta_{red} = \eta_{sp} / c = (\eta_{rel} - 1) / c \qquad (2\text{-}16)$$

where η is the viscosity of the solution, η_0 is the viscosity of the solvent, η_{sp} is the specific viscosity and c is the concentration. Due to non-ideality, the reduced viscosity of a solution shows concentration dependence, increasing with increasing concentration. The intrinsic viscosity, [η], of a macromolecule is defined as the limit as concentration tends to zero. Two forms of extrapolation can be used to calculate the intrinsic viscosity.

The *Huggins* equation:

$$\eta_{red} = [\eta](1 + K_H[\eta]c) \qquad (2\text{-}17)$$

or the *Kraemer* equation:

$$(\ln \eta_{rel})/c = [\eta](1 - K_K[\eta]c) \qquad (2\text{-}18)$$

Figure 2-3: Huggins and Kraemer plot for intrinsic viscosity. The common intercept gives $[\eta]$, the slope are $K_H[\eta]^2$ and $K_K[\eta]^2$. K_H is the Huggins constant and K_K the Kraemer constant. (Modified from Jumel 1994)

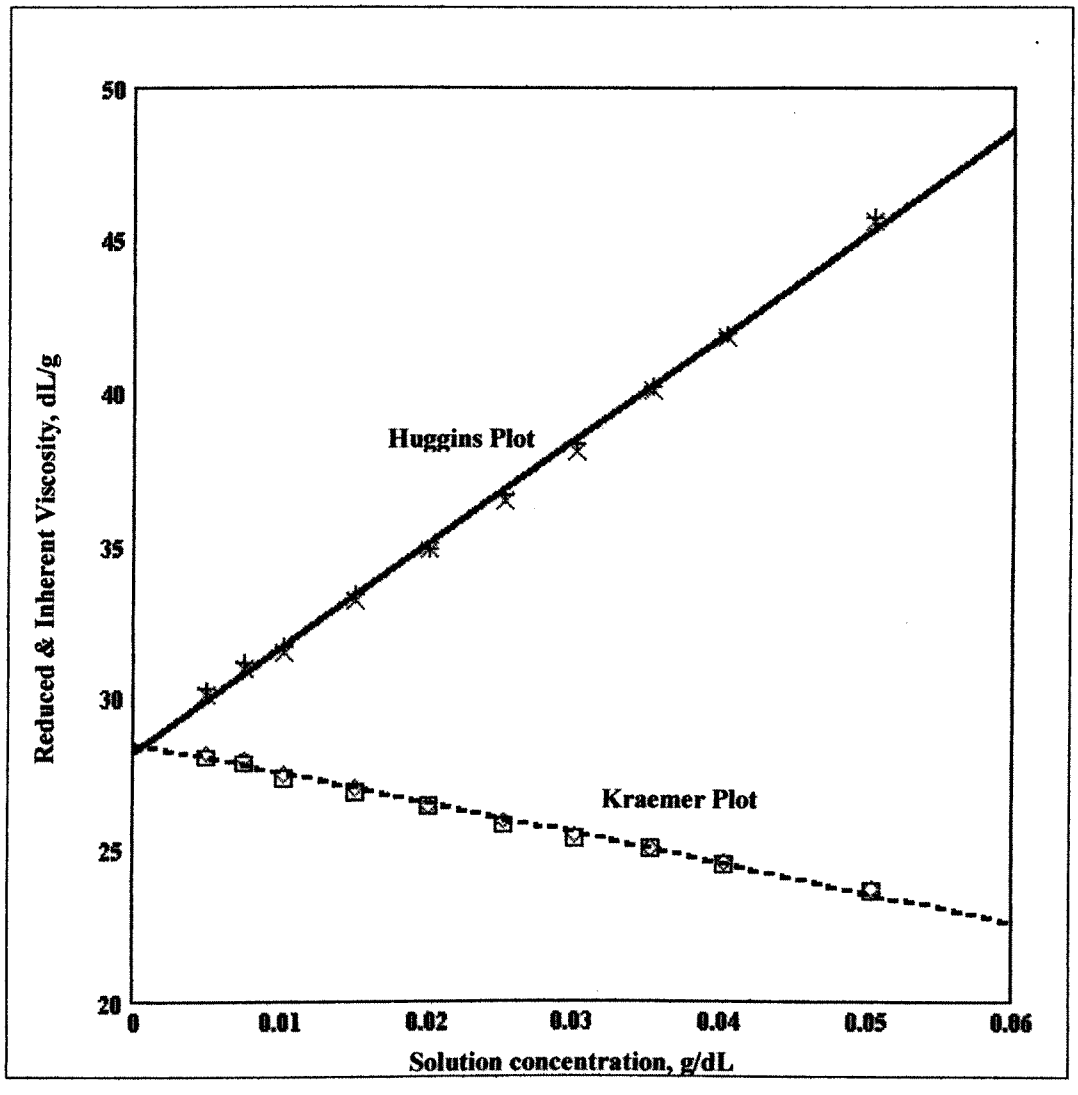

2.2.2.1 Capillary Viscometer

Viscosity measurements are performed by measuring the time for a solution (volume, V – usually 2ml) of a macromolecule dissolved in a solvent of viscosity η_0 to flow through a narrow capillary tube of radius r and length L under hydrostatic pressure.

The viscosity of the sample solution, η, given by:

$$\eta = \frac{\pi h g \rho r^4 t}{8LV} \qquad (2-19)$$

where h is the average liquid height; g the gravitational acceleration; and ρ the density of solution.

Since the flow times of the solvent (η_0) and of various concentrations of the macromolecule (η) are carried out under identical experimental conditions, the relative viscosity can be calculated from:

$$\eta_r = \frac{\eta}{\eta_0} = \frac{t\rho}{t_0\rho_0} \qquad (2-20)$$

where t and t_0 are the flow times of the solution and solvent respectively; and ρ and ρ_0, the density of the solution and solvent respectively.

Since the concentrations used for polysaccharides are usually sufficiently small (<5mg/ml) to neglect density corrections, it is reasonable to assume that kinematic viscosity parameters (no density correction) are approximately equal to dynamic viscosity parameters (corrected for density differences). (Tanford 1955) The intrinsic viscosity can then be calculated by extrapolation using the Huggins or Kraemer plot.

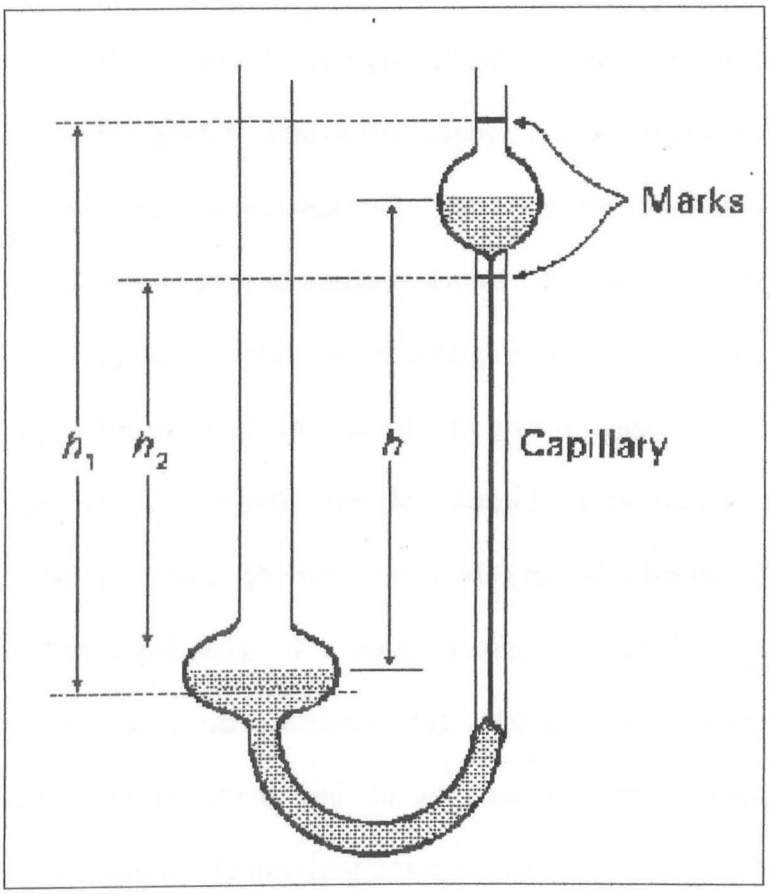

Figure 2-4: Ostwald capillary viscometer (Van Holde 1971)

2.2.2.2 Determination of Intrinsic Viscosity

The intrinsic viscosity of each chitosan sample was determined using the Ostwald capillary viscometer which was suspended in a temperature controlled water bath at 20.0°C. A 5 mg/ml chitosan solution was prepared in 0.2M acetate buffer, pH 4.3. 2 ml of this solution is transferred to the Ostwald capillary viscometer and suspended in the water bath for 10 minutes to ensure the sample is at 20.0°C prior to measurement of flow time. The flow time of the sample is recorded ten times and an average taken. The original sample is diluted using 0.2M acetate buffer, pH 4.3 to give a range of concentrations between 1 mg/ml and 5 mg/ml. The flow times for these diluted samples is recorded in the same way. The flow time is also recorded for the solvent (0.2 M acetate buffer, pH 4.3). For each sample concentration the reduced viscosity is calculated using equation (2-16). The reduced viscosities are then plotted against concentrations and the intrinsic viscosity is calculated by extrapolation to infinite dilution (Huggins method).

2.2.2.3 Determination of chitosan degradation using viscosity measurements

The viscosity of a macromolecule is related to its molecular weight using the Mark-Houwink-Kuhn-Sakarada equation – $[\eta] = K'M^a$ (Harding 1997). At solution concentration of 1 mg/ml the reduced viscosity of a chitosan solution is approximately equal to its intrinsic viscosity. Therefore changes in the reduced viscosity of a chitosan solution can be used as an indication of degradation that has occurred over a period of time.

The reduced viscosity of a chitosan solution is measured at the beginning of a storage trial. At two week intervals, a 2 ml aliquot of the sample is taken and the reduced viscosity measured. The change in reduced viscosity is used to

assess the degradation of chitosan under different storage conditions as examined in Chapters 4 and 5.

2.2.2.4 Concentration dependence of viscosity

As the concentration of a solution increases the relationship between viscosity and concentration is directly proportional. However, above a certain concentration a sharp increase in viscosity is observed. The cocnetration at which this occurs is known as the "Critical Overlap Concentration – C*". This can be clearly seen using a double logarithmic plot of η_{sp} against concentration (Morris *et al.* 1981). The increase in the gradient of the plot is due to the change from dilute solution conditions, where individual polymer molecules exist as isolated coils, to concentrated solutions where significant coil overlaps begins to occur. The concentration at which C* occurs is generally between 0.4 – 0.8 mg/ml for polysaccharides (Harding 1997).

2.2.3 Size Exclusion Chromatography coupled with Multi-Angle Laser Light Scattering (SEC-MALLS)

2.2.3.1 Size-Exclusion Chromatography

Chitosan is a polydisperse polymer, that comprises of a normally broad range of molecular weights. Chromatography can be used to separate the solution into different molecular weight fractions. Size-exclusion chromatography, as the name suggests, separates the chitosan sample into fractions of different sizes or molecular weight. The chitosan solution passes through a series of columns which are packed with beads of varying size. High molecular weight fractions are excluded from passing through the pores created between the packing material and pass through the columns faster than lower molecular weight fractions which are able to migrate into the packing material increasing their elution time. The results is that high molecular weight fractions elute

first and that a molecular weight distribution can then be obtained using the light scattering cell which is connected in series.

2.2.3.2 Multi-Angle Laser Light Scattering

The measurement of molecular weight by light scattering makes use of the intensity of the light scattered at some angle θ as a function of the intensity impinging on the scattered volume, V (Wyatt 1993).

In solution, light scattering data can be interpreted according to the fluctuation theory of light scattering which states that light is scattered as a result of changes of polarizability of the solution due to random fluctuations in the solute concentration in small volume elements. Based on this, the relationship between the Rayleigh excess factor and the physical characteristics of the scattering molecule has been calculated by Debye, Zimm and others as (Wyatt 1993):

$$Kc/R_\theta = 1/M_w P(\theta) + 2A_2 c + 3A_3 c^2 + \ldots\ldots \quad \textbf{(2 - 21)}$$

where:

K = the "polymer constant" = $(2\pi n^2/\lambda^4 N_A)(dn/dc)^2(1+\cos^2\theta)$

c = the concentration of solution

n = the refractive index of solution

λ = the wavelength *in vacuo*

N_A = Avogadro's number

dn/dc = the specific refractive index

A_2, A_3 = virial coefficients (A_2 is the same as B in equation (2-12))

R_θ = the Rayleigh excess factor = R_θ(solution) - R_θ(solvent)

$P(\theta)$ = the form factor which depends on shape and size of the scattering molecules

At limiting conditions where θ approaches zero angle, $P(\theta)$ approaches unity irrespective of size or shape of the scattering species. At low angles and concentrations, equation 1 can therefore be rewritten as:

$$Kc / R_\theta = 1 / M_w + 2A_2 c \qquad (2-22)$$

If A_2 is known, M_w can be determined from a single measurement of R_θ, which enables the continuous monitoring of SEC eluents. So, from the SEC trace shown, the molecular weight for uniform intervals on the elution curve is calculated from:

$$Kc_i / R_{\theta,i} = 1 / M_{w,i} + 2A_2 c_i \qquad (2-23)$$

The concentration c_i is most usually calculated from

$$c_i = (mx_i) / V_i x_i \qquad (2-24)$$

For each elution slice (i) in SEC the concentration (c_i) is obtained from a concentration sensitive detector, and R_0 is obtained from the MALLS (after extrapolation to zero angle). $M_{w,i}$ is then calculated according to equation (2-23). A_2 must be known from independent light scattering measurements, unless the sample concentration is kept so low that $A_2c << 1/M_w$. With SEC-MALLS, this is normally the case, since samples are diluted on the column.

2.2.3.3 Method

Acetate buffer, pH 4.3, was pumped at a flow rate of 0.8 ml/min through a column system consisting of TSK-G5000PW, TSK-G4000PW and TSK-G3000PW analytical columns protected by a guard column. Solutions of each chitosan sample were prepared as described in relevant study and 100 µl was injected onto the columns at ambient temperature (sample filtered through 0.45 µm filter to remove any insoluble material or dust prior to injection). The eluting fractions were monitored using a Dawn DSP, multi-angle light-

scattering photometer (Wyatt Technology, Santa Barbara, USA) fitted with a 5 mW He-Ne Laser and a differential interoferometric refractometer (Optilab 903, Wyatt Technology, Santa Barbara, USA). Apparent weight average molecular weights were obtained using the Debye plot method on the associated ASTRA software.

2.2.4 Preparation of Nanoparticles

2.2.4.1 Chitosan Nanoparticles

Chitosan nanoparticles were prepared according to the method described in (Dyer *et al.* 2002). A solution of a chitosan was prepared at a concentration of 2 mg/ml in distilled water. To this solution tripolyphosphate pentasodium (TPP) solution was added dropwise at the appropriate ratio whilst continuously stirring. This resulted in an opalescent solution. The solution was then divided into aliquots which were used for either determination of yield, loading capacity, or for use in chitosan stability experiments (see Chapter 6).

2.2.4.2 Chitosan-Insulin Nanoparticles

Insulin loaded chitosan nanoparticles are prepared in the same way as above except insulin is predissolved in the TPP solution at a concentration of 1.25 mg/ml. As with the chitosan nanoparticles the resulting nanoparticle suspension is divided into aliquots for determination of yield, etc. and for use in stability experiments.

2.2.5 Estimation of chitosan concentration

During the manufacture of chitosan nanoparticles it was necessary to determine the amount of chitosan present in the supernatant after

centrifugation to allow for calculation of nanoparticle yield. The chitosan content was calculated by means of the ninhydrin reaction.

Ninhydrin reacts with primary amino groups to produce a coloured product (diketohydrindylidene-diketodhyrindamine, also known as Ruhemann's purple). The method used here is based on that used by Prochazkova *et al.* (1999) and adapted by Leane *et al.* (2004).

2.2.5.1 Method

Lithium acetate buffer (10ml) was prepared by dissolving 4.08g of lithium acetate in approximately 6ml of deionised water. The pH of the solution was adjusted to 5.2 with glacial acetic acid and the volume adjusted to 10ml with deionised water. The ninhydrin was freshly prepared on the day of the assay by adding 4M lithium acetate buffer (10ml) to 0.8g ninhydrin and 0.12g hydrindantin in 30ml DMSO.

0.5ml of reagent was added to 0.5ml of sample in a glass bottle and shaken by hand. This was then heated in boiling water for 30 minutes to allow the reaction to proceed during which time a change in colour to purple is observed. The sample is then cooled and diluted with 15ml 50% ethanol and vortexed for 15 seconds to oxidise excess hydrindantin. The absorbance of each sample was measured at 570nm using a UV spectrophotometer and the concentration of chitosan calculated from a standard calibration curve (prepared on day of assay from the same chitosan used in the test sample).

2.2.6 Estimation of insulin concentration

The insulin concentrations of the various formulations were analyzed using a Gilson HPLC system fitted with a Vydac C18 5 μm pre-column and a Vydac

reverse phase C18 5μm 150 × 4.6 mm column (Hichrom, Reading, United Kingdom) (Dyer *et al.* 2002). Gradient conditions and a flow rate of 1.0 ml/min (ambient temperature) were used. The mobile phase was composed of eluent A, containing 95% ethanolamine (0.6%, pH 3) and 5% acetonitrile and eluent B, containing 40% ethanolamine (0.6%, pH 3) and 60% acetonitrile. The injection volume was 10 μl. The ultraviolet detector was set at 210 nm. The analysis run time was 18 min. Samples were prepared for analysis by dissolving/diluting the formulation in eluent B.

Chapter 3: Hydrodynamic Characterisation of Chitosan Samples

3.1 Introduction

For most applications of chitosan, and especially in the pharmaceutical industry, the molecular weight and degree of acetylation determine the properties and thereby the effectiveness of the chitosan for a particular application. Schipper *et al.* (1996) reported that for chitosan to enhance the absorption of hydrophilic drugs across mucosal surfaces, a low degree of acetylation and/or high molecular weight appeared to be necessary.

In this chapter chitosan samples are characterized under similar aqueous conditions in terms of molecular weight (using sedimentation equilibrium and SEC-MALLS) and their conformation determined using data obtained from sedimentation velocity and intrinsic viscosity measurements.

3.2 Methods

3.2.1 Intrinsic viscosity

Intrinsic viscosities were determined using an Ostwald-type viscometer of 2 ml capacity over a concentration range of 0.2 – 2.0 mg/ml as described in section 2.2.2.2. The flow times were recorded at (20.00 ± 0.01) °C. From the solution: solvent flow time ratio the kinematic relative viscosity was obtained. The intrinsic viscosity ($[\eta]$) was found by extrapolation to infinite dilution of both reduced viscosity using the Huggins equation and inherent viscosity using the Kraemer equation (see section 2.2.2).

3.2.2 Sedimentation Velocity

A Beckman XLI Analytical Ultracentrifuge was used for the determination of sedimentation coefficients at 20°C and a rotor speed of 45,000 rpm. Sedimentation coefficients were obtained by analysis of the change in concentration distribution in the centrifuge cell with time using the "time derivative" algorithm *DCDT+* (Philo 2000) and corrected to standard solvent conditions as described in section 2.2.1.2.1. Measurements were made at several concentrations (from 0.3 to 1.0 mg/ml) and the calculated $s_{20,w}$ values (or reciprocals thereof) were extrapolated to infinite dilution to yield $s^0_{20,w}$.

3.2.3 Sedimentation Equilibrium

Low-speed sedimentation equilibrium was used to determine the molecular weights (weight averages) of the various chitosan samples. Two analytical ultracentrifuges were employed.

Firstly, a Beckman XLI Analytical Ultracentrifuge was used for chitosan solutions in the range of concentrations 0.5 – 1.0 mg/ml, at rotor speeds of 14,000 rpm (chitosan G112) or 8,000 rpm (other chitosans) and a temperature of 20.0°C. The data collected from the Rayleigh interference optical system was analysed using the MSTARI program to give an apparent weight average molecular weight $M_{w,app}$ (see section 2.2.1.3.1).

A low concentration sample (0.3 mg/ml) was also analysed using a Beckman Model E Analytical Ultracentrifuge (at rotor speeds between 10,000 and 20,000 rpm, and at 20.0°C) equipped with Schlieren optics (section 2.2.1.1.2). The data was analysed by fitting to the Lamm equation (section 2.2.1.3.2) to yield the apparent z-average molecular weight ($M_{z,app}$). The data set was then

transformed by integrating with respect to r (distance from the meniscus) and analysed using MSTARI program to obtain $M_{w,app}$.

3.2.4 SEC-MALLS

The molecular weights (weight averages) of the chitosan samples was determined using SEC-MALLS as described in section 2.2.3. The data obtained was analysed using the Debye plot method to give an apparent weight average molecular weight, $M_{w,app}$.

3.3 Materials

Chitosan samples were used as provided by Pronova Ltd., Drammen, Norway. Solutions were prepared in 0.2M acetate buffer, pH 4.3 at appropriate concentrations for each method.

Table 3-1: Commercial manufacturer's data (courtesy of Pronova Ltd.)

Chitosan	G112	G114	G214	G213	G213*	CL210
Degree of Acetylation (%)	30	7	4	17	20	18
Viscosity of 1% solution (mPas)	5	18	59	79	153	126

NB: Chitosans G213 and G213* are different batches of the same chitosan

3.4 Results and Discussion

3.4.1 Viscosity

The intrinsic viscosity for each chitosan sample was calculated using both the Huggins equation and the Kraemer equation. Table 3-2 shows the intrinsic viscosities obtained from each method along with the corresponding constants. An example of the plots obtained for chitosan G214 using the Huggins and Kraemer equations is shown in Figure 3-1. The intercept of these two plots

with the y-axis gives the intrinsic viscosity and should be equivalent irrespective of the method used. The non-intersection seen in Figure 3-1 reflects the noise in the data. From the values in Table 3-2, the intrinsic viscosities obtained are very similar using both methods.

The manufacturer's data from apparent viscosity of the chitosan samples increases across the table – from left to right (Table 3-1). Comparing these with the intrinsic viscosities in Table 3-2, the same trend is apparent. The intrinsic viscosities obtained for chitosan G213 and chitosan CL210 are higher and lower, respectively, than would be expected from the manufacturer's data. This may be due to the different methods that have been used to obtain the two sets of data. The apparent viscosity is measured at a single concentration (10 mg/ml) whereas the intrinsic viscosities are determined using several measurements which are extrapolated to infinite dilution. The result of this extrapolation means that the intrinsic viscosity value obtained is not dependent on the chitosan concentration, only on the solvent used. The differences may also be due to aging of the samples, since the samples used had different manufacturing dates and some degradation may have occurred during storage.

3.4.2 Sedimentation Coefficients

The sedimentation coefficients calculated for each chitosan sample are shown in Table 3-3, with an example plot for chitosan G214 shown in Figure 3-2. As for the viscosity data, the sedimentation coefficients also increase in the same trend as seen in the manufacturer's data. The values obtained (in the range 1.6 – 3.0) are in good agreement with values obtained by other researchers for various chitosans (for example Rinaudo and Domard 1989; Anthonsen *et al.*

1993; Errington *et al.* 1993; Berth *et al.* 1998). As with intrinsic viscosity values, the sedimentation coefficient is dependent on the size of the macromolecule, and an increase in either of these parameter will indicate an increase in the molecular weight of the chitosan. The increasing values of the sedimentation coefficient agree with the molecular weight values that were obtained using sedimentation equilibrium and SEC-MALLS (the molecular weight values are discussed in section 3.4.3.).

As discussed in Section 2.2.1.2.2., sedimentation coefficients are dependent on concentration, the measured apparent sedimentation coefficient decreasing with increasing concentration (Wales and Holde 1954). The concentration dependence is due to the increased viscosity of the solution with increasing concentration resulting in a slower sedimentation of the solute particle and hence a larger sedimentation coefficient. This effect can be seen from Figure 3-2 were $1/s_{20,w}$ increased with increasing concentration. From the plot of $1/s_{20,w}$ vs concentration, the concentration dependence sedimentation coefficient, k_s, can be obtained from the slope of the extrapolated trend line (see equation (2-10)). The values for this coefficient are an indication of the effect that the concentration of the solute has on sedimentation coefficient. From Table 3-3 it can be seen that chitosan CL210 has a very large concentration dependence coefficient, whereas for chitosan G112 it is quite low. The significant variation in the extent of concentration dependence of the sedimentation coefficient, highlight the importance of standardising the sedimentation coefficient by extrapolation to infinite dilution after the sedimentation coefficients at each concentration have been converted to standard conditions (water and temperature 20°C using equation (2-9)).

Without this standardization, comparison of sedimentation coefficient for different chitosan or for the same chitosan by different researchers would be pointless.

Figure 3-1: Huggins and Kraemer plots for Chitosan G214

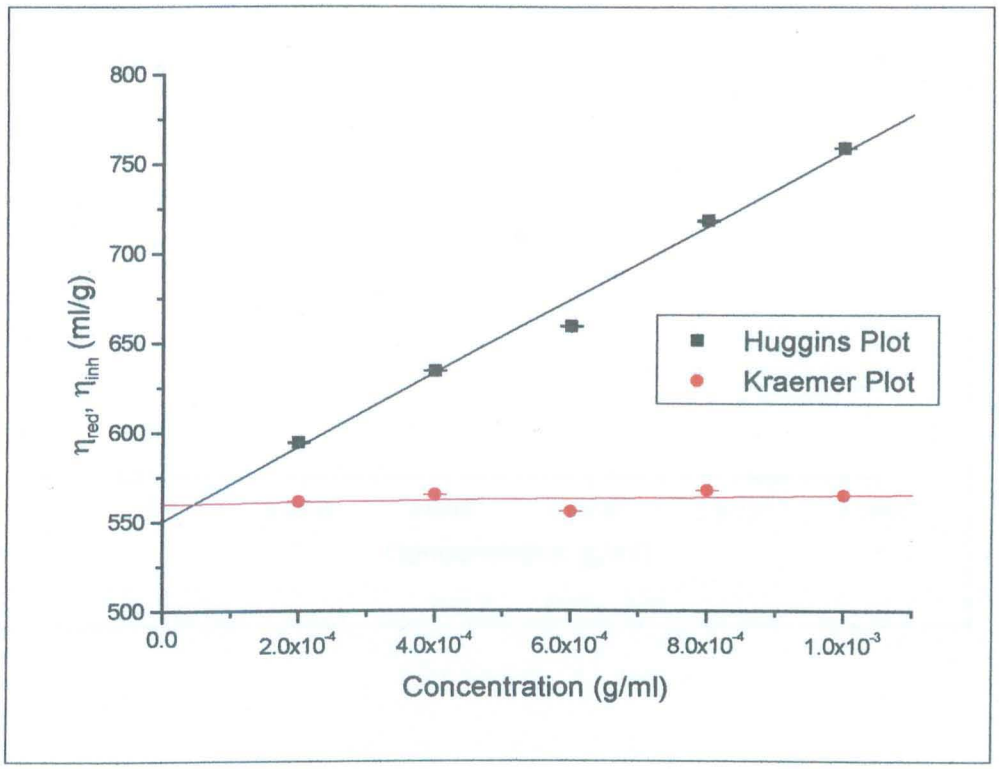

Table 3-2: Viscometric data for chitosan samples

Chitosan Sample	Huggins		Kraemer	
	[η] (ml/g)	K_H	[η] (ml/g)	K_K
G112	95 ± 6	3.18 ± 0.66	98 ± 6	-1.92 ± -0.56
G114	323 ± 10	0.38 ± 0.07	317 ± 7	-0.10 ± -0.04
G214	551 ± 6	0.68 ± 0.03	560 ± 5	0.02 ± 0.03
G213	418 ± 8	1.26 ± 0.09	433 ± 4	0.35 ± 0.06
G213*	611 ± 5	0.55 ± 0.03	615 ± 6	0.04 ± 0.03
CL210	842 ± 66	0.39 ± 0.07	882 ± 18	0.14 ± 0.02

[η] – intrinsic viscosity; K_H – Huggins constant; K_K – Kraemer constant

Figure 3-2: Determination of infinite dilution sedimentation coefficient for Chitosan G214

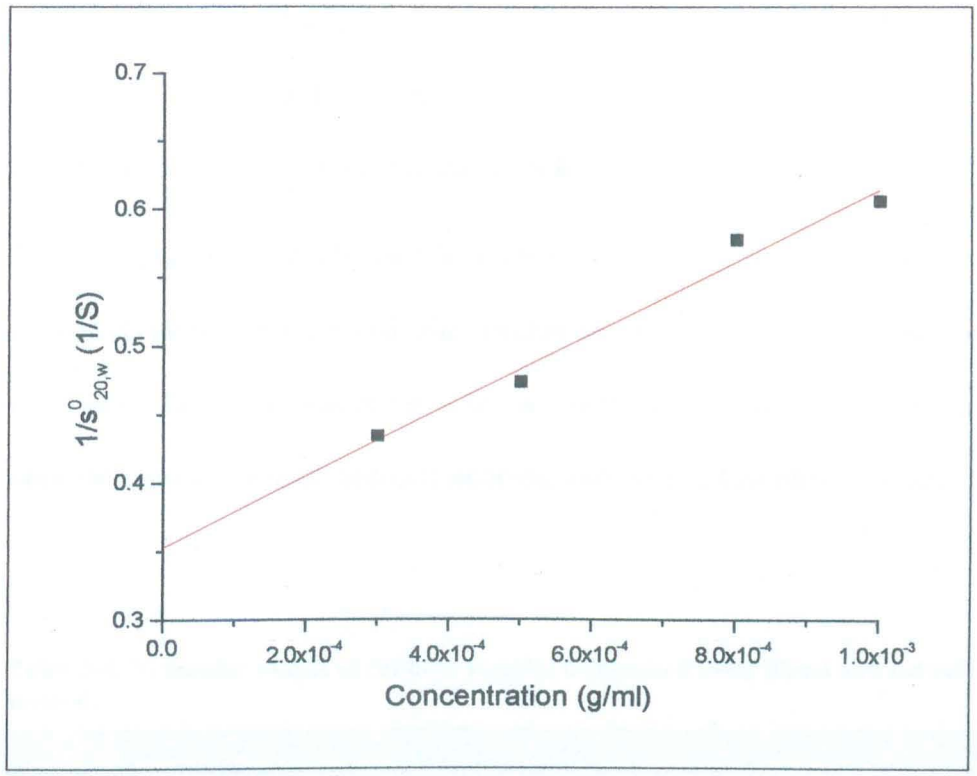

Table 3-3: Sedimentation velocity data for chitosan samples

Properties	Units	G112	G114	G214	G213	G213*	CL210
$s^0_{20,w}$	S	1.67 ± 0.04	1.90 ± 0.08	2.83 ± 0.15	2.88 ± 0.27	2.99 ± 0.09	2.49 ± 0.53
k_s	ml/g	389 ± 33	286 ± 65	740 ± 86	860 ± 158	884 ± 50	641 ± 233

$s^0_{20,w}$ - infinite dilution sedimentation coefficient, k_s – concentration dependence sedimentation coefficient

3.4.3 Molecular Weight Determination

The molecular weight of a polymer can be determined using absolute or relative methods. Absolute methods include analytical ultracentrifugion and light scattering methods and do not require calibration using materials of known molecular weight and identical conformation.

The two absolute methods used here are sedimentation equilibrium using the analytical ultracentrifuge and size exclusion chromatography coupled with multi-angle laser light scattering. The two methods are compared based on the data obtained for several chitosan samples, and the practicability discussed.

Table 3-4: Molecular weight of chitosan samples determined using direct and indirect methods

Property	Units	G112	G114	G214	G213	G213*	CL210
M_w (Sed. Equ.)	g/mol	57000 ± 8000	82000 ± 9000	132000 ± 15000	161000 ± 18000	-	173000 ± 12000
2BM (Sed. Equ.)	ml/g	-	2200	4100	46000	-	-
M_w (SEC-MALLS)	g/mol	42400 ± 3000	129000 ± 6000	172000 ± 6000	203000 ± 8000	207500 ± 8000	202000 ± 6000
M_z (SEC-MALLS)	g/mol	90000 ± 11000	386000 ± 30000	246500 ± 18000	442000 ± 30000	417000 ± 41000	1000000 ± 130000

M_w (Sed. Equ) – weight average molecular weight obtained from sedimentation equilibrium
2BM (Sed. Equ.)
M_w (SEC-MALLS) – weight average molecular weight obtained from SEC-MALLS
M_z (SEC-MALLS) – z-average molecular weight obtained from SEC-MALLS

3.4.3.1 Analytical Ultracentrifugation (AUC)

Measurement of molecular weight using the AUC requires the determination of molecular weight at several concentrations due to thermodynamic non-ideality.

In this study weight average molecular weights were determined at several concentrations using two AUCs. Firstly three concentrations (1.0, 0.8, and 0.5 mg/ml) were run on the XLI AUC and the apparent molecular weight determined from the interference data collected using the MSTAR program.

For 0.5 mg/ml chitosan solution the effects of non-ideality are still apparent (as indicated by the downwards curvature in the ln J versus ξ plot –Figure 3-3) and it is therefore best to also determine the molecular weight from data collected at lower concentrations (molecular weight determined at 0.3 mg/ml using Model E AUC as described in next paragraph). Chitosan is a polydisperse system, and this can normally be seen from upward curvature in the ln J versus ξ plot, however, the downward curvature in Figure 3-3 indicates that the effects of polydispersity are overshadowed by thermodynamic non-ideality (Cölfen and Harding 1997). Figure 3-4 shows the weight-average molecular weight versus ξ (normalized radial displacement function) and from this the apparent weight average molecular weight can be calculated (M^* at cell base is equal to $M_{w,app}$). Data at the base of the cell cannot always be observed completely and therefore extrapolation is necessary. In Figure 3-4, the data does not follow a clear downward curvature that levels out towards the base as would be seen with an ideal system. The data observed here is quite irregular due to the non-ideality associated with a chitosan system.

The XLI AUC uses 12mm path length centrepieces, which limits the minimum loading concentration. Since polysaccharides generally have refractive index increments in the range of 0.14 – 0.16 ml/g, the minimum loading concentration that can be used to obtain a sufficient fringe increment for molecular weight determination is ~0.5 – 0.6 ml/g in a 12 mm path length cell. The Model E AUC on the other hand, can use either 12 mm or 30 mm path length cells. By using a 30 mm cell, the minimum loading concentration is reduced to 0.2 – 0.3 mg/ml (Harding 1992; Harding 1995). An apparent molecular weight was determined at a loading concentration of 0.3 mg/ml using the Model E AUC.

Figure 3-5 shows the schlieren image produced in the Model E AUC (the principles of schlieren optics are described in section 2.2.1.1.2.). Data collected from this image can be plotted using the Lamm equation (example plot shown in Figure 3-6) to give an estimate of $M_{z,app}$, and by integration of the data with respect to r (distance from the meniscus), it can be analysed using MSTAR to determine $M_{w,app}$. The apparent molecular weights can be plotted against concentration using equation (2-12) (section 2.2.1.3.) to determine the true molecular weight for the chitosan. An example plot can be seen in Figure 3-7.

As previously mentioned, non-ideality causes the molecular weight for chitosan calculated from AUC data to be lower than the true molecular weight. There are two major contributing factors to this phenomenon: the excluded volume and the polyelectrolyte effect. The excluded volume arises from one molecule excluding another from the space occupied by it. For a sphere the excluded volume is eight times the volume, and the more extended the

conformation of the molecule the greater the excluded volume. Another contribution to exclusion volume comes from the swelling of the molecule through "hydration" or time-averaged association with water molecules. For a polysaccharide molecule in solution, the swollen volume can be 100 times its volume in the dry state (Harding 1995). The excluded volume can also be affected by interactions between the solute and solvent or by repulsion between solute molecules. The repulsion between solute molecules will be high for chitosan due to the high charge density on the molecule (~90 charges per 100 subunits) when in aqueous acidic solution. The intermolecular repulsion between the charged amino groups on chitosan results in a highly extended conformation. Chitosan will therefore have a large excluded volume and highly non-ideal behaviour when in solution. Increasing the ionic strength of the solution medium, thus reducing the electrostatic repulsion, can reduce the polyelectrolyte effect. However, for chitosan, large increases in ionic strength lead to reduced solubility and salting out can occur.

The term 2BM (second virial coefficient x molecular weight) is a measure of the non-ideality associated with the system (Van Holde 1971). For a spherical, uncharged molecule this would have a value of approximately 5-10 ml/g, and the value increases as the system deviates from ideality. From Table 3-4 it can be seen the 2BM values are in the range 1000-2000 ml/g indicating that chitosan is a highly non-ideal macromolecule.

At very low solute concentrations, ideal behaviour is approached (Van Holde 1998) and the effects of non-ideality should be small. Measurement at a single finite, but low (0.2 – 0.5 mg/ml) concentration can give an estimate of the apparent molecular weight within a few percent of the true molecular weight.

However, for chitosan the data obtained on the Model E AUC at a loading concentration of 0.3 mg/ml still showed non-ideality (deviation of data from trend line shown in Figure 3-6). Thus extrapolation to infinite dilution after measurement of the apparent molecular weight at several concentrations is necessary (see figure 3-7).

Figure 3-3: Plot of ln J versus ξ for chitosan G214 (concentration 0.5 mg/ml)

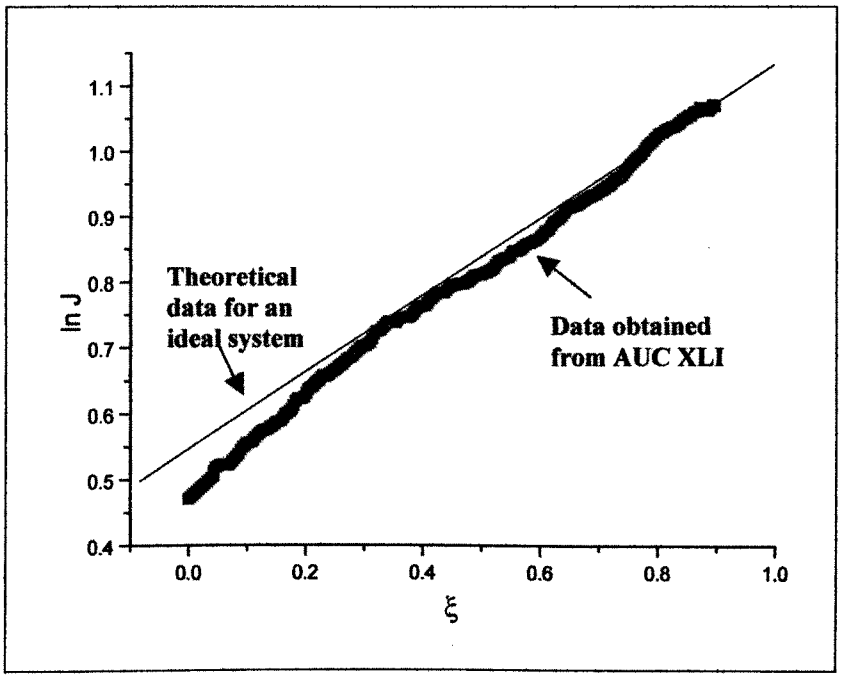

ξ - radial distance from centre of rotation normalized so that has a value of 0 at the solution meniscus and a value of 1 at the cell base

Figure 3-4: Plot of M_w^* versus ξ for chitosan G214 ($M^*(\xi\ 1)=M_{w,app}$) (concentration 0.5 mg/ml)

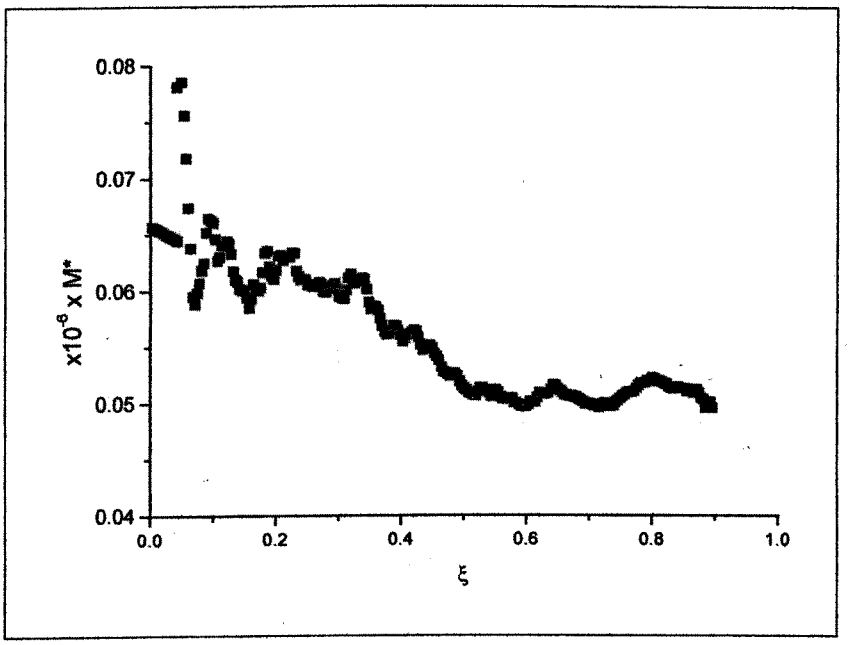

Figure 3-5: Schlieren image as produced on Model E AUC for chitosan G214 (concentration 0.3 mg/ml)

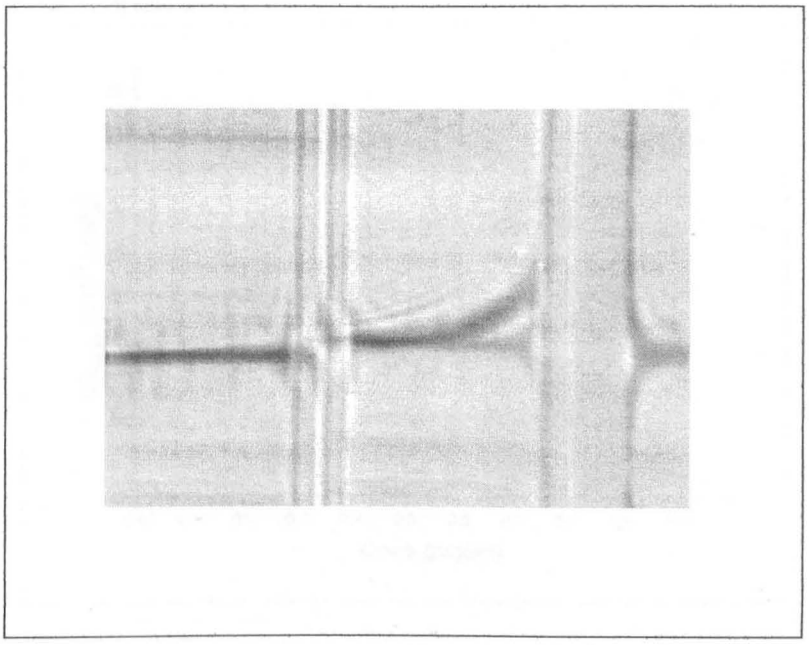

Figure 3-6: Lamm Plot for Chitosan G214 (concentration 0.3 mg/ml)

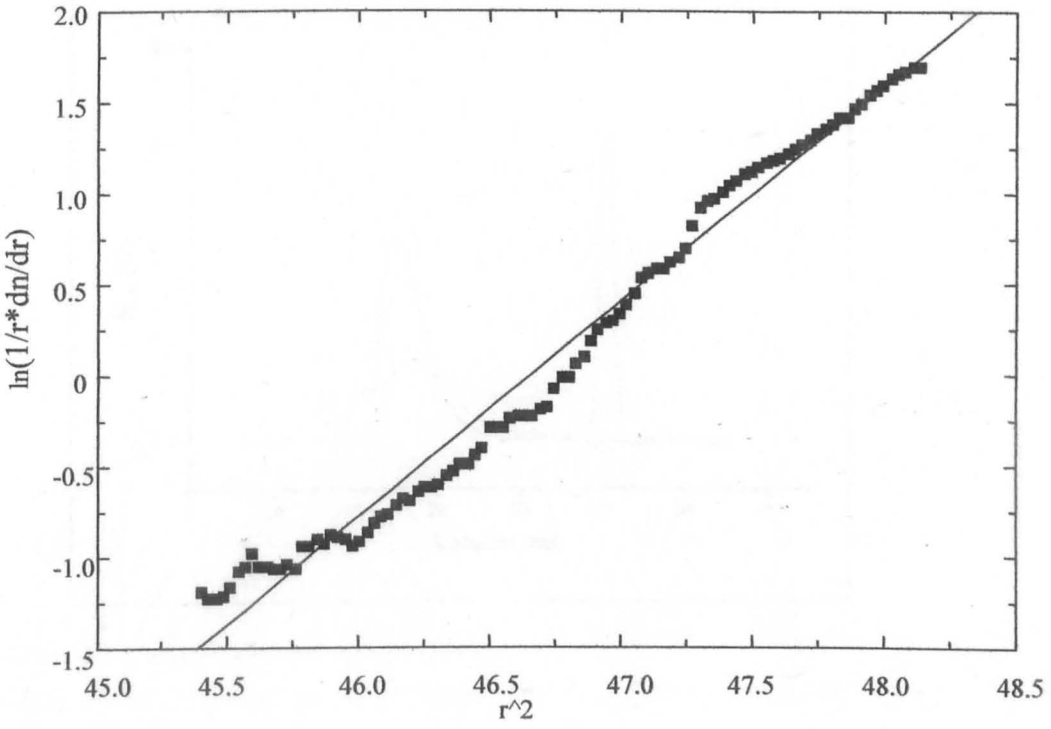

Figure 3-7: Extrapolation to infinite dilution for M_W determination of chitosan G214 from sedimentation equilibrium

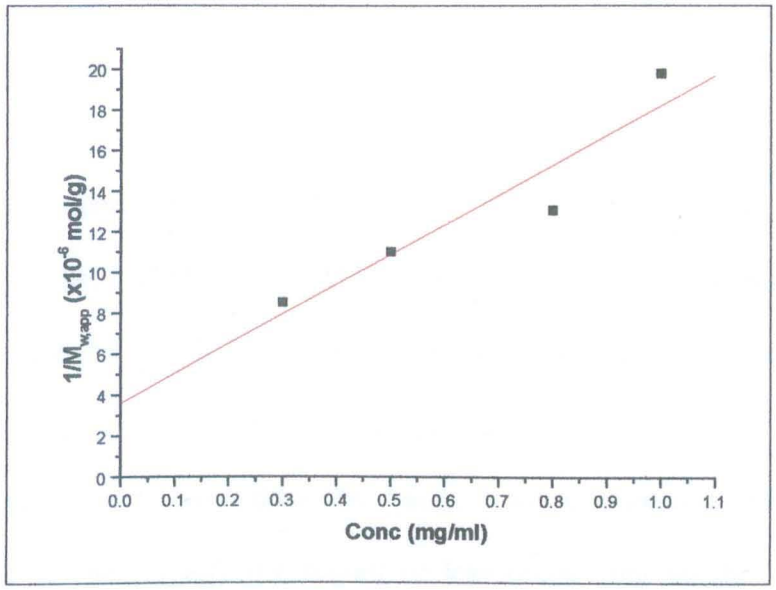

Figure 3-8: Light scattering (R_{90}) and Refractive Index (RI) traces obtained using SEC-MALLS for chitosan G214 (concentration 5mg/ml; solvent - 0.2M acetate buffer, pH 4.3)

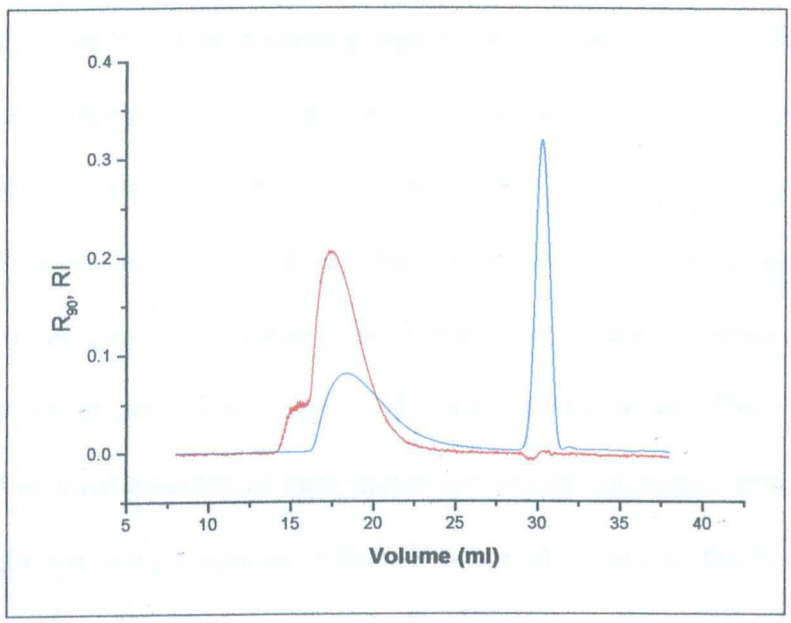

3.4.3.2 SEC-MALLS

SEC-MALLS also allows the direct evaluation of the absolute molecular weight of a macromolecule. However, with SEC-MALLS the measurements take approximately 60 minutes (after appropriate equilibration of the SEC columns) compared to up to 3 days for AUC measurements. Another advantage of SEC-MALLS over AUC is that no correction for non-ideality is required since the sample is diluted in the columns to such an extent that the concentrations of the volume "slices" passing through the light scattering detector are much lower than the initial loading concentration. These concentrations are usually 0.1 mg/ml or less (depending on the molecular weight of the scatterer), and corrections of non-ideality are not significant (Wyatt 1993).

Figure 3-8 shows an example of the trace produced using SEC-MALLS. The red trace shows the light scattering signal for chitosan, while the blue trace shows the refractive index signal. This is a measurement of the concentration of chitosan as it elutes and by combining the data from the two traces we can calculate the molecular weight distribution for each chitosan sample. From the light scattering traces it can be seen that in each case the peaks from the macromolecular component are skewed and not symmetrical. There was also evidence of trace amounts of high molecular weight aggregates from the 90° angle light scattering traces as indicated by the shoulders on the low elution volume or high molecular weight side of the light scattering peaks. However, except for sample G112 these light scattering signals are not accompanied by corresponding RI (concentration) signals indicating that only negligible amounts (<1%) are present in the samples. No such supramolecular particles

were observed from the sedimentation velocity g*(s) distributions obtained using time-derivative DCDT+ analysis, which showed only a single, approximately symmetrical peak in each case, including G112.

The molecular weights obtained from both AUC and SEC-MALLS measurements are in reasonable agreement (Table 3-4). Since SEC-MALLS is the more convenient technique, this will be used for measurement of molecular weight in the further experiments discussed in this thesis, however, for characterisation purposes it is advisable to also determine the molecular weight using the AUC to obtain a reliable and independent verification of the results.

3.4.4 Conformation of Chitosan

The conformation of chitosan is dependent upon the degree of acetylation of the molecule and the solvent conditions in which it is studied. The more deacetylated the molecule, the more extended the conformation due to the increase in charged amino groups along the chain. By altering the pH and ionic strength of the solution medium the conformation can be changed. Increases in ionic strength will reduce electrostatic repulsion leading to a more compact conformation, as will increases in pH since less amino groups will be charged.

3.4.4.1 Mark-Houwink Kuhn Sakarada relation

The Mark-Houwink Kuhn Sakarada (MHKS) exponent can be used as a conformation indicator. The most common form of the MHKS equation relates intrinsic viscosity to molecular weight (Harding 1997):

$$[\eta] = K' M^{a}$$

where K and a both depend on the polymer conformation. This relation was first suggested by Mark in 1938 and independently by Houwink in 1940. Similar relations exist for other hydrodynamic properties, e.g. sedimentation coefficients. The conformation of a molecule can be estimated depending on the value of these exponents are found in Table 3-5.

Table 3-5: MHKS exponents for general conformation types

Conformation	*a*	*b*	*ε*	*c*
Compact sphere	0	0.667	0.333	0.333
Rigid rod	1.8	0.15	0.85	1.0
Random coil	0.5 – 0.8	0.4 – 0.5	0.5 – 0.6	0.5 – 0.6

***a* – intrinsic viscosity exponent; *b* – sedimentation coefficient exponent; *ε* - diffusion coefficient exponent; *c* – radius of gyration exponent**

Figure 3-9 and Figure 3-10 show double logarithmic plots for the glutamate chitosans in terms of log $s^0_{20,w}$ versus log M_w and log [η] versus log M_w respectively. A linear fit to the log $s^0_{20,w}$ versus log M_w yielded an MHKS exponent b = (0.25 ± 0.04), i.e. between the limits of rod (0.15) and coil (0.4 – 0.5). Similarly a linear fit to the log [η] versus log M_w yielded an MHKS exponent a = (0.96 ± 0.10), again between the coil (0.5 – 0.6) and rod (1.8) limits. However, interpretation of such data should be done with caution because of the clear demonstration by others of a dependence conformation on the degree of acetylation (Anthonsen *et al.* 1993; Berth and Dautzenberg 2002). Despite this reservation, the values obtained appear similar to those for three chitosans with degrees of acetylation in the range 22-31% (Cölfen *et al.* 2001): a ~ 1 and b ~ 0.24. Furthermore, the data reassuringly shows consistency between the sedimentation coefficient and viscosity data.

Figure 3-9: Double logarithmic plot of sedimentation coefficient versus weight average molecular weight (SEC-MALLS) for chitosan samples (glutamate salts only)

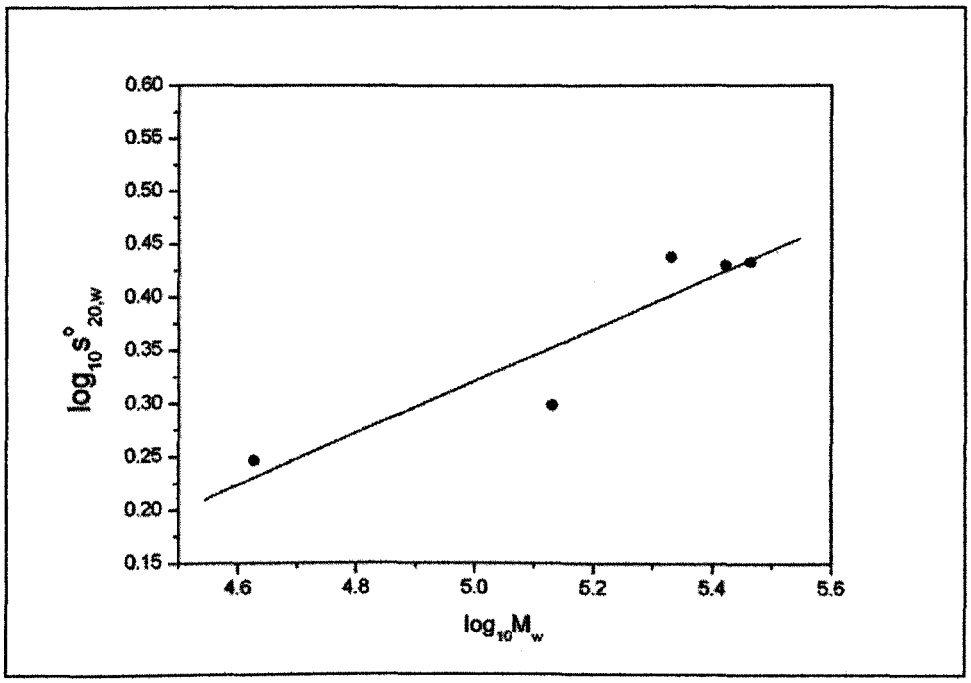

Figure 3-10: Double logarithmic plot of intrinsic viscosity versus weight average molecular weight (SEC-MALLS values) of chitosan samples (glutamate salts only)

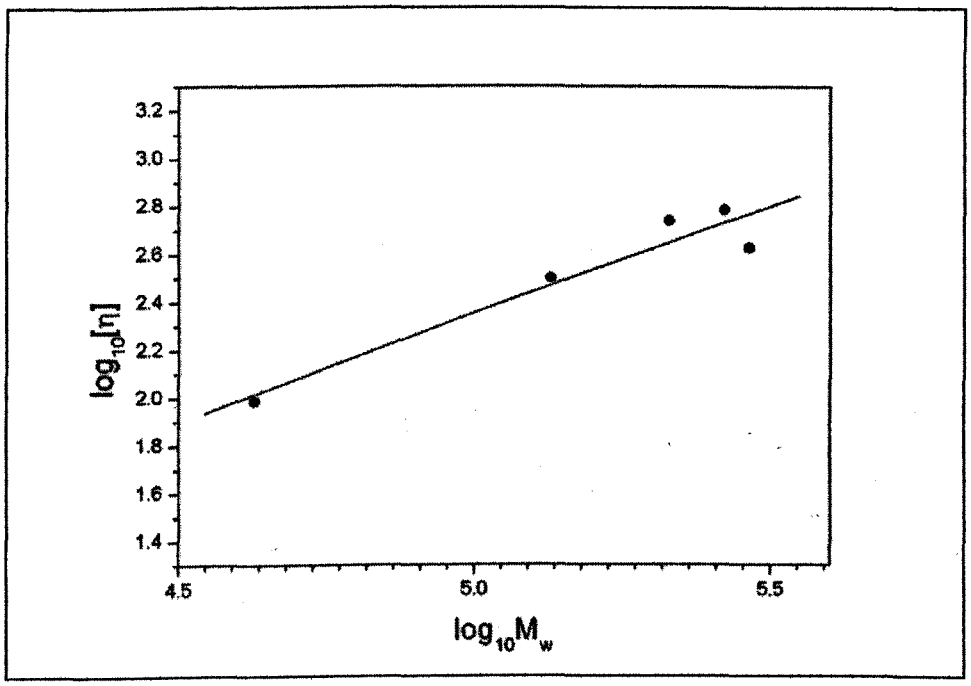

Chapter 4: Effect of Solvent Characteristics or Solvent Parameters on Degradation of Chitosan

4.1 Introduction

In this chapter the effect of various solvent parameters on chitosan degradation will be examined. It is known that the pH and ionic strength of a solvent affects the conformation of chitosan and these effects on conformation will be discussed in terms of the effects on degradation. Other conditions examined in this chapter are storage temperature; concentration of chitosan and the addition of scavenging agents which can be used to reduce oxidative reductive degradation (see section 1.2.2.2.).

In the first section of this chapter, the effect of individual parameters (pH, temperature, ionic strength, presence of scavenging agent) will be studied. In the second section, the effect of several factors is studied in a multi-factorial experiment.

4.2 Effect of Individual Factors on Chitosan Degradation

4.2.1 Materials and Methods

Degradation of chitosan was followed using both viscosity measurements and sedimentation data. 1.0 mg/ml chitosan solutions (Chitosan CL210) were prepared in either 0.2 M HCl (pH 1.28) or 0.1M acetate buffer at specified pH (pH 4 or 5) and ionic strength (I = 0.2 or 0.3M). Each sample was then stored in closed glass bottles (clear) at the appropriate temperature (4, 25, 40°C) and sampled weekly. Samples were prepared in triplicate.

In the study on the effect of scavenging agents, 7mM thiourea was added to the chitosan solution.

4.2.1.1 Viscosity data

Sample and solvent flow times were measured at 25°C using a 2 ml Ostwald viscometer. The reduced viscosity calculated using equation (2-16).

When viscosity vs time was plotted as a scatter graph, it could be seen that the decay or loss of viscosity followed first order kinetics. In first order degradation the rate of decay of a substance is proportional to the first power of the concentration of that substance, and independent of any other substance present.

By fitting each data set to a first order degradation curve (equation 4-1), a rate constant (k) can be obtained:

$$\eta_{red} = \eta_{resid} e^{-kt} \qquad (4-1)$$

where η_{red} is the reduced viscosity measured at time t, and η_{resid} is the residual viscosity after the period of study.

4.2.1.2 Sedimentation data

Sedimentation coefficients were determined from sedimentation velocity data (see section 2.2.1.2.) and converted to standard conditions using equation (2-9). Molecular weights ($M_{w,app}$) were determined from equilibrium data at concentration of 1mg/ml, 0.8mg/ml and 0.5mg/ml. This data was analysed using MSTAR and extrapolated to zero concentration to give M_w (g/mol).

4.2.1.3 Degradation rate

Degradation rates were determined using a method described in Vårum *et al.* (2001). Solutions of chitosan (CL210 – DA 18%) were prepared in a range of acid solutions (0.01 – 0.4 M HCl) at a concentration of 0.5 mg/ml. Each sample was stirred for one hour to ensure dissolution of the chitosan. 2 ml of

the sample was transferred to an Ostwald capillary viscometer suspended in a thermostatically controlled water bath at (60.0 ± 0.5°C) and allowed to equilibrate to temperature for 20 minutes before commencing flow time measurements. Flow times were recorded at 10-minute intervals over one hour. From the flow times, the degree of polymerisation was calculated (Nordtveit *et al.* 1994) using Mark-Houwink coefficients; a = 0.78, K = 5.58×10^{-2} (Anthonsen *et al.* 1993). Rate constants were calculated by plotting the degree of scission ($\alpha = 1/DP_n$) versus time, the value of the slope being equal to the reaction rate. Samples were measured in triplicate.

4.2.2 Results

4.2.2.1 Effects of Temperature

Figure 4-1 shows the effect of temperature on the reduced viscosity of chitosan samples. Each sample had approximately the same initial viscosity, which decreased over the eight-week period. The rate of degradation was fastest at 40°C (Rate = 0.775 $week^{-1}$), with a decrease in viscosity of 55% over the 8 week period, and slowest at 4°C (Rate = 0.087 $week^{-1}$), with a decrease in viscosity of 15%. This suggests that chitosan has greater stability at lower temperatures. This result was in agreement with Jia and Shen (2002) who showed that the intrinsic viscosity of chitosan decreased from 320 to 70 ml/g after only 8h storage at 40°C, while at ambient temperature the intrinsic viscosity remained at ~120ml/g after 35 days storages (solvent : 85% phosphoric acid).

The rate constants of most reactions increase as the temperature is raised. Typically, the degradation of chitosan requires the cleavage of bonds along the chitosan chain (usually the glycosidic bond joining the two glucosamine residues). The breaking of chemical bonds requires energy, i.e. it is an endothermic process. Therefore, as shown here, the rate of degradation will increase as the temperature increases since more energy is available.

Figure 4-1: Effect of temperature on reduced viscosity of chitosan solution (1mg/ml CL210; pH 4, I=0.2M, n=3)

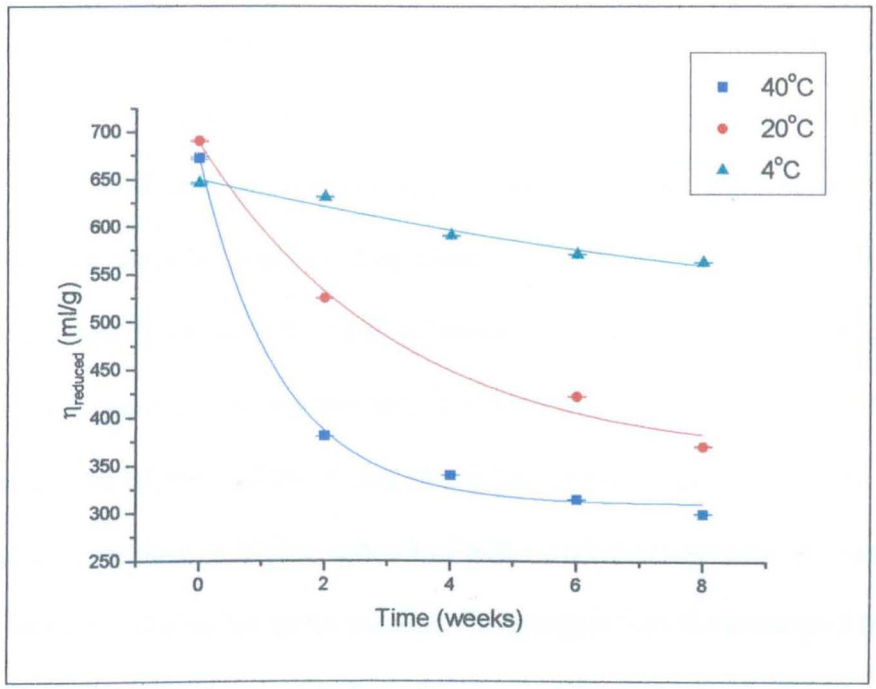

Table 4-1: Degradation rates for chitosan solutions at different temperatures

	k (week^{-1})
4°C	0.087
20°C	0.317
40°C	0.775

4.2.2.2 Effect of Ionic Strength

Figure 4-2 shows the effect of solution ionic strength on chitosan viscosity and degradation. In contrast to the results shown in Figure 4-1 the initial viscosities of the samples decreased as the ionic strength increased. This can probably be attributed to chitosan being a polyelectrolyte: the hydrodynamic behaviour of chitosan is affected by changes in the degree of protonation in different ionic strength and/or pH solutions. However, there is still much debate as to whether varying the degree of acetylation of chitosan affects the expansion and stiffness of the chains in solution (Ottøy *et al.* 1996; Berth *et al.* 1998). On one hand, a higher content of bulky acetyl groups may increase the stiffness of the chains for steric reasons. This effect was demonstrated by the Trondheim group, who found that chitosan exhibited higher expansion and stiffness with increasing DA (Anthonsen *et al.* 1993; Anthonsen *et al.* 1994; Ottøy *et al.* 1996). On the other hand, a lower DA means a higher amount of amino groups, which are charged in aqueous acidic solution. As described in Tanford (1961) for flexible polymer chains, the accumulation of charge leads to considerable expansion due to electrostatic repulsion. Errington *et al.* (1993) found that chitosans with a higher DA appeared to exhibit a less extended conformation due to a decrease in electrostatic charge on the molecule. In low ionic strength solutions, the charge effects dominate, which makes the chitosan molecule exist in an extended conformation due to electrostatic repulsion. However, in high ionic strength solutions, the concentration of the counter-ions are raised which screens the protonated amide groups and makes the molecule more contracted (Tanford 1961; Tsaih and Chen 1997). This change of the chitosan molecule with increasing ionic

strength will cause the solution viscosity to decrease as demonstrated in Figure 4-2.

Figure 4-2 also shows that over the eight-week period, the rate of degradation over ionic strength range 0.1 – 0.3M was approximately the same. This indicates that the changes in chitosan conformation over this ionic strength range have little effect on its stability in aqueous solution.

Figure 4-2: Effect of Ionic strength on reduced viscosity of chitosan solution (1 mg/ml CL210; pH 4; Temp = 20°C, n=3)

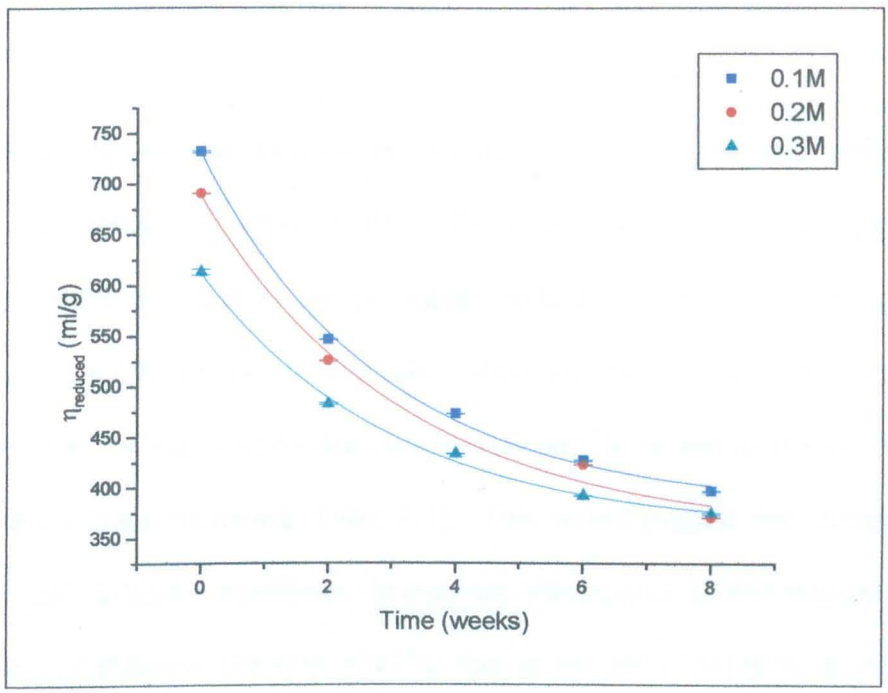

Table 4-2: Degradation rates for chitosan solutions at different ionic strengths

	k (week^{-1})
0.1M	0.356
0.2M	0.317
0.3M	0.336

4.2.2.3 Effect of pH

The main mechanism of degradation of chitosan in aqueous solution is believed to be acid degradation (Vårum *et al.* 2001); therefore it would be expected to observe increased degradation in more acidic conditions, i.e. low pH.

Figure 4-3 shows the decrease in viscosity over an eight week period in chitosan solutions of different pHs. The initial viscosities at each pH are similar, indicating that in the pH range studied there was little change in chitosan conformation. It was also observed that the rate of chitosan degradation, as indicated by decrease in viscosity, increased as the pH of the chitosan solution increased (Table 4-3). This would suggest that chitosan is more stable in acidic conditions. In contrast, Vårum *et al.* (2001) showed for a chitosan of different DA (DA = 62%) that as the pH of solution decreased, degradation increased, i.e. chitosan was susceptible to acid degradation.

An estimation of sedimentation coefficients can give a further indication of stability of chitosan stored at different pHs. Figure 4-4 and Figure 4-5 show the apparent sedimentation coefficient distributions for each sample. The peak maximum gives $s_{20,w}$ and the peak width gives an indication of the relative polydispersity of the sample (complications through particle diffusion obscure interpretation of absolute polydispersity). The area under the curve can be used to calculate the concentration of the species, however, it should be noted that this concentration does not include small fractions that may not have sedimented from the meniscus or large, aggregated fractions that will have rapidly sedimented to the base. Figure 4-4 shows the sedimentation coefficients of chitosan stored at pH 1.28. A significant decrease, as

expressed in Svedbergs, was observed in the first month, with minimal change in the second month. This decrease in sedimentation coefficient would appear to indicate that the chitosan has degraded by approximately 27% in the first month, with a much-reduced degradation (~2%) in the second month. These results are further supported by the weight-average molecular weights determined using sedimentation equilibrium (Table 4-4).

For the chitosan solution stored at pH 5, a steady, progressive decrease in the sedimentation coefficients and narrowing of the peak was observed over the two month period (Figure 4-5), resulting in a decrease of approximately 35%, i.e. greater than for the chitosan stored at pH 1.28.

Degradation occurred at a faster rate at a lower pH, i.e. in more acidic conditions, which is in agreement with Vårum *et al.* (2001), however after two months the extent of degradation in both cases was comparable.

Figure 4-3: Effect of pH on reduced viscosity of chitosan solution (1 mg/ml CL210; I=0.2M, Temp=20°C, n=3)

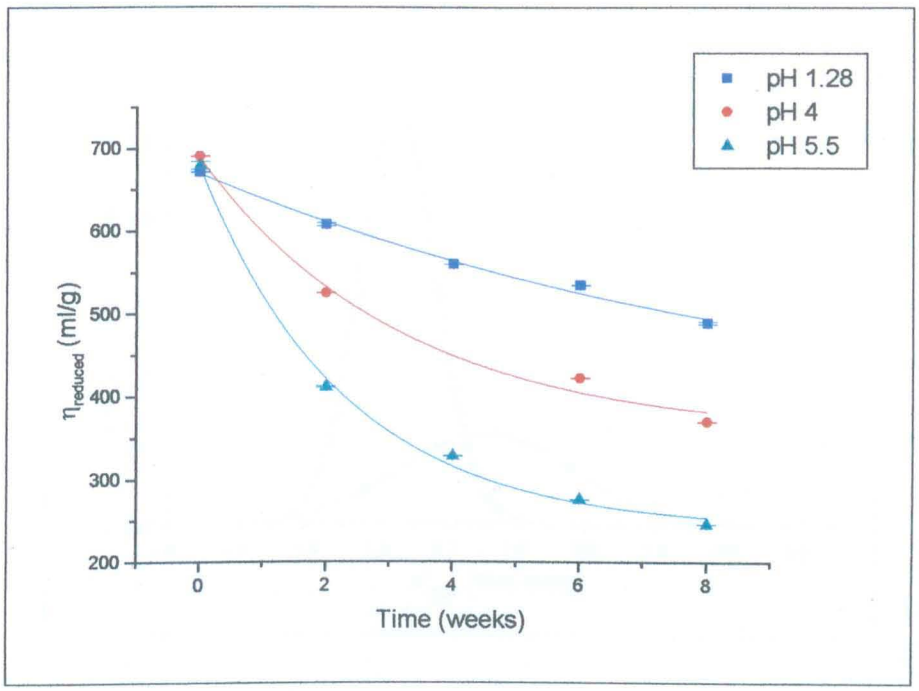

Table 4-3: Degradation rates for chitosan solutions at different pHs

	k (week^{-1})	% Decrease in Viscosity		
		0-8 wks	0-2 wks	2-8wks
pH 1.28	0.107	27	9	17
pH 4	0.317	46	24	22
pH 5.5	0.442	64	39	24

Figure 4-4: Distribution of apparent sedimentation coefficients for chitosan (1mg/ml) in 0.2M HCl (pH 1.28) at various time points (n=3)

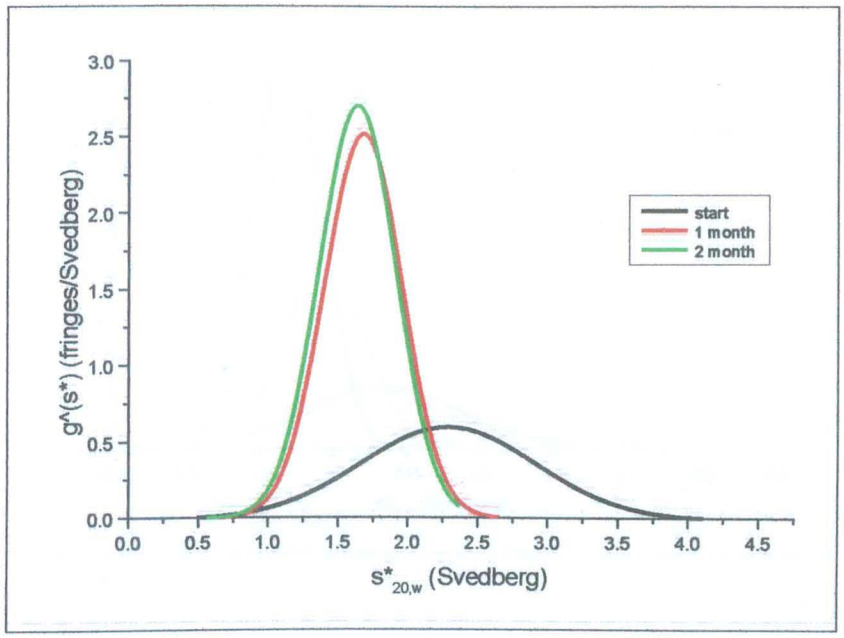

Table 4-4: Sedimentation coefficients (from sedimentation velocity analysis) and weight-average molecular weight (from sedimentation equilibrium) for chitosan (1mg/ml) in 0.2M HCl

Time	$s^*_{20,w}$ (S)	M_w (g/mol)
0	2.29 ± 0.01	174,000
1 month	1.68 ± 0.01	120,000
2 months	1.63 ± 0.01	121,000

Figure 4-5: Distribution of apparent sedimentation coefficients for chitosan (1mg/ml) in 0.1M Acetate buffer, pH 5 at various time points, (n=3)

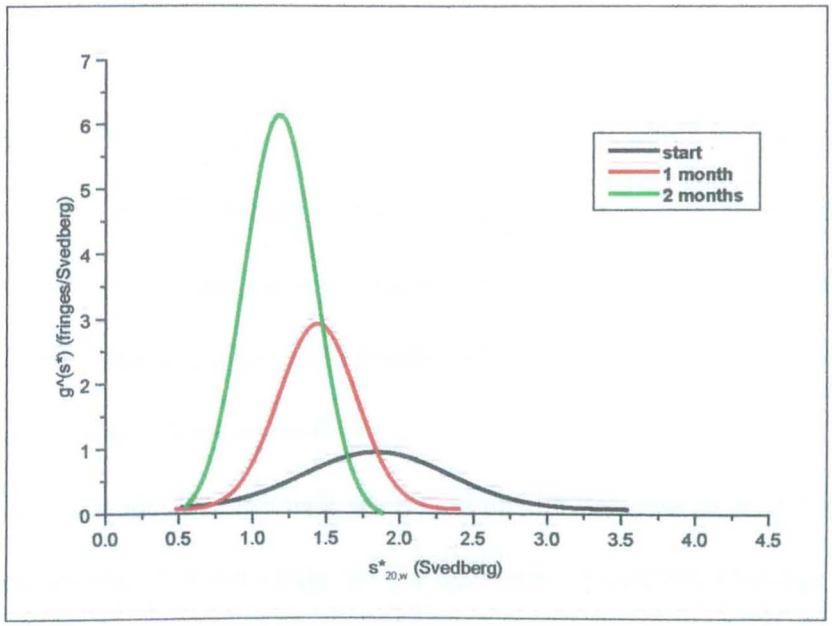

Table 4-5: Sedimentation coefficients and weight-average molecular weights for chitosan (1mg/ml) in 0.1M Acetate buffer, pH 5

Time	$s^*_{20,w}$ (S)	M_w (g/mol)
0	1.85 ± 0.01	176,000
1 month	1.44 ± 0.01	107,500
2 months	1.18 ± 0.01	106,500

It can be seen from Figure 4-3 and Table 4-3 that the difference in degradation rates due to the pH of solution occurred in the first two weeks. After this period, degradation occurred at a similar rate, irrespective of the pH of solution.

Again, a possible explanation for this may be a change in the conformation of chitosan. The initial viscosity reading for each sample was taken one hour after dissolution. During the subsequent two weeks degradation can occur at two possible sites; the glycosidic bonds linking the glucosamine residues or cleavage of the acetyl group on C4.

Breaking of the glycosidic bonds would result in a decrease in viscosity since the length of the chitosan chain would decrease. However, cleavage of the acetyl groups would results in more amide groups on the chitosan chain. In acidic solutions these amide groups are protonated, which might result in a more extended conformation and therefore an increase in viscosity. At low pH there are more hydrogen ions present which increases the chances of acetyl groups being cleaved from the chitosan chain as well as cleavage of the glycosidic bonds. Any increase in viscosity due to changes in conformation could mask the decrease in viscosity due to degradation of the chitosan chain, making it appear that chitosan degrades fastest in a high pH solution.

To confirm that acid hydrolysis does occur, the experiment reported by Vårum *et al.* (2001) was repeated. This experiment was carried out at two chitosan concentrations and the results can be seen in Figure 4-6. The rate of degradation increased as the acid concentration increased, which agrees with the data for a chitosan of higher DA studied by Vårum *et al.* (2001). Interestingly, the initial concentration of chitosan had an effect on the

degradation rate. Degradation appeared to occur faster at higher chitosan concentrations and this is probably due to the increased number of glycosidic bonds available for cleavage.

Comparing Vårum's results for a chitosan of DA=62% with the present data (DA=18%) obtained at the same concentration and using the same experimental conditions (Figure 4-7), there was a significant difference in the degradation rates (10 fold difference). This difference can be explained by the structural difference in the chitosans used in the two experiments (degree of acetylation), and is considered further in the Chapter 5.

Figure 4-6: Degradation rate constants as a function of acid concentration (HCl), determined by the viscosity assay at 60°C.

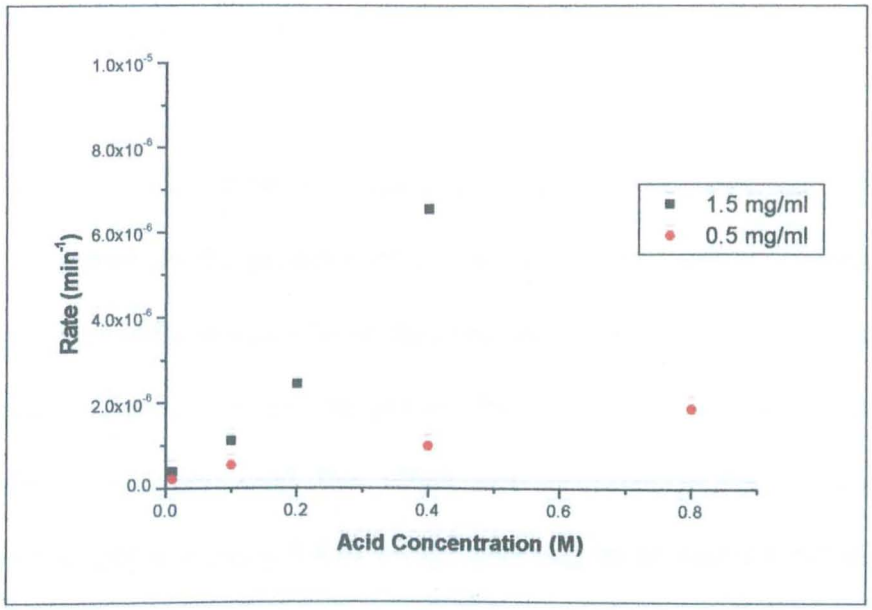

Figure 4-7: Degradation rate constants as a function of acid concentration (HCl), determined by the viscosity assay at 60°C. The data of Vårum *et al.* (2001), measured at 60°C, is also included for comparison.

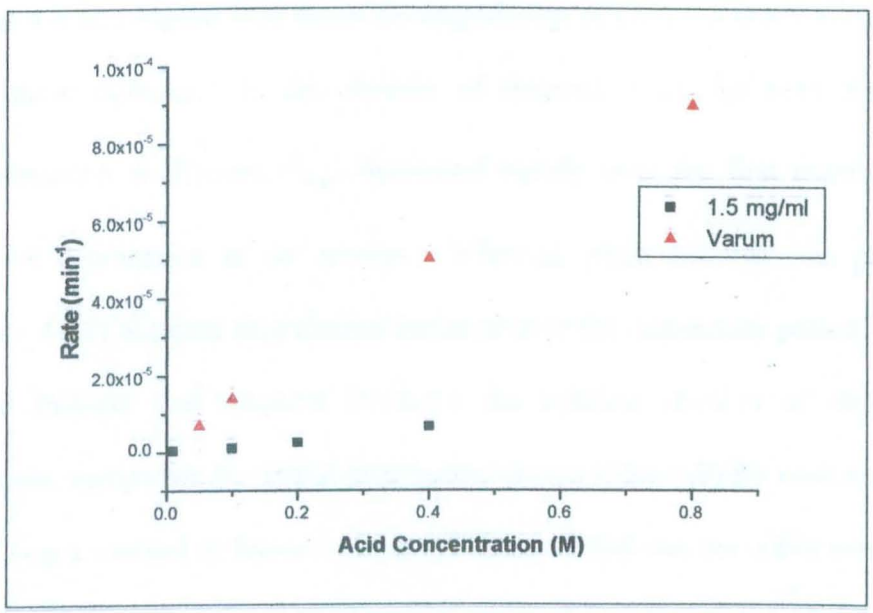

4.2.2.4 Effect of Scavenging agents

Another proposed mechanism of chitosan degradation is Oxidative Reductive Degradation (ORD). ORD involves a series of free radical reactions that ultimately lead to chain scission.

Figure 4-8 to Figure 4-10 show the degradation of chitosan under different acidic solutions, in the presence of various scavenging agents, measured by changes in the reduced viscosity of the chitosan solution.

As seen in Figure 4-3, as the pH of the solution increased, the rate of degradation increased, and this effect also occurred in the presence of scavenging agents (Figures 4-8 to 4-10). This may be explained by changes in chitosan conformation (see section 1.2.1.3.). At pH 1.28 and pH 5.5 (Figure 4-8 and Figure 4-10) the effect of scavenger on degradation was seen to be minimal. By contrast, at pH 4 (Figure 4-9), the presence of scavenger in the solution increased the stability of chitosan by approximately 18% (based on reduced viscosity after 8 weeks), which is not considered significant.

Figure 4-4 and Figure 4-11 show the degradation of chitosan at pH 1.28, with or without thiourea. In the absence of thiourea it can be seen that the sedimentation coefficient, $s^0_{20,w}$, decreased rapidly over the first month with minimal degradation in the second. Whereas, when thiourea was present (Figure 4-11) minimal degradation occurred over the one-month period. This would indicate that thiourea increased the solution stability of chitosan. However, comparing the initial distribution curves (time = 0) for each sample, there was a marked difference. In the absence of thiourea the curve was very broad and flat, whereas with thiourea present, it was narrower and taller. It would have been expected that at the start of each study, the sedimentation

coefficients for the two samples would have been similar and have a similar distribution. The differences in the initial distributions may be due to the presence of thiourea.

The molecular weight determined (using sedimentation equilibrium) at each time point (Table 4-4; pH 1.28) are in good agreement with the change in sedimentation coefficients for those samples not containing thiourea. However in the presence of thiourea, the initial calculated molecular weight was higher than expected (Table 4-6; pH 1.28). Again this may be due to some effect of thiourea on the conformation of chitosan.

Figure 4-5 and Figure 4-12 show the degradation of chitosan at pH 5, with or without thiourea. The results obtained are similar to those at pH 1.28 and again suggest that thiourea has had some effect on chitosan, possibly a conformation effect.

By studying the change in reduced viscosity at 60°C (Figure 4-13), the results indicate that as acid concentration increased the rate of degradation increased, which is suggestive of acid hydrolysis. However, the presence of thiourea does not have a significant effect ($t_{0.05,3df}$ = 3.182; t = 1.23 therefore not significant) on the degradation rate (Table 4.8).

In conclusion, acid hydrolysis does appear to be the main mechanism by which degradation of chitosan occurs. There may be some oxidative reductive degradation due to free radicals but this appears to be negligible.

Figure 4-8: Viscosity results for chitosan solutions in 0.2M HCl (pH 1.28, n=3)

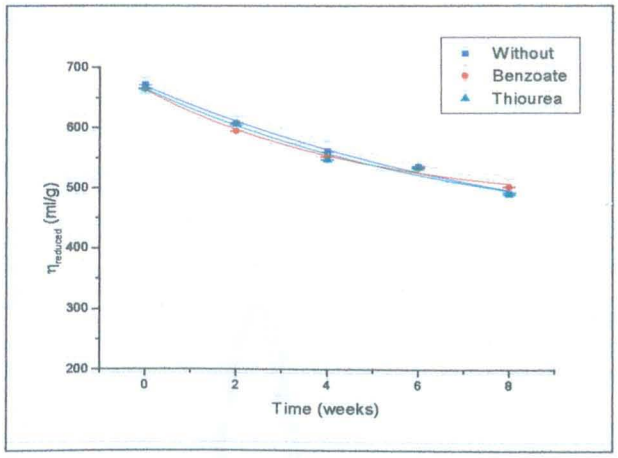

Figure 4-9: Viscosity results for chitosan solutions at pH 4 (n=3)

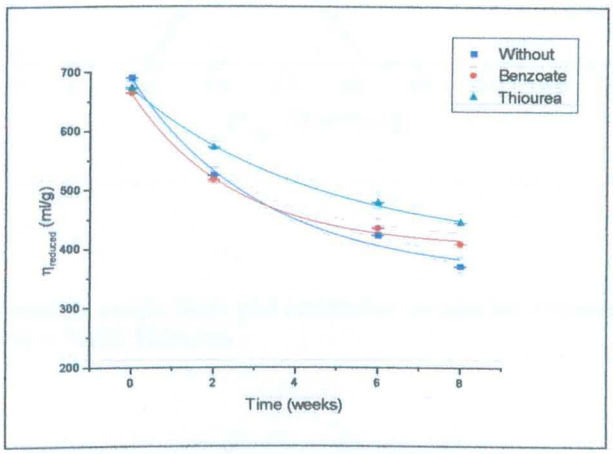

Figure 4-10: Viscosity results for chitosan solutions at pH 5.5 (n=3)

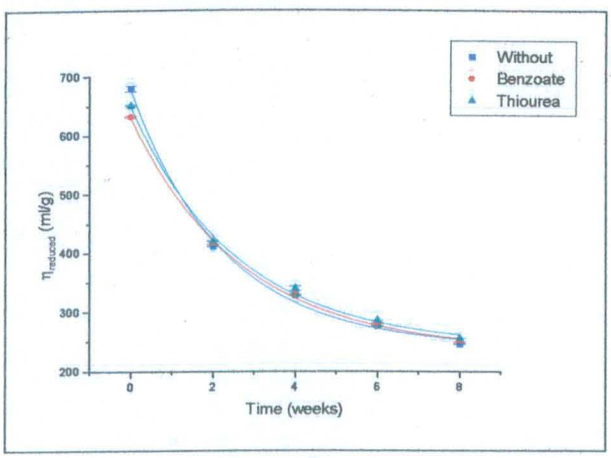

Figure 4-11: Distribution of sedimentation coefficients for chitosan (1mg/ml) in 0.2M HCl (pH 1.28) + 7mM Thiourea before and after storage for one month. No significant shift is evident, (n=3)

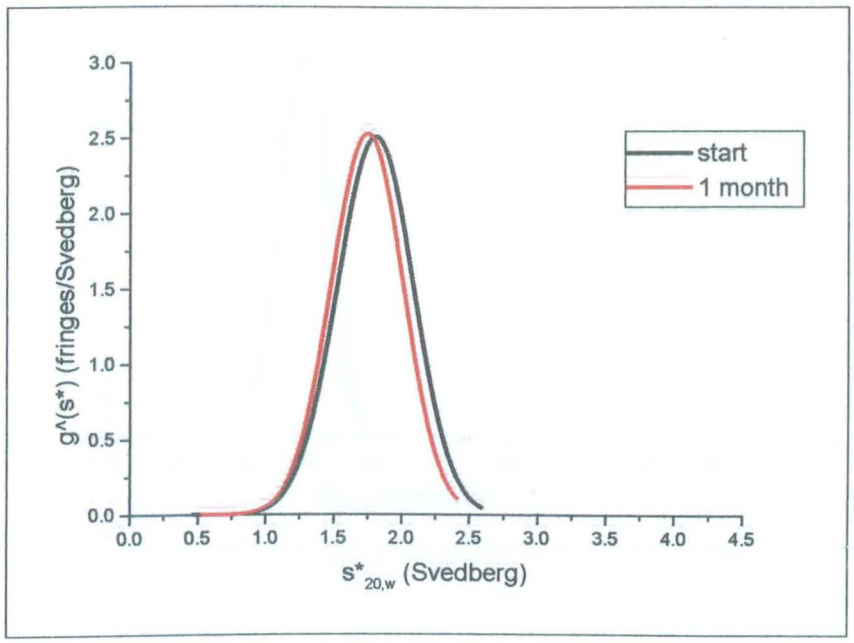

Table 4-6: Sedimentation coefficients and molecular weight for chitosan (1mg/ml) in 0.2M HCl (pH 1.28) + 7mM Thiourea

Time	$s^0_{20,w}$ (S)	M_w (g/mol)
Start	1.80 ± 0.01	251,000
1 month	1.74 ± 0.01	128,500

Figure 4-12: Distribution of sedimentation coefficients for chitosan (1mg/ml) in 0.1M Acetate buffer, pH 5 + 7mM Thiourea before and after storage for one month, (n=3)

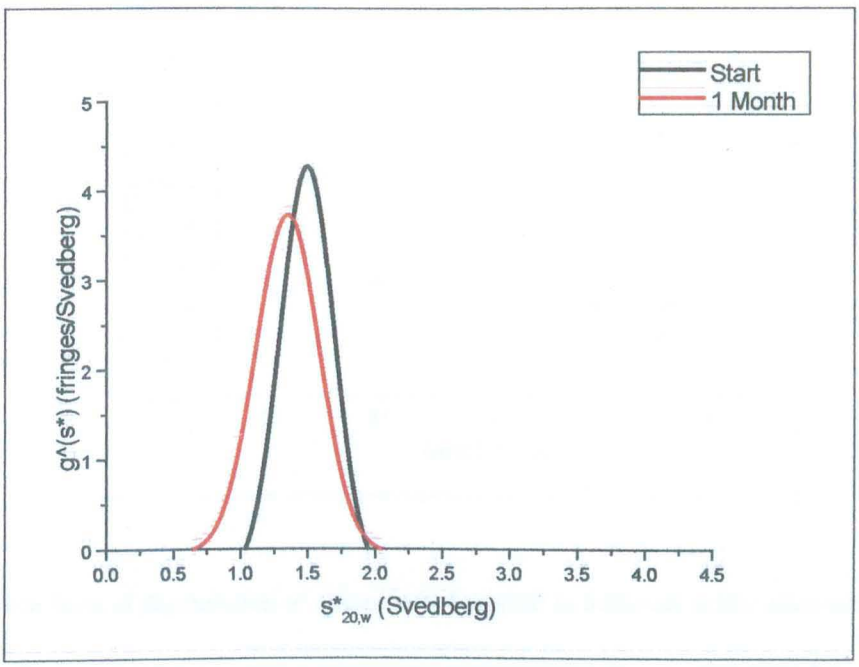

Table 4-7: Sedimentation coefficients and molecular weight for chitosan (1mg/ml) in 0.1M Acetate buffer, pH 5 + 7mM Thiourea

Time	$s^0_{20,w}$ (S)	M_w (g/mol)
Start	1.49 ± 0.01	149,500
1 month	1.35 ± 0.01	87,000

Figure 4-13: Degradation rates of chitosan as a function of acid concentration in the presence or absence of thiourea (n=3)

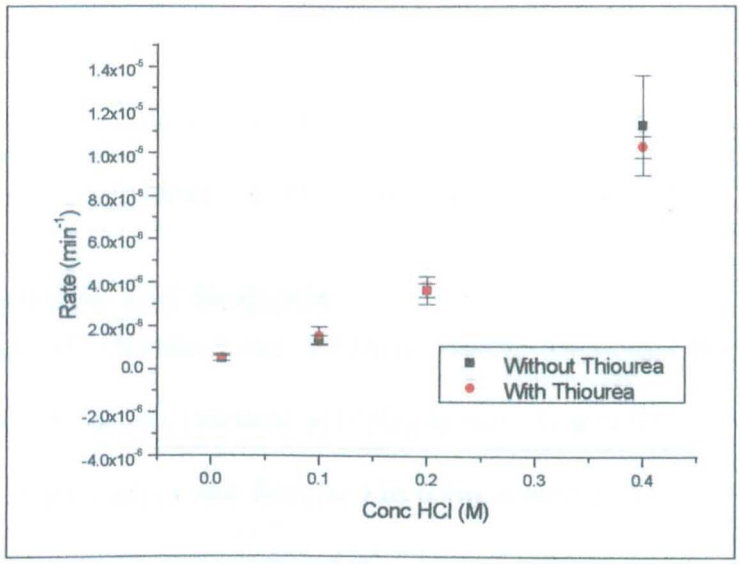

Table 4-8: Rate of degradation of chitosan (0.5 mg/ml) in different acidic solutions

Degradation Rate ($x\ 10^{-6}\ min^{-1}$)	Conc HCl (M)			
	0.4	0.2	0.1	0.01
Without Thiourea	11.33 ± 2.3	3.67 ± 0.31	1.36 ± 0.19	0.51 ± 0.12
With Thiourea	10.30 ± 0.5	3.67 ± 0.63	1.55 ± 0.44	0.53 ± 0.16

4.3 Multi-factorial Study

So far in this chapter the effect of several environmental parameters on chitosan stability have been assessed individually. However, in a pharmaceutical formulation, several parameters will be encountered. In this study four factors are looked at using a two level factorial design.

4.3.1 Materials and Methods

Degradation of chitosan was followed using viscosity measurements. Chitosan solutions were prepared in triplicate according to the details given in Table 4-9. Each sample was dissolved in 0.1M acetate buffer at the specified pH and ionic strength and contained 0.15 mg/ml benzalkonium chloride as a preservative to prevent bacterial growth. Each sample was stored in closed glass bottles (clear) at the appropriate temperature (25 or 40°C) and sampled at two week intervals.

4.3.1.1 Viscosity data

Sample and solvent flow times were measured at 25°C using a 2 ml Ostwald viscometer. The reduced viscosity calculated using equation (2-16).

At set time points of 2 weeks, 1month, 2 months and 3 months, a sample of each formulation was examined using viscosity as an indication of the degree of degradation (as described in section 2.2.2.3.).

4.3.1.2 Statistical Analysis

Statistical analysis of the viscosity data collected over the study period was carried out using a computer software package: Design Expert (Stat-Ease, Inc. 2000). The package enables data from factorial design to be analysed and the significant factors are selected using ANOVA.

Table 4-9: Details of samples

Sample	Conc. Chitosan (mg/ml)	Ionic Strength M	pH	Thiourea Conc (mM)
1	1	0.1	4.0	0
2	1	0.1	5.5	7
3	1	0.3	4.0	7
4	1	0.3	5.5	0
5	5	0.1	4.0	7
6	5	0.1	5.5	0
7	5	0.3	4.0	0
8	5	0.3	5.5	7

Table 4-10: Percentage Initial viscosity for stability study

Sample	2 weeks	4 weeks	8 weeks	12 weeks
1	66 ± 10	40 ± 14	51 ± 11	51 ± 12
2	79 ± 2	72 ± 7	66 ± 4	68 ± 2
3	76 ± 6	73 ± 6	69 ± 7	67 ± 3
4	70 ± 8	59 ± 6	51 ± 4	48 ± 5
5	69 ± 3	58 ± 6	51 ± 2	47 ± 2
6	48 ± 1	37 ± 1	27 ± 1	23 ± 1
7	64 ± 1	55 ± 1	45 ± 1	41 ± 2
8	60 ± 7	53 ± 5	44 ± 5	39 ± 4

Initial viscosity of all samples is 100%

4.3.2 Results

This study highlights the significant factors for chitosan stability. These were: pH, chitosan concentration and time. As was indicated in section 4.3.2., the ionic strength of the solution did not have a significant effect on degradation rate, and the presence of a scavenging agent did not improve stability.

The ANOVA analysis of the data obtained in this study also showed that ionic strength and presence of a scavenging agent did not have a significant effect on chitosan stability in solution ($P = 0.10$ and $P = 0.13$ respectively). For the other factors studied (pH, chitosan concentration, time), the ANOVA results showed a significant effect (Time: $P = 0.01$; pH: $P = 0.05$; chitosan concentration: $P = 0.04$).

Model graphs produced using the Design Expert software (Figure 4-14) show the effect of each significant factor on solution viscosity. From the graph for pH it can be seen that there was slightly increased stability at a low pH, but the difference was not high over the pH range studied here.

In conclusion, acid hydrolysis of chitosan does occur, however, over the pH range which is acceptable for nasal formulations there was little difference in the observed degradation rates.

Figure 4-14: Model plots showing the effect of each factor on chitosan stability in a multi-factorial design

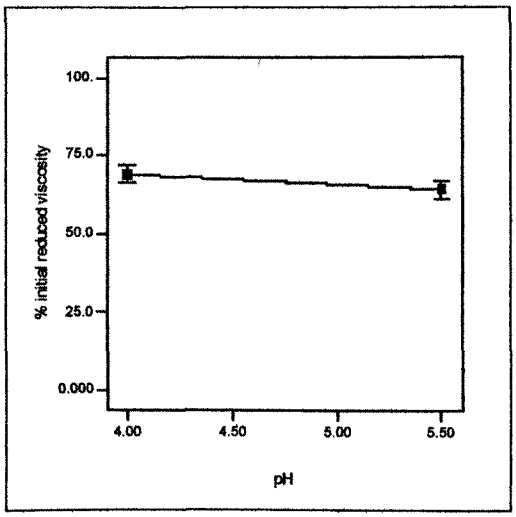

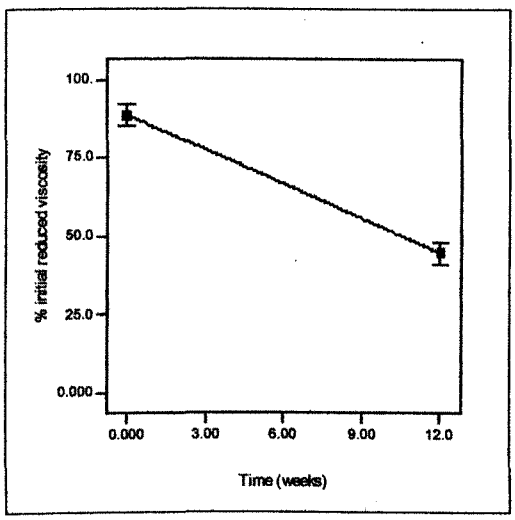

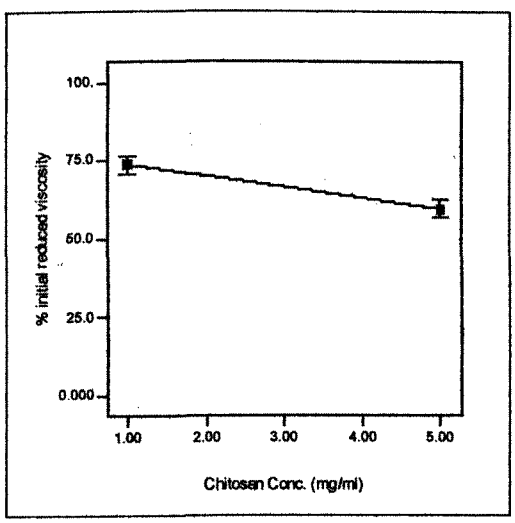

Chapter 5: Effect of Structural Factors on Degradation of Chitosan

5.1 Introduction

The structural properties of chitosan have an effect on its conformation and also on its functional applications. The lower the degree of acetylation of chitosan the more extended its conformation in solution which may make it more susceptible to acid degradation and attack from free radical species. However, it has also been stated that the charged amine groups can protect the subsequent glycosidic oxygen against protonation, which is the first stage in acid hydrolysis (Roberts 1992).

Schipper *et al.* (1996/9) looked at the influence of molecular weight and degree of acetylation on chitosan's ability to function as an absorption enhancer. Chitosans with a low degree of acetylation (1 and 15%) were active as absorption enhancers at low and high molecular weights. However, these chitosans displayed a clear dose-dependent toxicity. Chitosans with degrees of acetylation of 35 and 49% have been shown to enhance transport of ^{14}C-mannitol and with low toxicity, but only if a high molecular weight material is used. So it is possible to select chitosans with maximal effect on absorption and minimal toxicity.

In this chapter the effect of degree of acetylation and molecular weight on degradation are investigated and its attempted to relate this to the selection of the most appropriate chitosan for nasal delivery of therapeutic proteins and peptides.

5.2 Effect of molecular weight and degree of acetylation on degradation

5.2.1 Materials and Methods

The degradation of five chitosan samples (Table 5-1) was investigated over a one-month period. Samples were prepared in triplicate at a concentration of 2 mg/ml in 0.2M acetate buffer, pH 4.3, and stored at ambient temperature in clear glass, closed containers.

Table 5-1:Physical characteristics for chitosan samples

Chitosan	G112	G114	G214	G213	G213*
Molecular Weight*	42400	129000	172000	203000	**207500**
Degree of Acetylation (%)	30	7	4	17	20

*** Average molecular weight determined using SEC-MALLS in 0.2 M acetate buffer, pH 4.3**

Degradation of the chitosan samples was monitored using viscometry and SEC-MALLS. Reduced viscosities were determined for each sample (temperature 20.0°C) at one week intervals using equation (2-16), Chapter 2. Changes in reduced viscosity were used as an indication of degradation as described in section 2.2.2.3., Chapter 2. At two week intervals, the molecular weight of each chitosan sample was determined by SEC-MALLS using the method described in section 2.2.3.3., Chapter 2.

5.2.2 Results and Discussion

Table 5-2 and Table 5-3 show the reduced viscosities and the molecular weights for the chitosan samples over the one month period. The decrease in both reduced viscosity and molecular weight is also indicated as a percentage of the initial viscosity or molecular weight. Comparing the percentage decrease for the two parameters, it can be seen that reduced viscosity

measurements are a good indication of degradation since for all the chitosans except chitosan G112, the percentage decrease is in very good agreement. For chitosan G112, the percentage decrease at two weeks is in good agreement but at four weeks the percentage results are 74% for the reduced viscosity and 40% for the molecular weight. The reduced viscosity was determined at one week intervals and based on the decrease observed over the first three weeks, a percentage viscosity of 74% at four weeks seems reasonable. This suggests that the molecular weight determined using SEC-MALLS is incorrect. This may be due to the low molecular weight of this chitosan and the column system used may not have produced enough separation for accurate measurement of the molecular weight below 30000kDa.

Figure 5-1 shows the decrease in reduced viscosity of the chitosan samples over the one-month storage period in order of decreasing degree of acetylation and increasing molecular weight. With the exception of chitosan G112, the rate of degradation decreases with decreasing degree of acetylation. As the degree of acetylation decreases, the number of charged amino groups present on the chitosan chain will increase. As stated by Roberts (1992), the charged amino group is believed to protect the subsequent glycosidic oxygen against protonation, the first stage in acid hydrolysis. This theory is supported by the results obtained here. Chitosan G112 showed less degradation than the other samples, despite having the highest degree of acetylation. This may be due to the low starting molecular weight of this chitosan sample, and hence shorter chain length. Vårum *et al.* (2001) also examined the effect of degree of acetylation of degradation, and found that as the degree of acetylation decreased, the rate of degradation decreased (see Figure 5-2).

The effect of molecular weight on degradation was not as apparent as that of the degree of acetylation. No trend in the extent of degradation was observed with increasing molecular weight. Molecular weight may play a role in the extent of degradation but the range of molecular weights studied here may be too narrow for any trend to be observed. The results observed here would suggest that the main structural factor affecting degradation is the degree of acetylation.

Table 5-2: Reduced viscosity values (ml/g) for chitosan samples stored over a one-month period and as a percentage of the initial viscosity

Chitosan	Days								
	0	9		14		21		28	
G112	142 ± 10	124 ± 6	*88%*	124 ± 3	*88%*	115 ± 2	*81%*	105 ± 4	*74%*
G114	404 ± 5	361 ± 8	*89%*	356 ± 6	*88%*	348 ± 4	*86%*	289 ± 3	*72%*
G214	911 ± 21	800 ± 14	*88%*	787 ± 18	*86%*	751 ± 11	*82%*	686 ± 8	*75%*
G213	824 ± 15	643 ± 10	*78%*	587 ± 10	*71%*	532 ± 6	*65%*	393 ± 7	*48%*
G213*	989 ± 22	760 ± 11	*77%*	714 ± 13	*72%*	648 ± 10	*66%*	423 ± 9	*43%*

Table 5-3: Molecular weight determined using SEC-MALLS for chitosan samples stored over one-month period

Chitosan	Days				
	0	14		28	
G112	42400 ± 3000	37200 ± 5700	*88%*	16900 ± 3600	*40%*
G114	129000 ± 6000	101000 ± 3000	*78%*	90500 ± 2100	*70%*
G214	172000 ± 6000	140000 ± 3700	*81%*	122000 ± 4000	*71%*
G213	203000 ± 8000	140000 ± 4000	*69%*	99000 ± 4000	*49%*
G213*	207500 ± 8000	160000 ± 1500	*77%*	119000 ± 6300	*57%*

Figure 5-1: Change in viscosity of chitosan samples over one month period

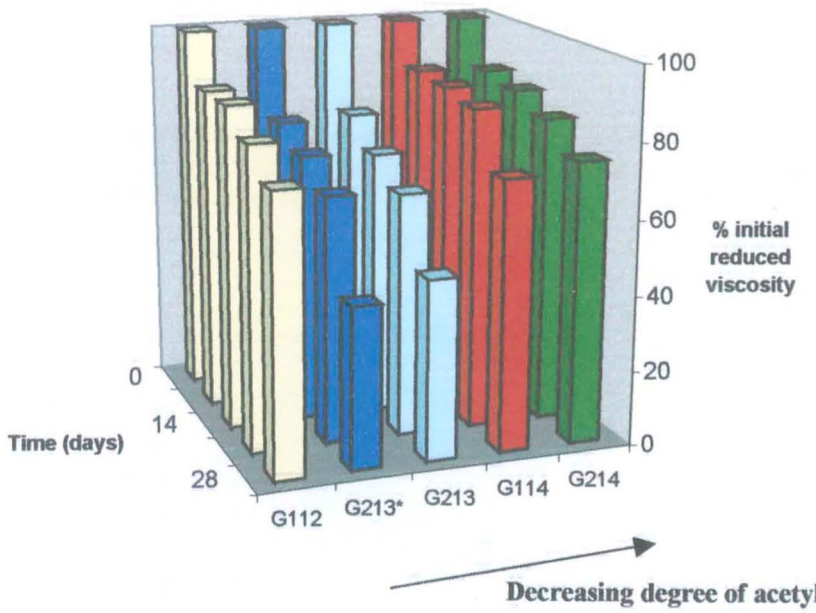

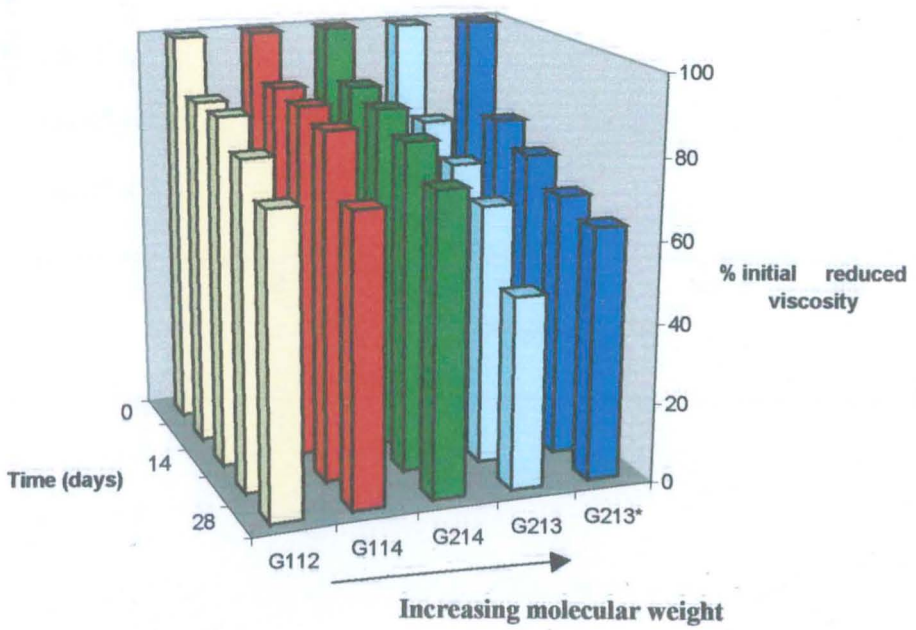

Figure 5-2: Degradation rate constant as a function of DA of the chitosan, determined by the viscosity assay at a chitosan concentration of 1.5mg/ml in 0.4M HCl at 60°C. Adopted from Vårum *et al.* (2001).

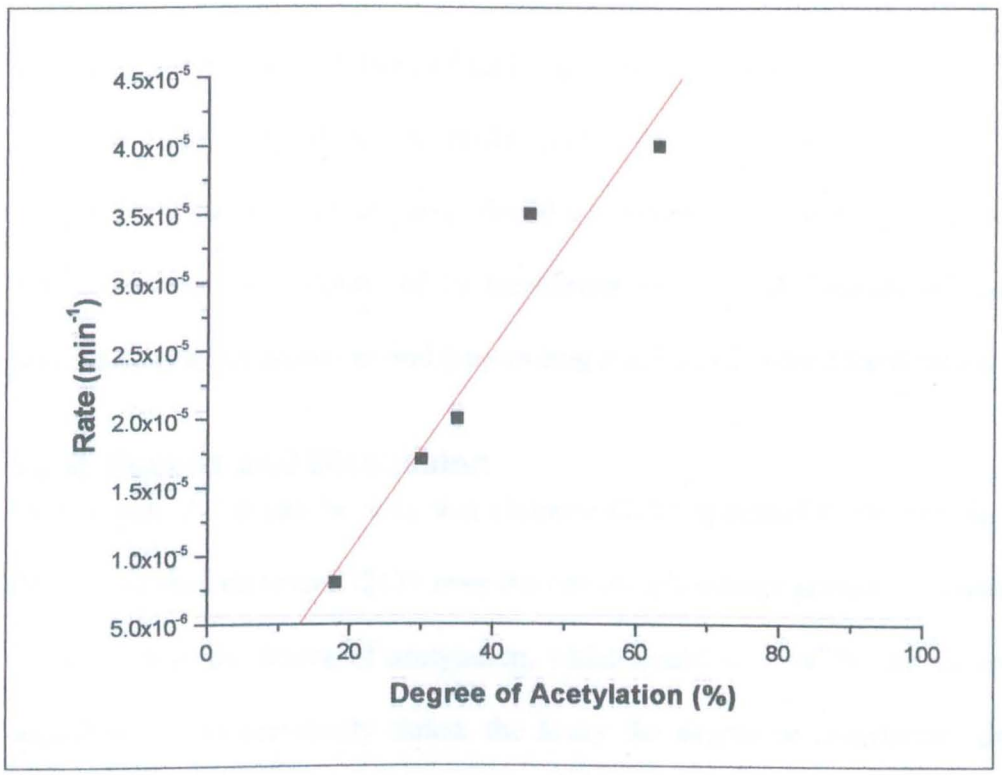

5.3 Comparison of degradation of two chitosans differing in degree of acetylation

5.3.1 Materials and Methods

In this study the aim was to investigate the effect of degree of acetylation on degradation over a range of pH. Two chitosans were chosen; these were chitosan G213* and chitosan G214. These chitosans have similar molecular weights, 207,500 Da and 172,000 Da but different degree of acetylation, 20% and 4%, respectively. Solutions of each chitosan were prepared in either 0.2M HCl (pH 1.28) or 0.1M acetate buffer (pH 4 or 5.5) at a concentration of 1 mg/ml and stored in clear glass, closed containers at ambient temperature. The degradation was monitored by measuring the reduced viscosity of each solution over a one-month period (see section 2.2.2.3., Chapter 2 for details).

5.3.2 Results and Discussion

From Figure 5-3 it can be seen that chitosan G214 appeared to degrade at a slower rate than chitosan G213* over the one month storage period. Chitosan G214 has a lower degree of acetylation, which could account for the slower degradation. As previously stated, the lower the degree of acetylation, the slower the degradation due to the charged amino groups protecting the glycosidic oxygens from protonation (Roberts 1992).

The effect of pH on chitosan degradation was also investigated. Both chitosans showed increased degradation with increasing pH (Table 5-4). The same result was observed in section 4.3.3. As discussed in section 4.3.3, the apparent increased stability of chitosan at low pH may be due to changes in its conformation. During degradation, deacetylation may also occur, which could lead to a more extended conformation masking the decrease in viscosity caused by chain scission.

Figure 5-3: Degradation of chitosans G214 and G213* stored in various pH solutions over an 8-week period

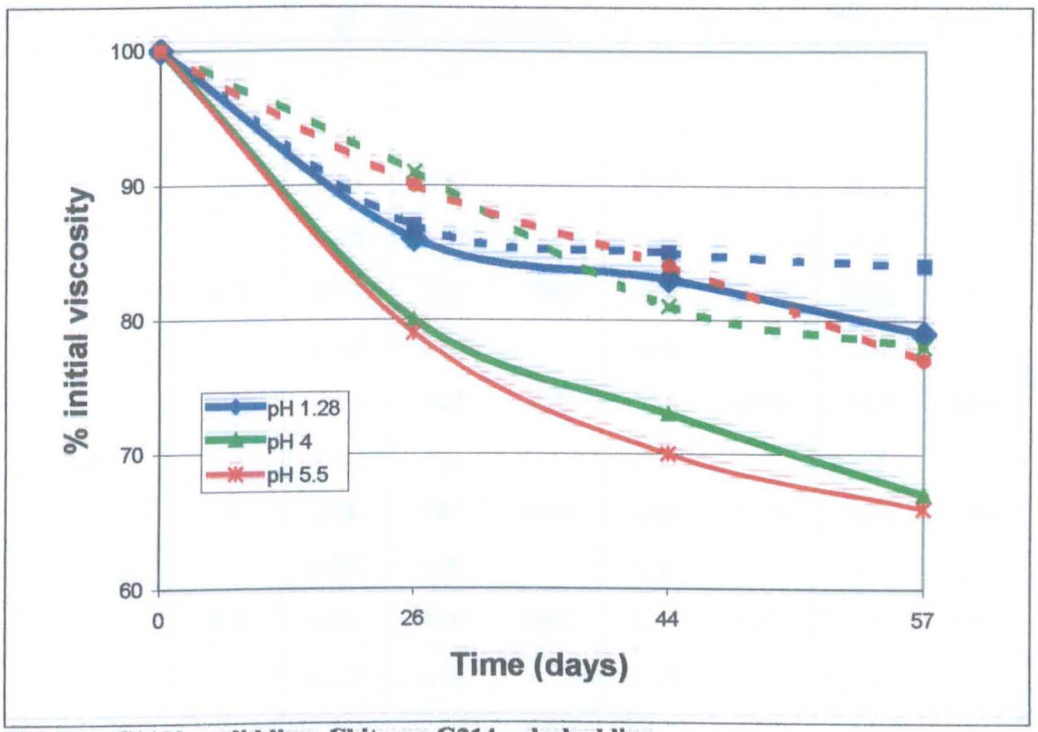

Chitosan G213* - solid line; Chitosan G214 – dashed line

Table 5-4: Reduced viscosity values for chitosans G214 and G213* solutions stored at various pHs over an 8-week period

Chitosan		Days						
	pH	0	26		44		57	
G213*	1.28	645 ± 57	556 ± 11	*86%*	531 ± 11	*83%*	504 ± 13	*79%*
	4	616 ± 16	492 ± 16	*80%*	452 ± 15	*73%*	412 ± 6	*67%*
	5.5	673 ± 60	527 ± 12	*79%*	472 ± 6	*70%*	442 ± 4	*66%*
G214	1.28	629 ± 60	543 ± 3	*86%*	545 ± 6	*87%*	543 ± 8	*86%*
	4	598 ± 26	543 ± 5	*91%*	484 ± 8	*81%*	464 ± 3	*78%*
	5.5	488 ± 37	438 ± 9	*90%*	410 ± 12	*84%*	377 ± 11	*77%*

Chapter 6: Nanoparticle Preparation

6.1 Introduction

The absorption enhancement abilities of chitosan are in part due to ionic interaction with sialic acid residues in mucus. By using nanoparticles to deliver a therapeutic protein, it is thought that the interaction between the protein and the nasal mucosa would be intensified (Fernández-Urrusuno *et al.* 1999). Also, a high concentration of the protein can be achieved at the site of absorption leading to increased absorption.

Chitosan nanoparticles are formed by ionotropic gelation with the anionic counterion tripolyphosphate pentasodium – TPP (Fernández-Urrusuno *et al.* 1999). Ionotropic gelation is a very mild process and occurs when the positively charged amino groups on chitosan interact with the negatively charged tripolyphosphate ions. Tripolyphosphoric acid ($H_5P_3O_{10}$) is a weak polyprotic acid-like phosphoric acid. When TPP is dissolved in water it dissociates into both hydroxyl ions (OH^-) and tripolyphosphoric ions ($P_3O_{10}^{5-}$, $HP_3O_{10}^{4-}$ and $H_2P_3O_{10}^{3-}$). Compared to polyanions, the use of low molecular weight anions to cross-link chitosan was found to be much simpler and milder (Shu and Zhu 2002). It was found that polyphosphate only bound on the surface of chitosan droplets, while TPP could diffuse into the chitosan droplets or films freely to form ionically cross-linked beads or films.

Chitosan nanoparticles prepared using this method show an excellent capacity for association with proteins such as BSA, tetanus toxoid or insulin. The mechanism of association of proteins to chitosan nanoparticles is mediated by the ionic interaction between both macromolecules. For example, insulin when dissolved in NaOH is negatively charged (pI 5.3), and electrostatic

interaction with the positively charged amino groups on chitosan is favoured. This mechanism was also supported by the observed partial neutralisation of the nanoparticle surface charge with increasing association with insulin (Fernández-Urrusuno *et al.* 1999; Janes *et al.* 2001). Although proteins of positive charge can form complexes with chitosan, other mechanism are involved in their association with chitosan nanoparticles. These include hydrophobic interactions, hydrogen bonding, other physicochemical forces dependent upon the specific nature of the associated protein and physical entrapment caused by gelation of chitosan with TPP in nanoparticulate form. These mechanisms enable significant amounts of insulin (15-30%) to be associated with the chitosan nanoparticles even at a pH where insulin is predominantly positively charged (Janes *et al.* 2001).

In this chapter, the yield of nanoparticles is studied using various methods and the effect of chitosan properties on yield are also examined.

6.2 Methods

6.2.1 Preparation of Nanoparticles

Chitosan nanoparticles were prepared using chitosan CL210 as described in section 2.2.4.1., Chapter 2. The ratio of chitosan to tripolyphosphate pentasoidum (TPP) was 6:1, as used by Dyer *et al.* (2002).

6.2.2 Estimation of yield and loading of chitosan nanoparticles

As with any manufacturing or production process it is important to determine the yield of the final product so that the efficiency of the process can be evaluated. The most commonly used method for the estimation of nanoparticle yield is to determine the dry weight of the nanoparticles. An

alternative method is to determine the concentration of chitosan in the supernatant layer using the ninhydrin assay. The details of these methods are described below.

6.2.2.1 Dry Weight Yield

Triplicate samples of nanoparticle suspension (10ml each) were transferred to pre-weighed glass tubes and centrifuged at approximately 3660 rpm for 30 minutes. The supernatant was discarded and the remaining pellet placed in an oven at 100°C until a constant weight was reached.

The theoretical weight of the nanoparticle was based solely on the weight of chitosan and TPP added to the nanoparticle mixture. For nanoparticles prepared at a 6:1 ratio (chitosan:TPP) the theoretical yield was 16.69mg.

$$\text{Yield}(\%) = \frac{\text{Weight dry nanoparticle}}{\text{Theoretical Yield}} \text{x}100 \quad \textbf{(6 - 1)}$$

For insulin loaded nanoparticles it is important to determine how much insulin is encapsulated. The amount of insulin present in the supernatant was determined using HPLC (as described in section 2.2.7) and from this the Loading Efficiency (LE) and Association Efficiency (AE) can be calculated.

$$\text{LE} = \frac{\text{Total Insulin - Amt Insulin in Supernatant}}{\text{Dry weight of nanoparticles}} \text{x}100 \quad \textbf{(6 - 2)}$$

$$\text{AE} = \frac{\text{Total Insulin - Amt Insulin in Supernatant}}{\text{Total Insulin}} \text{x}100 \quad \textbf{(6 - 3)}$$

6.2.2.2 Measurement of Chitosan in supernatant

The amount of chitosan present in the supernatant layer after centrifuging of the nanoparticle suspension can be determined using the ninhydrin assay (see section 2.2.5., Chapter 2). This assay is based on the reaction of ninhydrin with a primary amino group such as found on chitosan. The reaction results in a coloured product, diketohydrindylidene-diketohydrindamine (Ruhemann's purple), which has a λ_{max} at 570 nm. By preparing a standard calibration curve from solutions of known chitosan concentration, it is possible to determine the amount of chitosan present in the supernatant.

$$\text{Yield}(\%) = \frac{\text{Total Chitosan - Amt Chitosan in Supernatant}}{\text{Total Chitosan}} \text{x} 100 \qquad \textbf{(6 - 4)}$$

6.2.2.3 Estimation of Insulin Loading using AUC

The loading efficiency and association efficiency of nanoparticles can be calculated by measuring the insulin in solution using HPLC, and substituting this value into equations (6-2) and (6-3), respectively.

An alternative method is to run a sedimentation velocity type experiment on the analytical ultracentrifuge using absorption optics. The theory behind this is that by using UV optics, the movement of insulin, both encapsulated and in solution can be observed down the cell since chitosan will be invisible. For UV optics, the material being studied has to possess a chromophore to absorb the UV light. Insulin, like most proteins possesses a chromophore and a full UV scan showed that λ_{max} was at 280nm. Since chitosan does not possess a chromophore it will not absorb light in the UV region and should be invisible on the scans recorded.

Sedimentation velocity experiments were run at 2000 rpm and 45000 rpm for both chitosan and insulin-loaded nanoparticles. The results are discussed in the next section.

6.3 Results

6.3.1 Comparison of yields from dry weight and ninhydrin assay

The results from both methods of determining nanoparticles yield were compared in order to determine the validity of each method. These results are shown in Table 6-1.

Table 6-1: Yields for chitosan nanoparticles as determined using dry weight and the ninhydrin assay (n=3)

Method	Chitosan-insulin nanoparticles	Chitosan only nanoparticles
Dry Weight	26 ± 4	15 ± 2
Ninhydrin assay	29 ± 1	-

From comparison of the results obtained using insulin-loaded chitosan nanoparticles it would appear both methods produce similar results. This was confirmed by T-test that showed the two sample groups were not significantly different ($t_{0.05,3df} = 3.182$, $t = 1.22$).

For the estimation of yield using the ninhydrin assay the most important step in the method is the centrifugation of the nanoparticle suspension to separate the nanoparticles from the supernatant layer. If the centrifugation speed and duration is not sufficient to cause all the nanoparticles to sediment to the bottom of the sample tube, underestimation of yield could occur. To verify that the chosen speed and duration of centrifugation was sufficient to cause complete sedimentation of nanoparticles present, a second centrifugation step

was included and the supernatant after both step analysed using the ninhydrin assay. The chitosan concentration determined after each step was the same indicating that a speed of 3660 rpm and duration of 90 minutes is adequate to cause complete sedimentation of the nanoparticles.

Inclusion of insulin in the nanoparticles appears to result in increased yield. This could be due to interaction occurring between insulin and chitosan as well as between chitosan and TPP. However, the magnitude of this enhanced yield should be treated with caution, as the amount of insulin incorporated in the nanoparticles was not included in the calculation of yield.

6.3.2 Loading of nanoparticles estimated using AUC

6.3.2.1 Insulin Nanoparticles

Figure 6-1 shows a theoretical representation of the sedimentation of the nanoparticles during a sedimentation velocity experiment at 2000 rpm and 45000 rpm. At 2000 rpm, insulin incorporated in the chitosan nanoparticles should begin to sediment (Case A), whereas insulin that is free in solution should not (Case B). This is due to the difference in the molecular weight of the nanoparticles and insulin. Case C shows the theoretical sedimentation profile when insulin is partially incorporated in the chitosan nanoparticle. Sedimentation of the insulin incorporated in the nanoparticles will occur but the baseline remains high due to the free insulin in solution, which does not sediment at 2000 rpm. At 45000 rpm (case D), insulin in solution should in theory begin to sediment, although due to the low molecular weight (6000 Da), complete sedimentation to the cell base will most likely not occur.

Figure 6-1: Diagrammatic representation of sedimentation of insulin loaded chitosan nanoparticles

Case A: Insulin fully incorporated – 2000 rpm

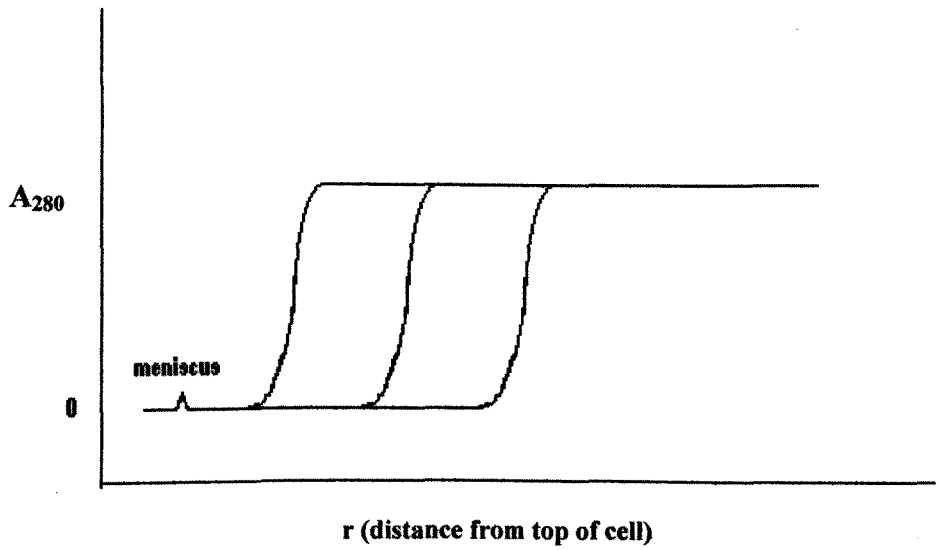

Case B: Insulin NOT incorporated (NB assuming chitosan nanoparticles do not have significant turbidity at 280nm) – 2000 rpm

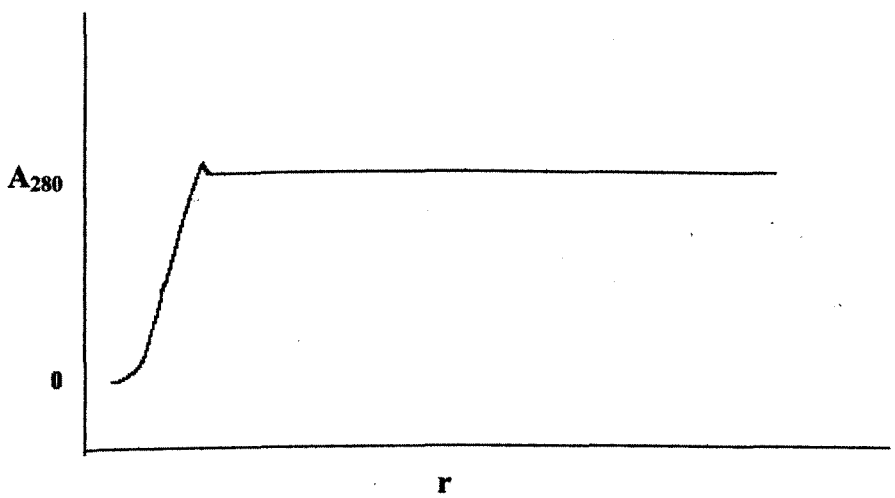

Case C: Insulin partially incorporated – 2000 rpm

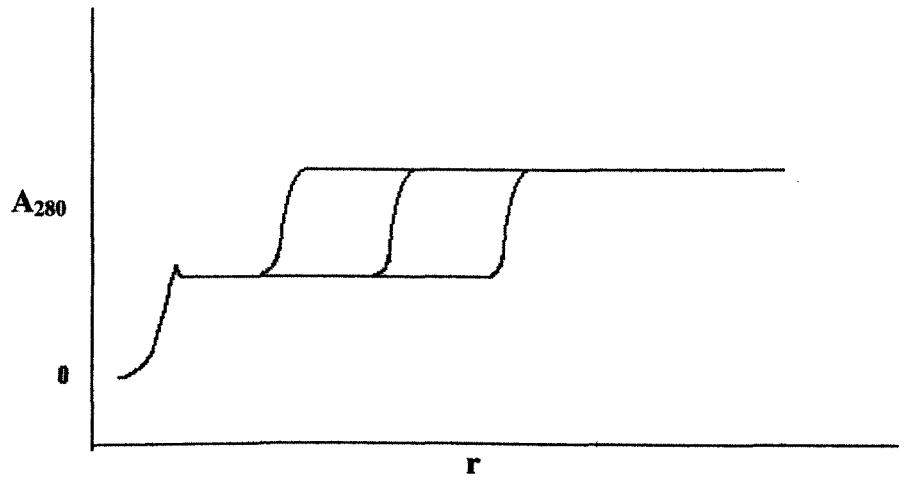

Case D: Insulin NOT incorporated – 45000 rpm

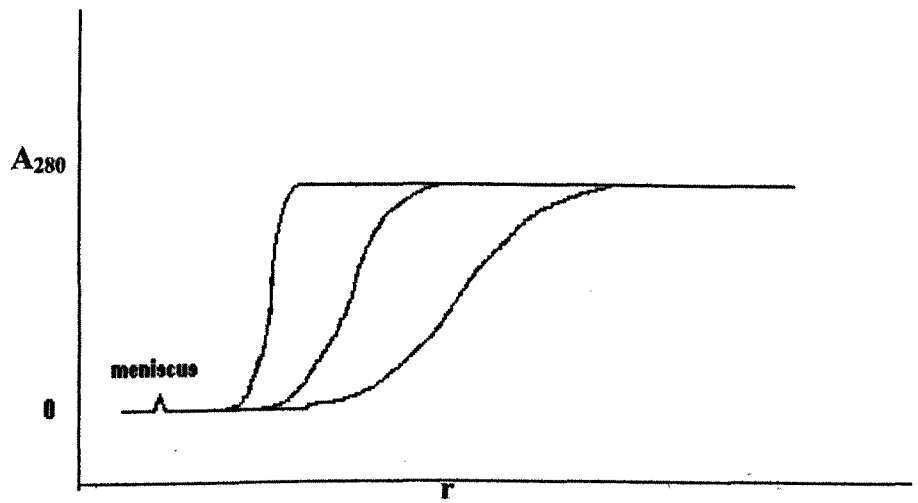

6.3.2.2 Results from sedimentation experiments – insulin nanoparticles

Figure 6.2 shows the actual sedimentation profile for insulin (1.5 mg/ml) at high and low centrifugation speeds. At 2000 rpm, no movement of insulin down the centrifuge cell was observed. This is due to the low molecular weight of insulin (MW ~ 6000Da). At 45000 rpm insulin began to redistribute.

As previously mentioned, since free insulin does not show significant redistribution at 2000 rpm, sedimentation observed at this speed should be due to insulin incorporated in the chitosan nanoparticles. Figure 6-3 shows the sedimentation of insulin loaded chitosan nanoparticles. At 2000 rpm sedimentation can be seen occurring over the three-hour period studied. This is likely to be due to the insulin encapsulated in the chitosan nanoparticles since chitosan should not absorb or scatter UV light at 280nm.

Comparison of Figure 6-3 (a and b) reveals a residual absorbance at the meniscus after the nanoparticles have begun to sediment to the base of the cell at 2000 rpm. This shows that some of the insulin has remained free in solution. By determining the value of this residual absorbance, the quantity of insulin that has been encapsulated in the chitosan nanoparticle can be estimated.

A control experiment was carried out of chitosan only nanoparticles to show that chitosan does not absorb or scatter UV light at 280 nm. The scans obtained at 2000 rpm and 45000 rpm are shown in Figure 6-4. It was hoped that these scans would show no absorbance, however the data obtained was very similar to that in Figure 6-3 for the insulin-loaded chitosan nanoparticles.

Due to the density of the chitosan nanoparticles, they cause scattering of UV light which is picked up by the XLA AUC.

Comparing Figure 6-3(a) and Figure 6-4(a), a difference in the level of absorbance can be seen (approximately 2.2 A and 1.4 A respectively). The difference in absorbance between the two nanoparticle solutions would be due to the insulin incorporated in the nanoparticles in Figure 6-3(a), however, since chitosan nanoparticles cause scattering of light, this may mask some of the absorbance from insulin so a quantitative measure of the insulin incorporated in the nanoparticles cannot be obtained.

In Figure 6-4(a), no residual absorbance was observed at the meniscus after the nanoparticles began to sediment, reinforcing that the residual absorbance observed in Figure 6-3(a) was due to free insulin in solution.

Figure 6-2: Sedimentation profiles of Insulin solution (1.5 mg/ml)

(a) 2000 rpm

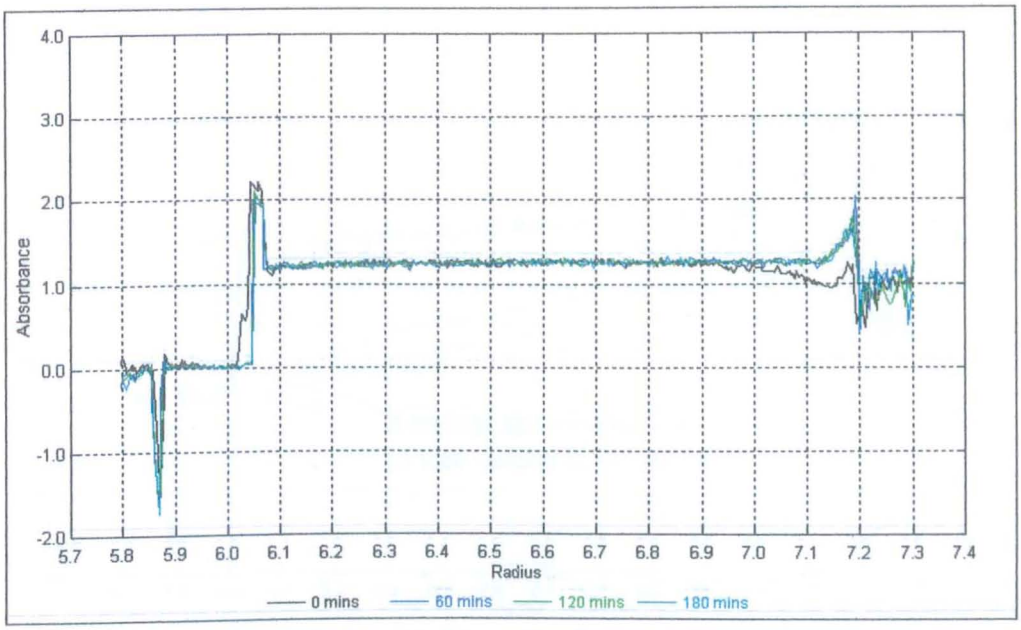

(b) 45000 rpm

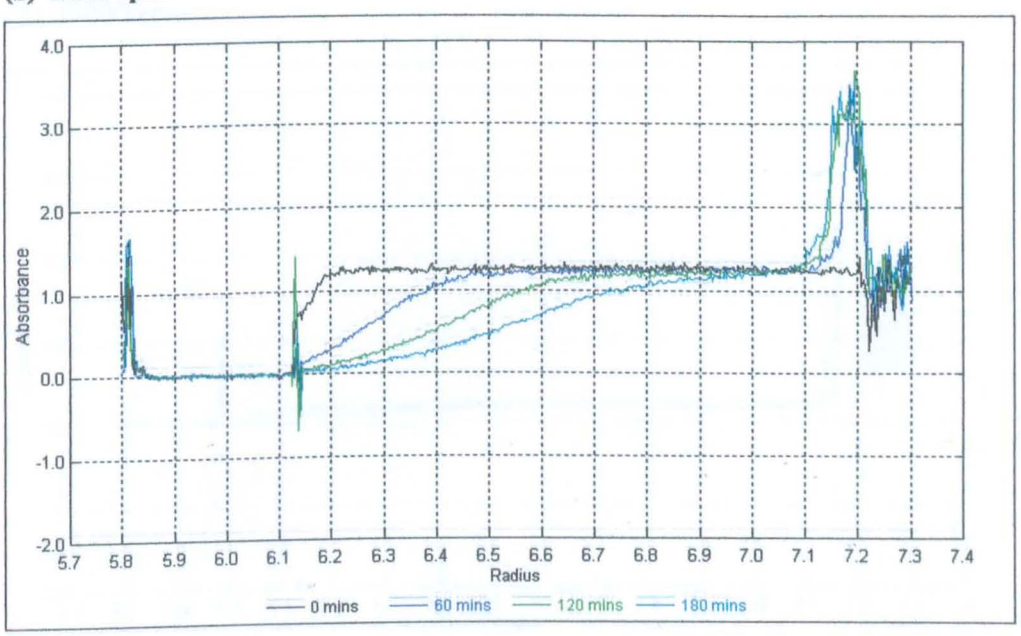

Figure 6-3: Sedimentation profiles of Insulin loaded chitosan nanoparticles

(a) 2000rpm

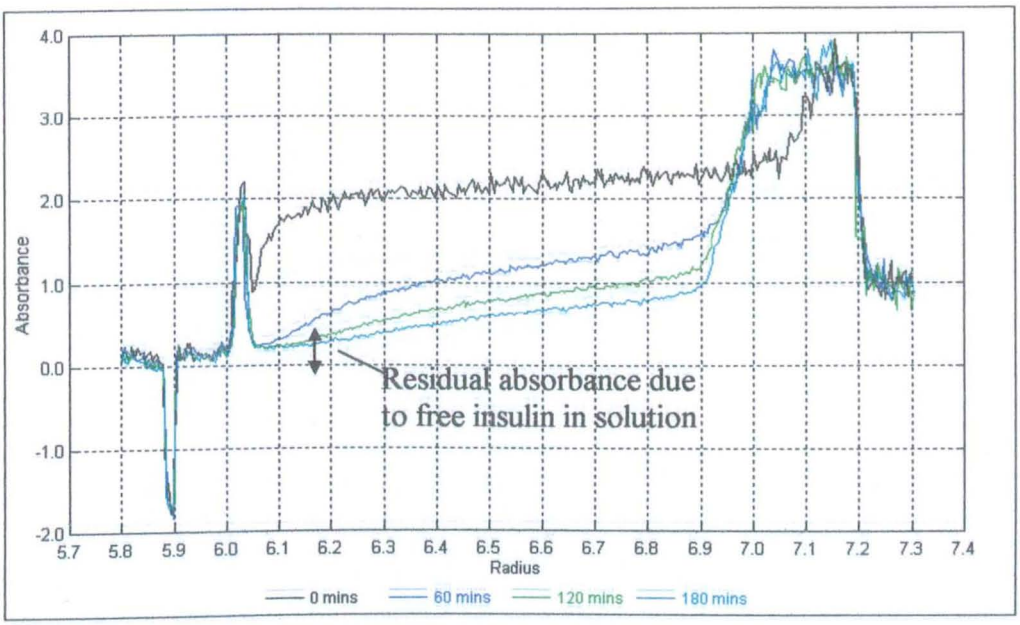

(b) 45000 rpm

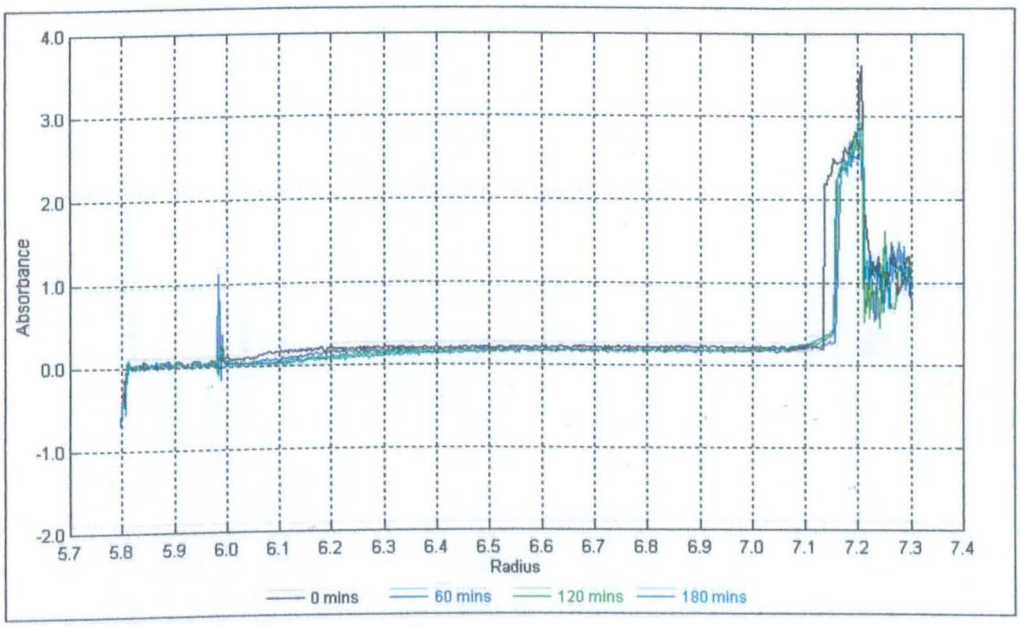

Figure 6-4: Sedimentation profiles of Chitosan only nanoparticles

(a) 2000rpm

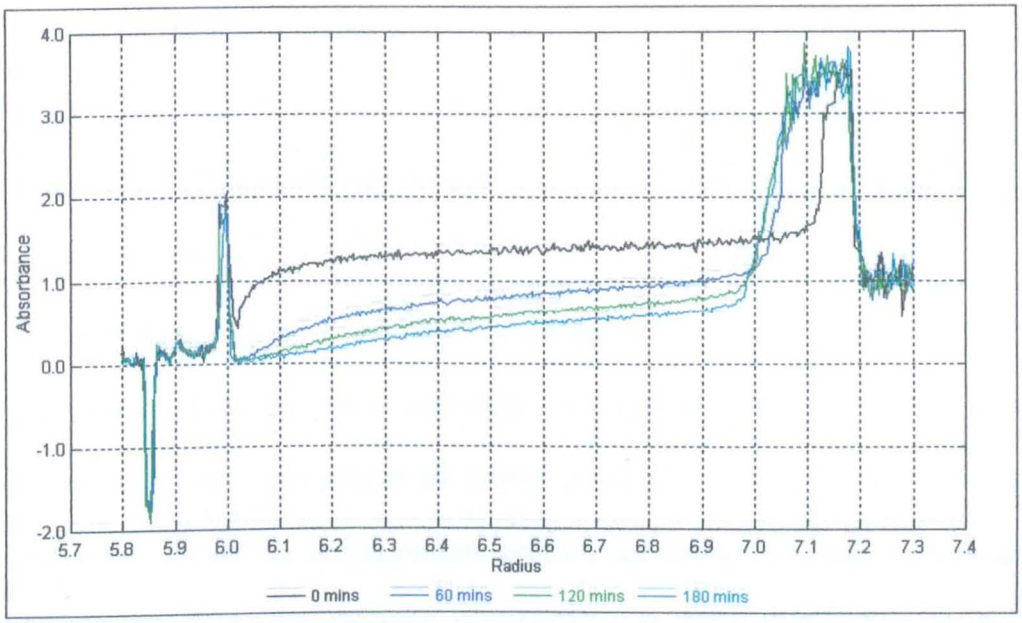

(b) 45000 rpm

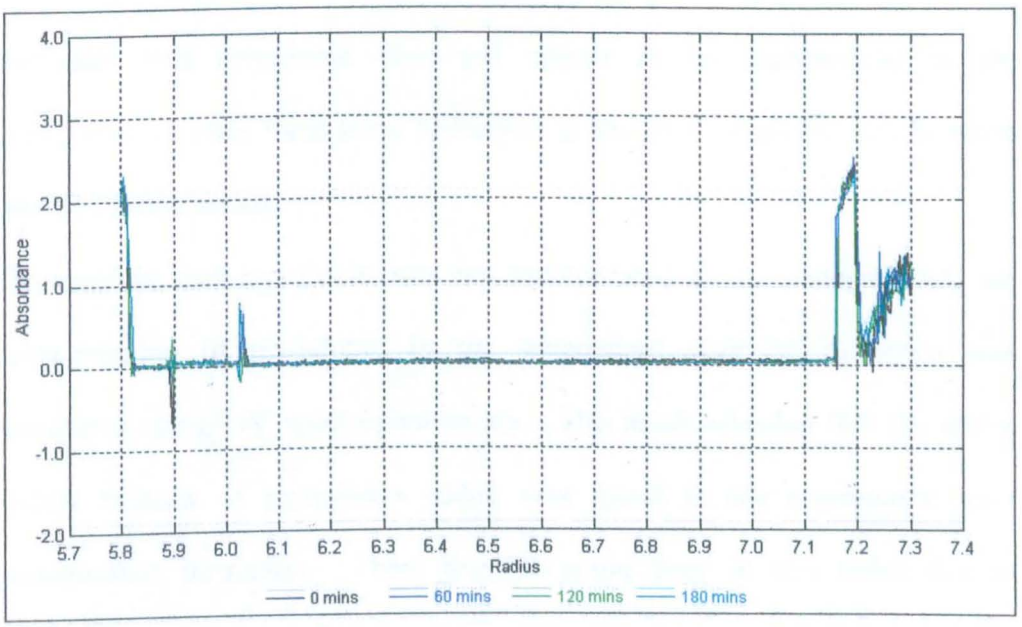

6.3.2.3 Results from sedimentation experiments – myoglobin nanoparticles

Since chitosan nanoparticles scattered light in the UV region, the method was evaluated using myoglobin incorporated into chitosan nanoparticles since myoglobin absorbs light in the visible region (λ_{max} = 410nm), and at the higher wavelength the nanoparticles should scatter less (scattering is approximately proportional to $1/\lambda^4$)

Sedimentation velocity scans obtained on the XLI AUC at 2000 and 45000 rpm should show the same behaviour for myoglobin as for insulin, with sedimentation only occurring at the higher speed.

Figure 6-5 shows the sedimentation profiles for myoglobin loaded chitosan nanoparticles and chitosan only nanoparticles at 2000 rpm. The profiles obtained are the same in both the presence and absence of myoglobin. This shows that firstly chitosan nanoparticles still scatter light at 410 nm, and secondly that myoglobin does not appear to be incorporated in the nanoparticles since there is no difference in the level of absorbance between the two formulations.

To confirm that myoglobin was not incorporated in the nanoparticles, the concentration of myoglobin in the supernatant after centrifugation was measured using UV spectrophotometry. The result revealed that the entire initial amount of myoglobin added was found in the supernatant after nanoparticle formation. There may be some error in this result due to fragments of nanoparticles that were not removed by filtration. Both insulin and myoglobin has similar isoelectric points (pI = 5.3 and 5.5 respectively) so both will be negatively charged during the formation of chitosan nanoparticles, and thus have the potential to form electrostatic bonds with the

amine groups on chitosan. The main difference between the two proteins is their molecular weight (6000 Da and 17000 Da for insulin and myoglobin respectively). Since the molecular weight of myoglobin is almost three times that of insulin this may affect its ability to penetrate within the chitosan network before the nanoparticle was formed by complexation with TPP. It is also possible that myoglobin could be adsorbed onto the surface on the chitosan nanoparticles after formation, but the high speeds used in centrifugation cause it to dissociate into the supernatant layer.

Figure 6-5: Sedimentation velocity scans of Chitosan nanoparticles at 410 nm

(a) Chitosan nanoparticles containing myoglobin at 2000 rpm

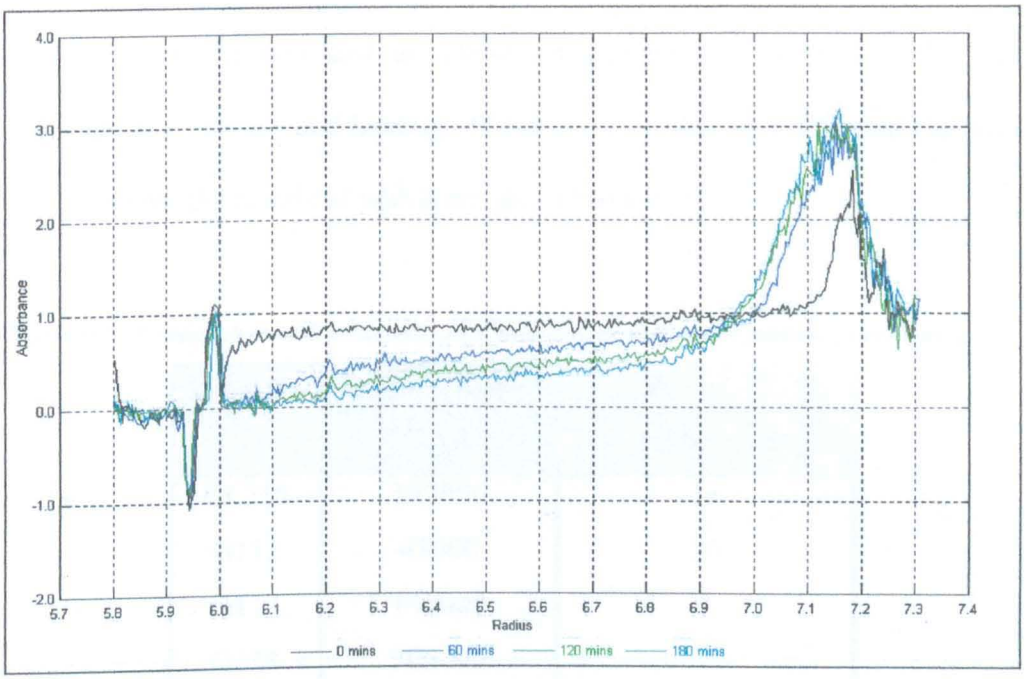

(b) Chitosan only nanoparticles at 2000 rpm

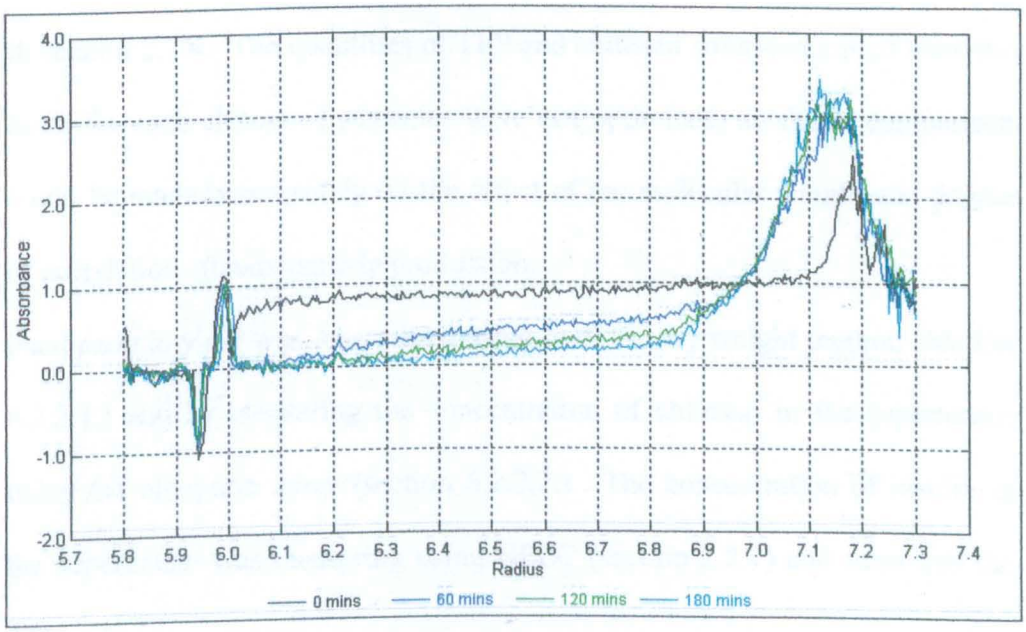

6.4 Effect of physicochemical properties of Chitosan on nanoparticle yield and loading capacity

The aim of this set of experiments was to investigate if the physicochemical properties of chitosan had an effect on nanoparticle yield and also the association efficiency and loading efficiency of insulin. Six different chitosan were studied, the details of which are given in Table 6-2.

Table 6-2: Physicochemical properties of Chitosans used in nanoparticle preparation

Chitosan	Molecular Weight	Degree of Acetylation
CL210	173000	18
G112	45000	30
G114	141000	7
G214	205000	4
G213	263000	17
G213*	277000	20

The nanoparticles were prepared according to the method previously described in section 2.2.4. The quantities of TPP and chitosan solutions mixed were the same for each chitosan (quantities were not optimised) so that a comparison could be made based solely on the effect of the molecular weight and degree of acetylation on nanoparticle production.

Nanoparticle yield was determined using both the dry weight method (section 6.2.2.1.) and by measuring the concentration of chitosan in the supernatant using the ninhydrin assay (section 6.2.2.2.). The concentration of insulin in the supernatant was measuring using HPLC (section 2.2.7) and from this the

association and loading efficiency of the nanoparticles was determined. Each measurement was carried out in triplicate.

6.4.1 Results and Discussion

Table 6-3: Yields and insulin loading of nanoparticles prepared from various chitosan samples

Chitosan	Yield (%)		Association Efficiency (AE) %	Loading Efficiency (LE) %
	Dry Weight	Chitosan Conc.		
G112	61 ± 11	32 ± 6	54 ± 7	20 ± 6
G114	48 ± 5	37 ± 1	63 ± 9	29 ± 7
G214	26± 1	27 ± 3	34 ± 5	29 ± 6
G213	28 ± 4	18 ± 2	72 ± 6	55 ± 12
G213*	30 ± 3	21 ± 2	83 ± 4	59 ± 5
CL210	26 ± 4	43 ± 2	-	-

6.4.1.1 Yield

The yields obtained using the two methods are not consistent for each chitosan. For chitosan G112, the yield obtained from the dry weight method was almost twice that obtained using the ninhydrin assay. As mentioned in section 6.3, the most important step in determining the concentration of chitosan in the supernatant layer is the centrifugation step. It was concluded that the speed and duration of this centrifugation step was sufficient to remove all the nanoparticles from the supernatant layer as no decrease in chitosan concentration was observed after further centrifugation. This would suggest that in this case the results obtained from the dry weight method might be an overestimation of yield possibly due to inadequate drying.

From the yield obtained using the concentration of chitosan in the supernatant, chitosan CL210 resulted in the highest yield of nanoparticles. Chitosan CL210 is a hydrochloride salt, which contains approximately 82% chitosan base, whereas the other chitosans studied are all glutamate salts, which contains about 55% chitosan base. Therefore chitosan CL210 would contain more chitosan base per volume, which would account for the higher yield observed. By studying the results obtained from the glutamate salts, the effect of degree of acetylation and molecular weight can be examined (Figure 6-6). Neither parameter showed any trend for its effect on yield. With the exception of chitosan G112, there appears to be a slight tendency for decreasing degree of acetylation to increase yield. This could be explained by the increase in charged amino groups with decreasing acetylation. This would allow more ionic interaction to occur between chitosan and TPP leading to an increase in yield. With increasing molecular weight it may have been expected that the yield would increase due to the longer chain lengths of the chitosan molecules and hence an increase in charged amino groups (Figure 6-7). This effect was not observed, however, it is important to remember that in this study the effect of degree of acetylation and molecular weight could not be studied independently.

Figure 6-6: Yield of nanoparticles produced from various chitosan shown as a function of degree of acetylation of chitosan

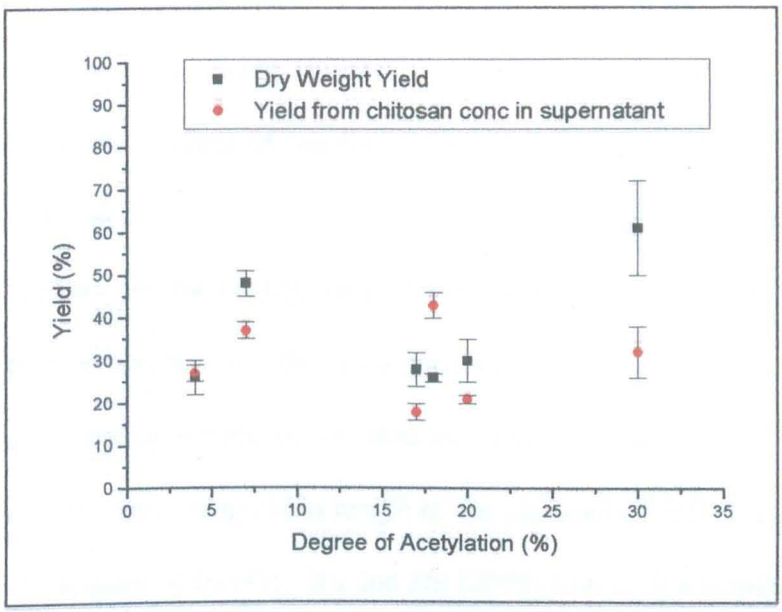

Figure 6-7: Yield of nanoparticles produced from various chitosans shown as a function of molecular weight of chitosan

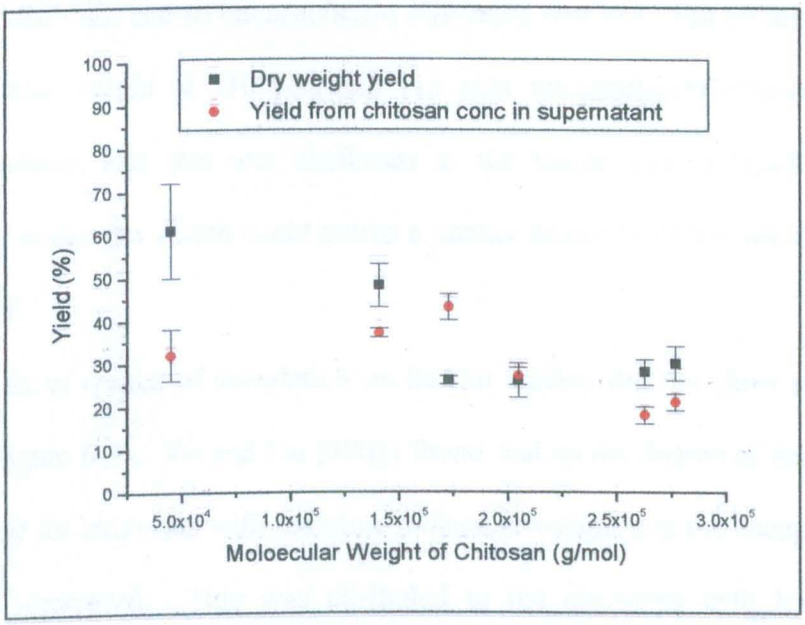

6.4.1.2 Insulin Loading

Insulin loading of the chitosan nanoparticles was determined by measuring the loading efficiency and association efficiency as described in section 6.2.2.1. Nanoparticles produced using chitosan CL210 did not appear to encapsulate any insulin as the amount of insulin in the supernatant was the same as the total amount added.

From the results obtained using the glutamate salts, the association efficiency and loading efficiency of the nanoparticles appeared to increase with increasing molecular weight of the chitosan used (Figure 6-8). This can be explained by the increasing chain length of the chitosans, leading to increased physical entrapment of insulin. Xu and Du (2003) found, in a similar manner, that as the molecular weight of chitosan increased (same DA), the encapsulation of BSA increased. Chitosan with a molecular weight of 48 kDa has a relatively short chain length compared to BSA, which makes entrapment of BSA difficult, and so encapsulation efficiency was low. For chitosans with a molecular weight of 210 kDa and 115 kDa, encapsulation efficiency was much greater, and this was attributed to the longer chains length of the chitosan molecules which could entrap a greater amount of BSA when gelated with TPP.

The effect of degree of acetylation on insulin loading did not show a distinct trend (Figure 6-9). Xu and Du (2003) found that as the degree of acetylation decreased for chitosans with the same molecular weight that the encapsulation of BSA increased. This was attributed to the chitosans with lower DA containing more functional groups that could complex with the acid groups of BSA and gelate with TPP so increasing the encapsulation efficiency of BSA.

Chitosans G213 and G213* show the highest loading. This may be attributed to their high molecular weight and relatively low degree of acetylation (17 – 20%).

For these chitosans it would be necessary to determine the optimal concentrations of chitosan and TPP, so as to further increase yield and insulin loading.

Figure 6-8: Insulin loading of nanoparticles produced from various chitosans as a function of molecular weight of chitosan

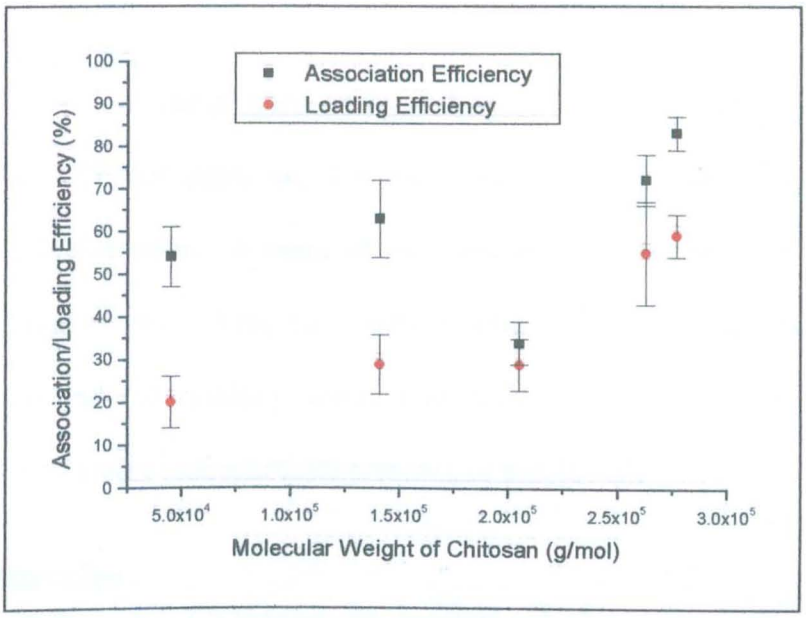

Figure 6-9: Insulin loading of nanoparticles produced from various chitosans as a function of degree of acetylation of chitosan

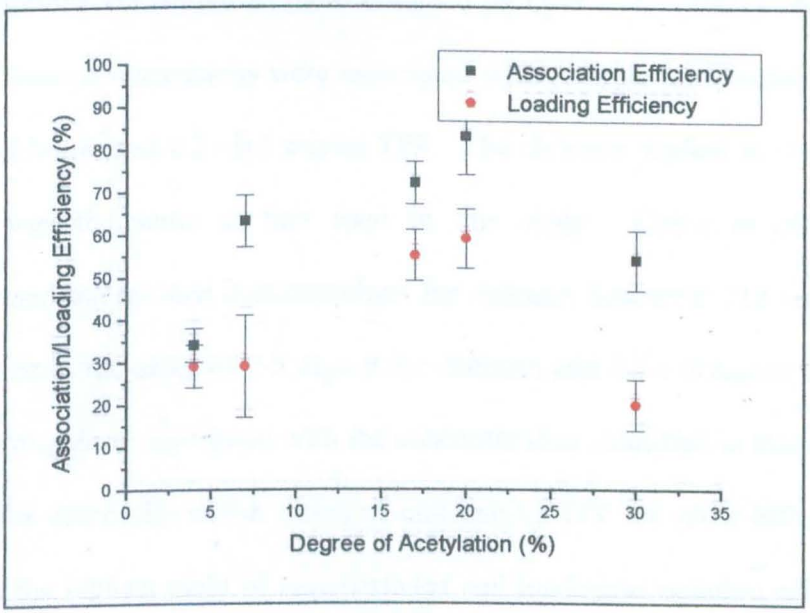

6.5 Optimisation of Chitosan:TPP ratios for Chitosan G213

6.5.1 Methods

Preliminary experiments were performed to identify the optimal chitosan G213 and TPP concentrations for the achievement of ionic gelation and nanoparticle formation. A range of chitosan samples was prepared over the concentration range 1 – 5 mg/ml. To these solutions, varying amounts of TPP was added and the resulting solution identified as clear (no nanoparticles formed), opalescent (nanoparticles present), or precipitate.

6.5.2 Results

The results (Figure 6-10) indicate the resulting solution characteristics at each ratio of chitosan and TPP. For chitosan G213 it would appear that the most appropriate concentration of chitosan in the final nanoparticle solution is between 1 – 5 mg/ml and for TPP between 0.25 – 0.5 mg/ml. These concentrations are similar to those obtained by Dyer *et al.* (2002) who found that opalescent suspensions were associated with formulations containing 1-3 mg/ml chitosan and 0.2 –0.5 mg/ml TPP. The chitosan studied in Dyer *et al.* (2002) was the same as that used in this study. Calvo *et al.* (1997) investigated the optimal concentrations for chitosan Seacure® 213 and found these to be in the order of 1-3 mg/ml for chitosan and 0.2-1.0 mg/ml for TPP, which are again in agreement with the concentrations identified in this study.

To further determine which ratios of chitosan to TPP are most efficient i.e. produce the highest yield of nanoparticles and loading/association efficiency, several chitosan/TPP ratios were chosen predicted to result in an opalescent solution.

Figure 6-10: Identification of chitosan G213 and TPP concentrations appropriate to nanoparticle formation

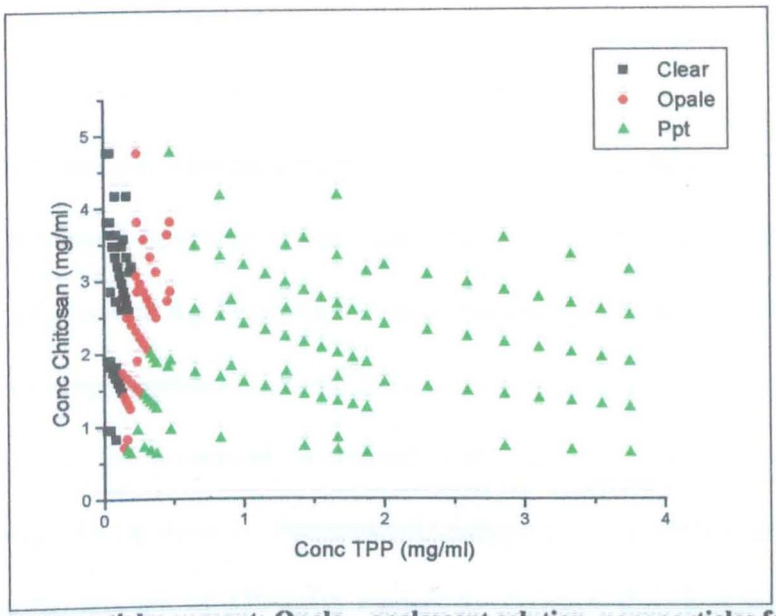

Clear – no nanoparticles present; Opale – opalescent solution, nanoparticles formed; Ppt – precipitate

Table 6-4: Nanoparticle yields obtained using different ratios of chitosan G213 and TPP

Conc. Initial CS solution (mg/ml)	Conc. Initial TPP solution (mg/ml)	Ratio CS:TPP (w:w)	Yield (%)	
			Dry Weight	Chitosan Conc.
2	1	5.7 : 1	25 ± 6	39 ± 4
3	1	6.7 : 1	19 ± 3	30 ± 12
3	5	6 : 1	30 ± 2	42 ± 7
4	1	6.7 : 1	25 ± 2	29 ± 3

Table 6-5: Insulin loading of chitosan nanoparticles at different ratios of chitosan G213 and TPP

Ratio CS:TPP	Yield	Loading Efficiency (%)	Association Efficiency (%)
6 : 1	31 ± 5	16 ± 2	25 ± 2
7 : 1	24 ± 1	20 ± 3	28 ± 4

Table 6-4 shows the yields obtained using different ratios of chitosan to TPP. The highest yield was obtained when the ratio was 6:1. In general the yield increased as the ratio decreased.

The yield of nanoparticles may be expected to increase as the concentration of chitosan increases; however, if the concentration of TPP is not high enough, the level of crosslinking between the two species would not be sufficient to cause enough aggregation to result in nanoparticle formation. This theory is reinforced by the observed increased yield at lower ratios, since the crosslinking will be denser. Fernández-Urrusuno *et al.* (1999) found that by increasing the amount of TPP with respect to chitosan, the nanoparticle yield increased which reinforces our findings.

As the ratio of chitosan to TPP increases, the surface charge in the nanoparticles will also increase. This may result in higher loading of insulin due to increased ionic interaction between insulin and chitosan. Nanoparticles were prepared at ratios of 6:1 and 7:1 and the yield and insulin loading determined. The results are shown in Table 6-5. The yield of nanoparticles was greatest at the lower ratio due to the increased level of crosslinking as explained previously (Table 6-5). The loading efficiency and association efficiency was lowest for those nanoparticles prepared at the lower ratio despite the higher yield. This can be explained due to the reduced charge on the nanoparticles due to increased crosslinking with TPP. As mentioned previously insulin loading with chitosan nanoparticles is due to ionic interaction with the positively charged chitosan as well as hydrophobic interaction, hydrogen bonding and some physical entrapment. As the ratio of chitosan to TPP increases, the amount of remaining charged amino groups on

chitosan increases, and this will enable more interaction with insulin, and hence increased loading capacity. Fernández-Urrusuno *et al.* (1999) also found that the loading capacity was affected by the insulin concentration and the chitosan:TPP ratio. Data indicated that insulin loading was directly related to the amount of insulin and chitosan but inversely related to the amount of TPP. This suggested that there was a competition between TPP and insulin in their ionic interaction with chitosan.

Chapter 7: Stability of Chitosan in complex

7.1 Introduction

In this chapter the effect on chitosan stability of i) complexation of chitosan with tripolyphosphate pentasodium (TPP) and ii) chitosan being in the solid state, is investigated. Chitosan nanoparticles, as discussed in the previous chapter, were formed by ionotropic gelation using TPP as the counterion. In order to investigate the effect of complexation, and hence storage of chitosan in the solid state, on the stability of chitosan it is necessary to be able to dissociate the complex back to the starting components. To separate the complex formed between chitosan and TPP requires harsh conditions which could degrade chitosan in the process. It was therefore decided to evaluate the chitosan stability using a complex formed between chitosan and insulin that can be dissociated by altering the pH of the solution.

7.2 Methods

7.2.1 Preparation of Chitosan-Insulin Complex

A 4 mg/ml chitosan solution (chitosan G213*) was prepared by dissolving 200 mg chitosan G213 in 40 ml ultrapure water and adjusting the pH to 5.5 by adding 0.1M NaOH and making up the volume to 50 ml with ultrapure water.

A 4 mg/ml human zinc insulin solution was prepared by dissolving 200 mg zinc insulin in 40 ml ultrapure water adjusted to pH 4.0 with 0.1M NaOH. When the insulin was dissolved the pH was adjusted to 7.0 with 0.1M HCl and the volume made up to 50 ml with water.

The complexes were prepared by adding dropwise 50ml of 4 mg/ml insulin solution to 50ml of the 4 mg/ml chitosan solution under vigorous stirring with a magnetic stirrer. The pH of the final solution was between 5.5 – 5.7.

The complex was divided into 10ml aliquots and stored under ambient conditions until the required testing date.

7.2.2 Molecular Weight Determination

To determine the molecular weight of chitosan after the stated storage period, dissociation of the complex is necessary. The isoelectirc point of insulin is 5.3; above this pH insulin is negatively charged and will form ionic interaction with chitosan resulting in a complex. Below this pH, insulin becomes predominantly positively charged. Therefore by lowering the pH of the medium in which the chitosan-insulin complex is suspended, the complex will dissociate since both components are now positively charged, soluble and will repel each other.

The 10ml aliquot was divided into two, one 5ml aliquot is centrifuged and the supernatant removed and stored. To the supernatant and the other 5 ml aliquot a drop of 1M HCl is added to dissociate any complex (pH of solution ~ 4). This solution is then filtered through a 0.45 μm filter and analysed using SEC-MALLS as described in Section 2.2.3.1. and the molecular weight determined. The use of SEC-MALLS to determine the molecular weight of chitosan in this solution is possible since the insulin, which will still be present in the solution, will not be detectable on the column system used here.

7.2.3 Stability of Chitosan-Insulin Complex

During storage it is possible that the chitosan-insulin complex may dissociate. To determine the stability of the complex over the storage period, the amount

of chitosan and insulin in the supernatant was determined at each time interval using the ninhydrin assay and HPLC respectively (see sections 2.2.6. and 2.2.7.).

7.3 Results

7.3.1 Stability of Chitosan in complex

As mentioned in section 7.2.2., the determination of the molecular weight of chitosan using SEC-MALLS is possible without the removal of insulin from the solution since insulin is not detectable in the system used. Insulin has a molecular weight of 9000 kDa whereas the chitosan used in the study has an initial molecular weight of 207500 kDa. The system chosen will elute the insulin at the end of the run (volume 30ml). An example of the SEC-MALLS traces for insulin and chitosan G213* are shown in Figures 7-1 and 7-2 respectively. The insulin trace shows no recorded light scattering or refractive index signal during the experimental run time.

Table 7-1 shows the molecular weight determined using SEC-MALLS for chitosan stored as a complex over a two-month period. Degradation of chitosan does occur with a decrease in molecular weight of approximately 10% ($t_{0.05,3df} = 3.182$; $t = 1.22$ therefore not significantly different). The same chitosan (G213*) was stored in acetate buffer, pH 4.3 for a two-month period and a decrease in molecular weight of approximately 43% was observed (results also shown in Table 7.1).

From these results it would appear that by storing chitosan as a complex and thereby in the solid state, and also possibly in nanoparticle form, the stability in aqueous solution is increased. However, it should be noted that the pHs of the two storage media were different. The complex was suspended in water at

approximately pH 5.7, whereas the chitosan solution was in acetate buffer, pH 4.3. As was shown in Figure 4.6, Section 4.3.3., as the pH of the chitosan solution decreases, the rate of degradation of chitosan increases due to acid hydrolysis occurring. These effects were also shown by Vårum *et al.* (2001). The results obtained here should therefore be treated with caution due to the different storage conditions. In order to clarify that storage of chitosan in nanoparticle form or as a complex does improve its stability, it would be necessary to compare its degradation in solution at the same pH as the medium in which the nanoparticles/complex are suspended.

7.3.2 Stability of Chitosan-Insulin Complex

It has been demonstrated that storage of chitosan as a complex may improve its stability. However, it is also necessary to show that the chitosan-insulin complex remains intact over the storage period. To demonstrate this, the amount of insulin and chitosan in the supernatant was determined over the two-month period, as well as the total amount present after dissociation of the complex. The results are shown in Table 7-2.

After two weeks, the amount of chitosan and insulin present in the complex has increased. This would indicate that after the initial measurement, that further complexation occurred. Over the next six weeks, the amount of chitosan and insulin complexed remained constant, indicating that the chitosan-insulin complex was steady over the two-month storage period.

Figure 7-1: SEC-MALLS trace for insulin solution (2 mg/ml)

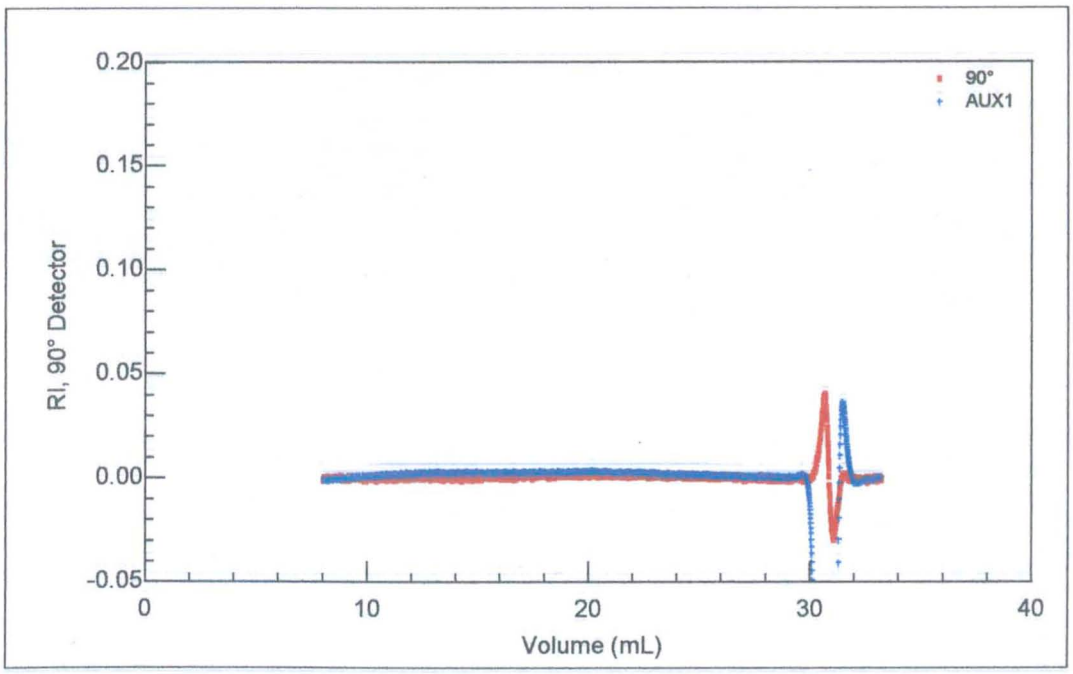

Figure 7-2: SEC-MALLS trace for Chitosan G213* (2mg/ml)

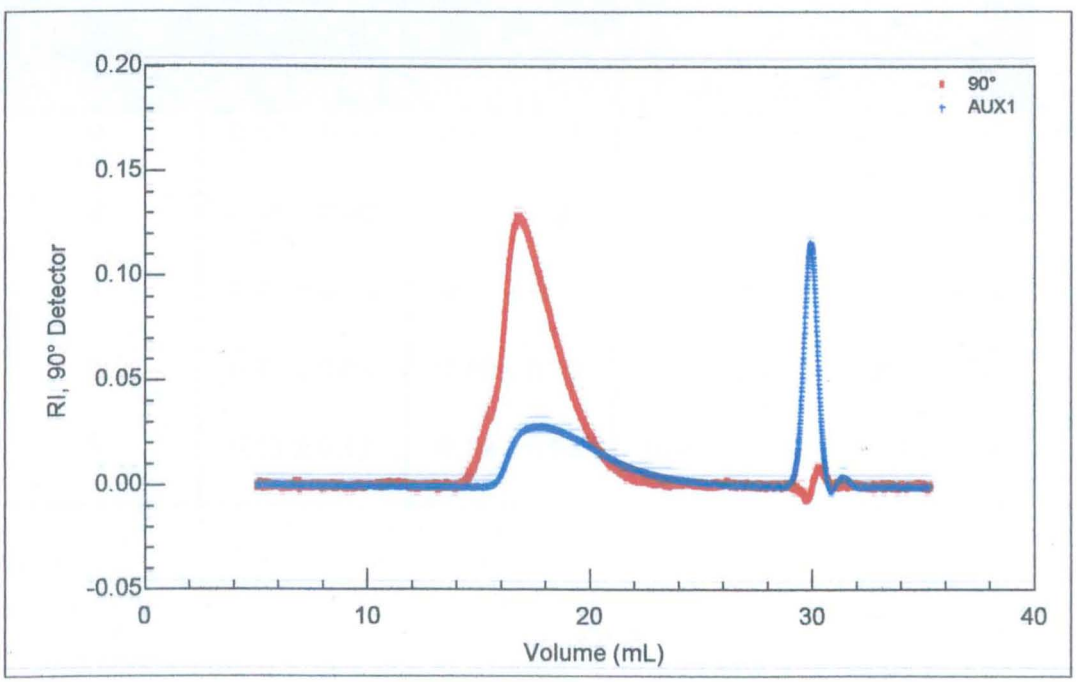

Table 7-1: Molecular Weight of chitosan determined using SEC-MALLS after storage in solution and as a complex with insulin

Time (weeks)	Chitosan-Insulin Complex		G213* (0.1M acetate buffer, pH 4.3)
	Complex	Supernatant	
0	204500 ± 8000	193000 ± 7000	207500 ± 8000
4	189000 ± 9000	-	160000 ± 1500
8	185000 ± 6000	-	119000 ± 6300

Table 7-2: Insulin and Chitosan concentrations in complex over two-month storage period under ambient conditions

Time (weeks)	Insulin (mg/ml)		Chitosan (mg/ml)	
	Complex	Supernatant	Complex	Supernatant
0	0.67 ± 0.10	0.34 ± 0.05	0.74 ± 0.13	0.22 ± 0.10
2	0.84 ± 0.07	0.12 ± 0.02	0.91 ± 0.17	0.05 ± 0.03
4	0.82 ± 0.13	0.16 ± 0.03	0.93 ± 0.14	0.11 ± 0.06
6	0.87 ± 0.08	0.15 ± 0.10	0.92 ± 0.11	0.05 ± 0.02
8	0.83 ± 0.11	0.19 ± 0.08	0.89 ± 0.13	0.17 ± 0.09

Chapter 8: Conclusions and Suggested Further Work

In this study I have investigated the characterisation of a range of chitosan samples using various hydrodynamic techniques. These studies have highlighted the problems that are encountered when determining the molecular weight of chitosan due to non-ideality and how the use of SEC-MALLS can provide a quick and accurate measure. The main focus of the project has been the degradation of chitosan in solution and the possibilities of constructing stable chitosan based nanoparticles for nasal delivery of therapeutic proteins and peptides.

8.1 Molecular Weight Determination and Conformation

The measurement of molecular weight of a polymer can provide information on its potential applications in the pharmaceutical industry. It is therefore important to be able to accurately measure the molecular weight by a convenient method.

The molecular weight of chitosan was determined using two absolute techniques: sedimentation equilibrium using the analytical ultracentrifugation (AUC) and SEC-MALLS. The time required for these techniques is very different. AUC requires the measurement of molecular weight at several concentrations, and the experiment takes approximately three days to perform. Several concentrations are required due to non-ideality as was explained in Chapter 3. SEC-MALLS, on the other hand, only requires the measurement of the molecular weight using one concentration and the experiment only take one hour to perform. The effects of

non-ideality are negligible due to dilution of the sample that occurs as it flows through the column system.

The column system chosen for SEC-MALLS provided good separation of the chitosan sample and there was excellent sample recovery (~90%), which indicated that the chitosan did not interact with the column packing material. The results obtained from both techniques were in good agreement showing that SEC-MALLS can be used as a quick and simple method for the determination of the molecular weight of chitosan.

Information on the conformation of chitosan can help us to understand the application of chitosan as a bioadhesive material in drug delivery. From the information we gathered using the power-law or "Mark Houwink Kuhn Sakurada exponents, we can see that chitosan exists as an extended coil in aqueous acidic solutions (power law coefficients $b = 0.25 \pm 0.04$ and $a = 0.96 \pm 0.10$). These parameters appear consistent with the data obtained from other groups (Anthonsen *et al*, 1993, and Berth, Cölfen and Dautzenberg 2002), although interpretations in terms of conformation can be complicated by the existence of possible solvent draining effects from the chain (see Berth, Colfen and Dautzenberg, 2002). Since chitosan exists in an extended conformation there is likely to be a greater chance of interaction between that negatively charged sialic acid groups present in the mucus lining the mucosal membranes and the positively charged amino groups on chitosan. This will favour increased bioadhesion and facilitate improved absorption of the protein or peptide that is being delivered, vindicating the choice of chitosan as a mucoadhesive system.

8.2 Degradation of Chitosan in aqueous solution

In the first section of this thesis, the stability of chitosan was investigated. It was found that an increase in temperature increased the degradation rate and that changes in ionic strength over the range studied had no effect on degradation rate. The ionic strength range that was studied was narrow and it may have been found that over a greater range an effect on degradation may have been observed. This may have been due to changes in the conformation of chitosan with larger increases in ionic strength. If the ionic strength were increased sufficiently, chitosan would exist as a coiled molecule in solution due to shielding of the charged amino groups along the chain. This may increase its stability, as it would be harder for the hydroxyl ions to penetrate into the coiled molecule and hydrolysis the glycosidic bonds.

The most important factor was found to be the pH of the solution. It was found that as the pH of the solution decreased, i.e. as the solution became more acidic, the rate of degradation increased. This result indicates that acid hydrolysis, which results in the cleavage of the glycosidic bonds, plays an important role in the degradation of chitosan.

Initial studies on the effect of pH showed the opposite effect, i.e. increased degradation at elevated pH, but I attributed this to incomplete dissolution of the chitosan under low-acidic conditions, a consequence of the cationic nature of this polysaccharide. Scavenging agents, which will be effective in reducing degradation caused by oxidative reductive degradation, were also investigated but showed no significant effect on degradation, suggesting that oxidative degradation

was not a accountable for a significant amount of chitosan degradation in solution.

In conclusion, the main mechanism of degradation of chitosan in aqueous solution appears to be acid hydrolysis, and, encouragingly, for the pH range that would be used for a nasal formulation, the amount of degradation is not significant as was shown by the multi-factorial three month stability study.

The effect of molecular weight and degree of acetylation on chitosan degradation is also worthy of serious comment. For the molecular weight range studied, no significant effect was observed. However, it was found that the rate of degradation decreased as the DA of the chitosan decreased. I attributed this to the increase in the number of charged amino groups on chitosan as the DA decreased, which protects the glycosidic oxygen from protonation i.e. the first stage in acid hydrolysis. As the number of charged groups on the chitosan molecule increases, there may also be enhanced bioadhesion which would also be advantageous in drug delivery via mucosal membranes. Taking into account these two parameters (degradation and degree of bioadhesion) it would appear that the most important structural parameter to consider when selecting a chitosan is its degree of acetylation.

8.3 Nanoparticle Production and Chitosan Stability

For the nasal delivery of insulin, current research is focussed on the use of chitosan nanoparticles. These possess both the mucoadhesive and absorption enhancing properties of chitosan as well as delivery the drug to the site of absorption in a high concentration.

The effect of molecular weight and degree of acetylation of the yield and loading capacity of chitosan nanoparticles was investigated. It was found that to improve the yield of nanoparticles a decrease in the degree of acetylation, DA of the chitosan molecule was beneficial. This can be explained by the increase in the number of charged groups on the chitosan molecule, which increases the possible sites for interaction between chitosan and tripolyphosphate, TPP. To increase the loading of the nanoparticles it was found that higher molecular weight chitosans were best. By increasing the molecular weight, the chain length of the chitosan molecule will increase, which could increase the physical entrapment of insulin.

The effect of DA on loading capacity did not show any distinct trend but it would be expected that as with yield, a lower DA would be best due to the increased number of charged amino groups.

I also investigated the effect of formulating nanoparticles on the stability of chitosan was investigated. The stability of the nanoparticles was assessed by determining the molecular weight of chitosan using SEC-MALLS after the chitosan-insulin complex had been dissociated. The results obtained were compared with the degradation of chitosan only in a solution of the same pH. The results showed a small improvement in stability (approximately 30%), but this was not significant.

It is worth making the comment that the time scale of the stability trail was relatively short (only two months) and this is rather short compared with the storage data that would be required for a marketed pharmaceutical product. It may be found that over a longer storage period, the amount of degradation

observed when chitosan is in a dispersion in complexed nanoparticle form compared to the case of a molecular solution form, is significantly different – this is clearly a case for further study.

8.4 Further Work

It is still not sure how the level of degradation observed in both chitosan solution and chitosan nanoparticles will affect the absorption enhancing properties of chitosan.

This could be investigated by simultaneously measuring degradation and bioadhesion. A factorial experiment could be carried out to look at the effect of molecular weight and degree of acetylation (over a wider range tan covered in this thesis) on degradation and along side the molecular weight or viscosity measurements taken a measure of bioadhesion could be taken.

After evaluation of these experiments, a study could be carried out in sheep using a selected range of chitosan sample (best, worst and middle), to investigate the effect of degradation of the absorption enhancing properties.

These experiments could be carried out using both a simple chitosan solution as well as using chitosan nanoparticles. From this study we may find that as the chitosan sample is degraded the bioadhesion and absorption enhancing properties decrease due to a reduced number of charged amine groups on the chitosan chain.

References

Angelo, R., D. Malkov, H. Tang, H. Wang, E. Flanders, S. Dinh and I. Gomez-Orellana (2002). Oral Insulin Absorption with EMISPHERE Drug Delivery Agents. Mechanistic Studies using Intestinal Epithelial Cells. 2nd Annual Diabetes Technology Meeting.

Anthonsen, M. W., K. M. Vårum and O. Smidsrød (1993). "Solution properties of chitosans: conformation and chain stiffness of chitosans with different degrees of *N*-acetylation." *Carbohydrate Polymers* **22**: 193-201.

Anthonsen, M. W., K. M. Vårum, A. M. Hermansson, O. Smidsrød and D. A. Brant (1994). "Aggregates in acidic solutions of chitosans detected by static laser light scattering." *Carbohydrate Polymers* **25**: 13-23.

Artursson, P., T. Lindmark, S. S. Davis and L. Illum (1994). "Effect of chitosan on the permeabliltiy of monolayers of intestinal epithelial cells (caco-2)." *Pharmaceutical Research* **11**: 1358-1361.

Aspden, T. J., J. Adler, S. S. Davis and L. Illum (1995). "Chitosan as a nasal delivery system: Evaluation of the effect of chitosan on mucociliary clearance rate in the frog palate model." *International Journal of Pharmaceutics* **122**: 69-78.

Aspden, T. J., L. Illum and O. Skaugrud (1996). "Chitosan as a nasal delivery system: evaluation of insulin absorption enhancement and effect on nasal membrane integrity using rat models." *European Journal of Pharmaceutical Sciences* **4**: 23-31.

Aspden, T. J., J. D. T. Mason, N. S. Jones, J. Lowe, O. Skaugrud and L. Illum (1997). "Chitosan as a Nasal Delivery System: The Effect of Chitosan Solutions on in Vitro and in Vivo Mucociliary Transport Rates in Human Turbinates and Volunteers." *Journal of Pharmaceutical Sciences* **86**(4): 509-513.

Aulton, M. E. (2002). Pharmaceutics: The Science of Dosage Form Design. London, Churchill Livingstone.

Behl, C. R., H. K. Pimplaskar, A. P. Sileno, J. deMeireles and V. D. Romeo (1998). "Effects of physicochemical properties and other factors on systemic nasal drug delivery." *Advanced Drug Delivery Reviews* **29**: 89-116.

Behl, C. R., H. K. Pimplaskar, A. P. Sileno, W. J. Xia, W. J. Gries, J. C. deMeireles and V. D. Romeo (1998). "Optimization of systemic nasal drug delivery with pharmaceutical excipients." *Advanced Drug Delivery Reviews* **29**: 117-133.

BeMiller, J. N. (1967). "Acid-catalyzed hydrolysis of glycosides." *Advances in Carbohydrate Chemistry* **22**: 25-108.

Bernkop-Schnurch, A. (2000). "Chitosan and its derivatives: potential excipients for peroral peptide delivery systems." *International Journal of Pharmaceutics* **194**: 1-13.

Berth, G., H. Dautzenberg and M. G. Peter (1998). "Physico-chemical characerization of chitosans varying in degree of acetylation." *Carbohydrate Polymers* **36**: 205-216.

Berth, G. and H. Dautzenberg (2002). "The degree of acetylation of chitosans and its effect on the chain conformation in aqueous solution." *Carbohydrate Polymers* **47**: 39-51.

Berth, G., H. Cölfen and H. Dautzenberg (2002). *Prog. Coll. Polym. Sci.* **119**: 50-57

Bodmeier, R., H. Chen and O. Paeratakul (1989). "A novel approach to the delivery of microparticles or nanoparticles." *Pharmaceutical Research* **6**: 413-417.

Borchard, G., H. L. LueBen, A. G. de Boer, J. Coos Verhoef, C.-M. Lehr and H. E. Junginger (1996). "The potential of mucoadhesive polymers in enhancing intestinal peptide drug absorption. III: Effects of chitosan-glutamate and carbomer on epithelial tight junctions in vitro." *Journal of Controlled Release* **39**: 131-138.

Boryniec, S., G. Strobin, H. Struszczyk, A. Niekraszewicz and M. Kucharska (1997). "GPC Studies of Chitosan Degradation." *International Journal of Polymer Analysis and Characterisation* **3**: 359-368.

Calvo, P., C. Remunan-Lopez, J. L. Vila-Jato and M. J. Alonso (1997). "Novel Hydrophilic Chitosan-Polyethylene Oxide Nanoparticles as Protein-Carriers." *Journal of Applied Polymer Science* **63**: 125-132.

Carino, G. P., J. S. Jacob and E. Mathiowitz (2000). "Nanosphere based oral insulin delivery." *Journal of Controlled Release* **65**: 261-269.

Carino, G. P. and E. Mathiowitz (1999). "Oral insulin delivery." *Advanced Drug Delivery Reviews* **35**: 249-257.

Chang, K. L. B., M.-C. Tai and F.-H. Cheng (1999). "Kinetics and Products of the Degradation of Chitosan by Hydrogen Peroxide." *American Chemical Society.*

Chang, K. L. B., G. Tsai, J. Lee and W. Fu (1997). "Heterogeneous *N*-acetylation of chitin in alkaline solution." *Carbohydrate Research* **303**: 327-332.

Chen, R. H., J. R. Chang and J. S. Shyur (1997). "Effects of ultrasonic conditions and storage in acidic solutions on changes in molecular weight and polydispersity of treated chitosan." *Carbohydrate Research* **299**: 287-294.

Clement, S., P. Dandona, J. Gordon Still and G. Kositic (2004). "Oral Modified Insulin (HIM2) in patients with Type I Diabetes Mellitus: Results from a Phase I/II Clinical Trial." *Metabolism.*

Clewlow, A. C., N. Errington and A. J. Rowe (1997). "Analysis of data captured by an on-line image capture system from an analytical ultracentrifuge using schlieren optics." *European Journal of Biophysics* **25**: 311-317.

Cölfen, H. and S. E. Harding (1997). "MSTARA and MSTARI: interactive PC algorithms for simple, model independent evaluation of sedimentation equilibrium data." *European Journal of Biophysics* **25**: 333-346.

Cölfen, H., G. Berth and H. Dautzenberg (2001). "Hydrodynamic studies on chitosans in aqueous solution." *Carbohydrate Polymers* **45**: 373-383.

Couvreur, P., V. Lenaerts, B. Kante, K. Roland and P. Speiseret (1980). "Oral and parenteral administration of insulin associated to hydrolzable nanoparticles." *Acta Pharmaceutical Technology* **26**: 220-222.

Creeth, J. M. and S. E. Harding (1982). "Some observations on a new type of point average molecular weight." *Journal of Biochemical and Biophysical Methods* **7**(1): 25-34.

Damge, C., M. Michael, A. Aprahamian and P. Couvreur (1988). "New approach for oral administration of insulin with poly-alkylcyanoacrylate nanocapsules as oral carrier." *Diabetes* **37**: 247-251.

Damge, C., C. Michel, A. Aprahamian, P. Couvreur and J. P. Devissaguetet (1990). "Nanocapsules as carriers for oral peptide delivery." *Journal of Controlled Release* **13**: 233-239.

Davis, S. S. (1999). "Delivery of peptide and non-peptide drugs through the respiratory tract." *Pharmaceutical Science and Technology Today* **2**(11): 450-456.

Denker, B. M. and S. K. Nigam (1998). "Molecular structure and assembly of the tight junction." *American Journal of Physiology* **274**: F1-F9.

Dodane, V. and V. D. Vilivalam (1998). "Pharmaceutical applications of chitosan." *Pharmaceutical Science and Technology Today* **1**(6): 246-253.

Dodane, V., M. Amin Khan and J. R. Merwin (1999). "Effect of chitosan on epithelial permeability and structure." *International Journal of Pharmaceutics* **182**: 21-32.

Donovan, M. D., G. L. Flynn and G. L. Amidon (1990). "Absorption of polyethylene glycols 600 through 2000: the molecular weight dependence of gastrointestinal and nasal absorption." *Pharmaceutical Research* **7**: 863-868.

Dyer, A. M., M. Hinchcliffe, P. Watts, J. Castile, I. Jabbal-Gill, R. Nankervis, A. Smith and L. Illum (2002). "Nasal Delivery of Insulin Using Novel

Chitosan Based Formulations: A Comparative Study in Two Animal Models between Simple Chitosan Formulations and Chitosan Nanoparticles." *Pharmaceutical Research* **19**(7): 998-1008.

Edman, P., E. Bjork and L. Ryden (1992). "Microspheres as a nasal delivery system for peptide drugs." *Journal of Controlled Release* **21**: 165-172.

Ermak, T. H., E. P. Dougherty, H. R. Bhagat, Z. Kabok and J. Pappo (1995). "Uptake and transport of copolymer biodegradable microspheres by Rabbit Peyer's patch M cells." *Cell Tissue Research* **279**: 433-436.

Errington, N., S. E. Harding, K. M. Varum and L. Illum (1993). "Hydrodynamic characterization of chitosans varying in degree of acetylation." *International Journal of Biological Macromolecules* **15**: 113-117.

Farraj, N. F., B. R. Johansen, S. S. Davis and L. Illum (1990). "Nasal administration of insulin using bioadhesive microspheres as a delivery system." *Journal of Controlled Release* **13**: 253-361.

Fernández-Urrusuno, R., P. Calvo, C. Remuñán-López, J. L. Vila-Jato and M. J. Alonso (1999). "Enhancement of Nasal Absorption of Insulin Using Chitosan Nanoparticles." *Pharmaceutical Research* **16**(10): 1576-1581.

Fernández-Urrusuno, R., D. Romani, P. Calvo, J. L. Vila-Jato and M. J. Alonso (1999). "Development of a freeze-dried formulation of insulin-loaded chitosan nanoparticles intended for nasal administration." *S.T.P. Pharma Sciences* **9**(5): 429-436.

Fiebrig, I., S. E. Harding, B. T. Stokke, K. M. Varum, D. Jordan and S. S. Davis (1994). "The potential of chitosan as a mucoadhesive drug carrier: studies on its interaction with pig gastric mucin on a molecular level." *European Journal of Pharmaceutical Sciences* **2**: 185.

Fisher, A. N., K. Brown, S. S. Davis, G. D. Parr and D. A. Smith (1987). "The effect of molecular size on the nasal absorption of water-soluble compounds in the albino rat." *Journal of Pharmacy and Pharmacology* **39**: 357-362.

Fisher, A. N., L. Illum, S. S. Davis and E. H. Schacht (1991). "Di-iodo-L-tyrosine-labelled dextrans as molecular size markers of nasal absorption in the rat." *Journal of Pharmacy and Pharmacology* **44**: 550-554.

Furst, A. (1997). "The XL-I analytical ultracentrifuge with Rayleigh interference optics." *European Journal of Biophysics* **35**: 307-310.

Harding, S. E. (1992). Sedimentation analysis of polysaccharides. Analytical Ultracentrifugation in Biochemistry and Polymer Science. S. E. Harding, A. J. Rowe and J. C. Horton. Cambridge, Uk, Royal Society of Chemistry.

Harding, S. E. (1995). "Some recent developments in the size and shape analysis of industrial polysaccharides in solution using sedimentation analysis in the analytical ultracentrifuge." *Carbohydrate Polymers* **28**: 227-237.

Harding, S. E. (1997). "The intrinsic viscosity of biological macromolecules. Progress in measurement, interpretation and application to structure in dilute solution." *Progress in Biophysics and Molecular Biology* **68**(2/3): 207-262.

Harding, S. E., S. S. Davis, M. P. Deacon and I. Fiebrig (1999). "Biopolymer Mucoadhesives." *Biotechnology and Genetic Engineering Reviews* **16**: 41-85.

He, P., S. S. Davis and L. Illum (1998). "In vitro evaluation of the mucoadhesive properties of chitosan microspheres." *International Journal of Pharmaceutics* **186**: 75-88.

Hejazi, R. and M. Amiji (2003). "Chitosan-based gastrointestinal delivery systems." *Journal of Controlled Release* **89**: 151-165.

Hinchcliffe, M. and L. Illum (1999). "Intranasal insulin delivery and therapy." *Advanced Drug Delivery Reviews* **35**: 199-234.

Holme, H. K., H. Foros, H. Pettersen, M. Dornish and O. Smidsrød (2001). "Thermal depolymerization of chitosan chloride." *Carbohydrate Polymers* **46**: 287-294.

Hussain, A. A. (1998). "Intranasal drug delivery." *Advanced Drug Delivery Reviews* **29**: 39-49.

Illum, L., N. F. Farraj, H. Critchley and S. S. Davis (1988). "Nasal administration of gentamicin using a novel microsphere delivery system." *International Journal of Pharmaceutics* **46**: 261-265.

Illum, L., N. F. Farraj and S. S. Davis (1994). "Chitosans as a novel nasal delivery system for peptide drugs." *Pharmaceutical Research* **11**: 1186-1189.

Illum, L., A. N. Fisher, I. Gill, M. Miglietta and L. M. Benedetti (1994). "Hyaluronic acid ester microspheres as a nasal drug delivery system for insulin." *Journal of Controlled Release* **29**: 133-141.

Illum, L., A. N. Fisher, I. Jabbal-Gill and S. S. Davis (2001). "Bioadhesive starch microspheres and absorption enhancing agents act synergistically to enhance the nasal absorption of polypeptides." *International Journal of Pharmaceutics* **222**: 109-119.

Illum, L., I. Jabbal-Gill, M. Hinchcliffe, A. N. Fisher and S. S. Davis (2001). "Chitosan as a novel nasal delivery system for vaccines." *Advanced Drug Delivery Reviews* **51**: 81-96.

Illum, L., H. Jorgensen, H. Bisgard, O. Krogsgaard and N. Rossing (1987). "Bioadhesive microspheres as a potential nasal drug delivery system." *International Journal of Pharmaceutics* **39**: 189-199.

Janes, K. A., P. Calvo and M. J. Alonso (2001). "Polysaccharide colloidal particles as delivery systems for macromolecules." *Advanced Drug Delivery Reviews* **47**: 83-97.

Jia, Z. and D. Shen (2002). "Effect of reaction temperature and reaction time on the preparation of low-molecular-weight chitosan using phosphoric acid." *Carbohydrate Polymers* **49**(4):393-396

Jones, N. (2001). "The nose and paranasal sinuses physiology and anatomy." *Advanced Drug Delivery Reviews* **51**: 5-19.

Jumel, K. (1994). PhD Dissertation, University of Nottingham, U.K.

Kotzé, A. F., B. J. de Leeuw, H. L. Lueßen, A. G. de Boer, J. C. Verhoef and H. E. Junginger (1997). "Chitosans for enhanced delivery of therapeutic peptides across intestinal epithelia: in vitro evaluation in caco-2 cell monolayers." *International Journal of Pharmaceutics* **159**: 243-253.

Kotzé, A. F., H. L. Lueßen, B. J. de Leeuw, A. G. de Boer, J. C. Verhoef and H. E. Junginger (1998). "Comparison of the effect of different chitosan salts

and *N*-trimethyl chitosan chloride on the permeability of intestinal epithelial cells (Caco-2)." *Journal of Controlled Release* **51**: 35-46.

Kotzé, A. F., M. Thanou, H. L. Lueßen, A. G. de Boer, J. C. Verhoef and H. E. Junginger (1999). "Enhancement of paracellular drug transport with highly quaternized *N*-trimethyl chitosan chloride in neutral environments: in vitro evaluation in intestinal epithelial cells (caco-2)." *Journal of Pharmaceutical Sciences* **88**: 253-257.

Kublik, H. and M. T. Vidgren (1998). "Nasal delivery systems and their effect on deposition and absorption." *Advanced Drug Delivery Reviews* **29**: 157-177.

Leane, M. M., R. Nankervis, A. Smith and L. Illum (2004). "Use of the ninhydrin assay to measure the release of chitosan from oral solid dosage forms." *International Journal of Pharmaceutics* **271**(1-2): 241-249.

Lehr, C.-M., J. A. Bouwstra, E. H. Schacht and H. E. Junginger (1992). "In vitro evaluation of mucoadhesive properties of chitosan and some other natural polymers." *International Journal of Pharmaceutics* **78**: 43-48.

Lloyd, P. H. (1974). Optical Methods in Ultracentrifugation, Electrophoresis and Diffusion. Oxford.

Lueßen, H. L., B. J. de Leeuw, A. G. Langemeÿer, A. G. de Boer, J. C. Verhoef and H. E. Junginger (1996). "Mucoadhesive polymers in peroral

peptide drug delivery. VI. Carbomer and chitosan improve the intestinal absorption of the peptide drug buserelin in vitro." *Pharmaceutical Research* **13**: 1668-1672.

Marttin, E., N. G. M. Schipper, J. C. Verhoef and F. W. H. M. Merkus (1998). "Nasal mucociliary clearance as a factor in nasal drug delivery." *Advanced Drug Delivery Reviews* **29**: 13-38.

McMartin, C., L. E. F. Hutchinson, R. Hyde and G. E. Peters (1987). "Analysis of Structural Requirements for the Absorption of Drugs and Macromolecules from the Nasal Cavity." *Journal of Pharmaceutical Sciences* **76**(7): 535-540.

Meza, I., M. Sabanero, E. Stefani and M. Cereijido (1982). "Occluding junctions in MDCK cells: Modulation of transepithelial permeability by the cytoskeleton." *Journal of Cellular Biochemistry* **18**(4): 407-421.

Mygind, N. and D. Dahl (1998). "Anatomy, physiology and function of the nasal cavities in health and disease." *Advanced Drug Delivery Reviews* **29**: 3-12.

Nordtveit, R. J., K. M. Vårum and O. Smidsrød (1994). "Degradation of fully water-soluble, partially *N*-acetylated chitosans with lysozyme." *Carbohydrate Polymers* **23**: 253-260.

Ohwaki, T., H. Ando, S. Watanabe and Y. Miyake (1985). "Effect of dose, pH and osmolarity on nasal absorption of secretin in rats." *Journal of Pharmaceutical Sciences* **74**: 550-552.

Ohya, Y., M. Shiratani, H. Kobayashi and T. Ouchi (1994). "Release behaviour of 5-fluorouracil from chitosan-gel nanospheres immobilizing 5-fluorouracil coated with polysaccharides and their cell specific cytotoxicity." *Journal of Macrolmolecular Science - Pure and Applied Chemistry* **A31**(5): 629-642.

Ottøy, M. H., K. M. Vårum and O. Smidsrød (1996). "Compositional hetergeneity of heterogeneously deacetylated chitosans." *Carbohydrate Polymers* **29**(1): 17-24.

Ottøy, M. H., K. M. Vårum, B. E. Christensen, M. W. Anthonsen and O. Smidsrød (1996). "Preparative and analytical size-exclusion chromatography of chitosans." *Carbohydrate Polymers* **31**: 253-261.

Paradossi, G., E. Chiessi, M. Venanzi and B. Pispisa (1992). "Branched-chain analogues of linear polysaccharides: a spectroscopic and conformational investigation of chitosan derivatives." *International Journal of Biological Macromolecules* **14**: 73-80.

Pettersen, H., A. Sannes, H. K. Holme, A. H. Kristensen, M. Dornish and O. Smidsrød (1997). Thermal depolymerization of chitosan salts. 7th

International Conference on Chitin and Chitosan, Lyon, France, Jacques Andre.

Philo, J. S. (2000). "A Method for Directly Fitting the Time Derivative of Sedimentation Velocity Data and an Alternative Algorithm for Calculating Sedimentation Coefficient Distributions Functions." *Analytical Biochemistry* **279**: 151-163.

Price, N. C. and R. A. Dwek (1979). Solutions of Macromolecules. Principles and problems in physical chemistry for biochemists. Oxford, Clarendon Press.

Prochazkova, S., K. M. Vårum and K. Østgaard (1999). "Quantitative determination of chitosans by ninhydrin." *Carbohydrate Polymers* **38**: 115-122.

Pujara, C. P., Z. Shao, M. R. Duncan and A. K. Mitra (1995). "Effects of formulation variables on nasal epithelial cell integrity: Biochemical evaluations." *International Journal of Pharmaceutics* **114**: 197-203.

Qin, C. Q., Y. M. Du and L. Xiao (2002). "Effect of hydrogen peroxide treatment on the molecular weight and structure of chitosan." *Polymer Degradation and Stability* **76**: 211-218.

Ralston, G. (1993). Introduction to Analytical Ultracentrifugation.

Rege, P. R. and L. H. Block (1999). "Chitosan processing: influence of process parameters during acidic and alkaline hydrolysis and effec of the processing sequence on the resultant chitosan's properties." *Carbohydrate Research* **321**: 235-245.

Rinaudo, M. and A. Domard (1989). Solution Properties of Chitosan. Chitin and Chitosan: Sources, Chemistry, Biochemistry, Physical Properties and Applications. G. Skjak-Braek, T. Anthonsen and P. Sandford. London, Elsevier Applied Science: 71-86.

Rinaudo, M., G. Pavlov and J. Desbrieres (1999). "Influence of acetic acid concentration on the solubilization of chitosan." *Polymer* **40**: 7029-7032.

Roberts, G. A. F. (1992). Chemical Behaviour of Chitin and Chitosan. Chitin Chemistry. London, Macmillian Press Ltd: 249-261.

Rossi, S., F. Ferrari, M. C. Bonferoni and C. Caramella (2000). "Characterization of chitosan hydrochloride-mucin interaction by means of viscoimetric and turbidimetric measurements." *European Journal of Pharmaceutical Sciences* **10**: 251-257.

Schachman, H. K. (1992). Is There a Future for the Ultracentrifugation? Analytical Ultracentrifugation in Biochemistry and Polymer Science. S. E. Harding, A. J. Rowe and J. C. Horton. Cambridge, The Royal Society of Chemistry.

Schipper, N. G. M., K. M. Vårum and P. Artusson (1996/9). "Chitosans as absoprtion enhancers of poorly absorbable drugs: influence of molecular weight and degree of acetylation." *European Journal of Pharmaceutical Sciences* **4**(1): S153.

Schipper, N. G. M., K. M. Vårum and P. Artursson (1996). "Chitosans as absorption enhancers for poorly absorbable drugs. 1. Influence of molecular weight and degree of acetylation on drug transport across human intestinal epithelial (Caco-2) cells." *Pharmaceutical Research* **13**: 1686-1692.

Schipper, N. G. M., S. Olsson, J. A. Hoogstraate, A. G. deBoer, K. M. Vårum and P. Artursson (1997). "Chitosans as absorption enhancers for poorly absorbable drugs. 2. Mechanism of absorption enhancement." *Pharmaceutical Research* **14**: 923-929.

Schipper, N. G. M., K. M. Vårum, P. Stenberg, G. Ocklind, H. Lennernas and P. Artursson (1999). "Chitosans as absorption enhancers of poorly absorbable drugs 3: Influence of mucus on absorption enhancement." *European Journal of Pharmaceutical Sciences* **8**: 335-343.

Shigemasa, Y., K. Saito, H. Sashiwa and H. Saimoto (1994). "Enzymatic degradation of chitins and partially deacetylated chitins." *International Journal of Biological Macromolecules* **16**(1): 43-49.

Shin-ya, Y., M.-Y. Lee, H. Hinode and T. Kajiuchi (2001). "Effects of *N*-acetylation degree on *N*-acetylated chitosan hydrolysis with commercially available and modified pectinases." *Biochemical Engineering Journal* **7**: 85-88.

Shu, X. Z. and K. J. Zhu (2000). "A novel approach to prepare tripolyphospate/chitosan complex beads for controlled release drug delivery." *International Journal of Pharmaceutics* **201**: 51-58.

Shu, X. Z. and K. J. Zhu (2002). "The influence of multivalent phosphate structure on the properties of ionically cross-linked chitosan films for controlled drug release." *European Journal of Pharmaceutics and Biopharmaceitics* **54**: 235-243.

Smith, J., E. Wood and M. Dornish (2004). "Effect of Chitosan on Epithelial Cell Tight Junctions." *Pharmaceutical Research* **21**(1): 43-49.

Soane, R. J., M. Frier, A. C. Perkins, N. S. Jones, S. S. Davis and L. Illum (1999). "Evaluation of the clearance characteristics of bioadhesive systems in humans." *International Journal of Pharmaceutics* **178**: 55-65.

Sugimoto, M., M. Morimoto, H. Sashiwa, H. Saimoto and Y. Shigemasa (1998). "Preparation and characterization of water-soluble chitin and chitosan derivatives." *Carbohydrate Polymers* **36**: 49-59.

Tanford, C. (1955). "Intrinsic Viscosity and Kinematic Viscosity." *Journal of Physics and Chemistry* **59**: 798.

Tanford, C. (1961). Flexible Linear Polyelectrolyes. Physical Chemistry of Macromolecules. London, John Wiley & Sons: 489-508.

Tanioka, S., Y. Matsui, T. Irie, T. Tanigawa, Y. Tanaka, H. Shibata, Y. Sawa and Y. Kono (1996). "Oxidative Depolymerization of Chitosan by Hydroxyl Radical." *Bioscience, Biotechnology and Biochemistry* **60**(12): 2001-2004.

Thanou, M., J. C. Verhoef and H. E. Junginger (2001). "Oral drug absorption enhancement by chitosan and its derivatives." *Advanced Drug Delivery Reviews* **52**: 117-126.

Tolaimate, A., J. Desbrieres, M. Rhazi, A. Alagui, M. Vincendon and P. Vottero (2000). "On the influence of deacetylation process on the physicochemical characteristics of chitosan from squid chitin." *Polymer* **41**: 2463-2469.

Tominaga, S., T. Takaizawa and M. Yamada (1998). Colon drug delivery system. *Journal of Polymer Application.* **10:** 642.

Tozaki, H., J. Komoike, C. Tada, T. Maruyama, A. Terabe, T. Suzuki, A. Yamamoto and S. Muranishi (1997). "Chitosan capsules for colon-specific

drug delivery: improvement of insulin absorption from the rat colon." *Journal of Pharmaceutical Sciences* **86**: 1016-1021.

Tsaih, M. L. and R. H. Chen (1997). "Effect of molecular weight and urea on the conformation of chitosan molecules in dilute solutions." *International Journal of Biological Macromolecules* **20**: 233-240.

Van Holde, K. E. (1971). Viscosity. Physical Biochemistry. New Jersey, Prentice-Hall.

Van Holde, K. E. (1998). Principles of Physical Biochemistry.

Vårum, K. M., M. H. Ottøy and O. Smidsrød (1994). "Water-solubility of partially *N*-acetylated chitosans as a function of pH: effect of chemical compostition and depolymerisation." *Carbohydrate Polymers* **25**: 65-70.

Vårum, K. M., H. K. Holme, M. Izume, B. T. Stokke and O. Smidsrød (1996). "Determination of enzymatic hydrolysis specificity of partially *N*-acetylated chitosans." *Biochimica et Biophysica Acta* **1291**: 5-15.

Vårum, K. M., M. M. Myhr, R. J. N. Hjerde and O. Smidsrød (1997). "In vitro degradation rates of partially *N*-acetylated chitosans in human serum." *Carbohydrate Research* **299**: 99-101.

Vårum, K. M., M. H. Ottøy and O. Smidsrød (2001). "Acid hydrolysis of chitosans." *Carbohydrate Polymers* **46**: 89-98.

Wales, M. and V. Holde (1954). "The Concentration Dependence of the Sedimentation Constants of Flexible Macromolecules." *Journal of Polymer Science* **14**: 81-86.

Wang, W., S. Bo, S. Li and W. Qin (1991). "Determination of the Mark-Houwink equation for chitosans with different degrees of deacetylation." *International Journal of Biological Macromolecules* **13**: 281-285.

Wyatt, P. J. (1993). "Light Scattering and the absolute characterization of macromolecules." *Analytica Chimica Acta* **272**: 1-40.

Xu, Y. and Y. Du (2003). "Effect of molecular structure of chitosan on protein delivery properties of chitosan nanoparticles." *International Journal of Pharmaceutics* **250**:215-226.

Eur Biophys J (2003) 32: 457–464
DOI 10.1007/s00249-003-0317-8

ARTICLE

Monica Fee · Neil Errington · Kornelia Jumel
Lisbeth Illum · Alan Smith · Stephen E. Harding

Correlation of SEC/MALLS with ultracentrifuge and viscometric data for chitosans

Received: 7 January 2003 / Revised: 28 March 2003 / Accepted: 8 April 2003 / Published online: 14 June 2003

Abstract Attempts have been made to correlate estimates of molecular weight for a group of cationic polysaccharides known as chitosans between the highly popular technique of size-exclusion chromatography coupled to multi-angle laser light scattering, "SEC-MALLS", and the less convenient but more established technique of sedimentation equilibrium in the analytical ultracentrifuge. Four pharmaceutical grade chitosans of various molecular weights and degrees of acetylation (4–30%) were chosen. Better correlation than previous was achieved, although some batch variability was observed. Despite the broad spectrum in degree of acetylation, a $\log s^{\circ}_{20,w}$ versus $\log M_w$ scaling plot appeared to fit a straight line with power-law exponent $b = 0.25 \pm 0.04$, i.e. between the limits of rod (0.15) and coil (0.4–0.5), although this may be the average of a lower b value at low M_w and higher b at high M_w. With regard to viscosity, a $\log[\eta]$ versus $\log M_w$ scaling plot appeared to also fit a straight line with power-law exponent $a = 0.96 \pm 0.10$, again between the coil (0.5–0.7) and rod (1.8) limits.

Keywords Chitosan · Conformation · Molecular weight · SEC-MALLS · Sedimentation equilibrium

Presented at the conference for Advances in Analytical Ultracentrifugation and Hydrodynamics, 8–11 June 2002, Grenoble, France

M. Fee · N. Errington · K. Jumel · S. E. Harding (✉)
NCMH Physical Biochemistry Laboratory,
School of Biosciences,
University of Nottingham,
Sutton Bonington, LE12 5RD, UK
E-mail: steve.harding@nottingham.ac.uk

L. Illum · A. Smith
West Pharmaceutical Services,
Drug Delivery and Clinical Research Centre Ltd,
Albert Einstein Centre,
Nottingham Science and Technology Park,
Nottingham, NG7 2TN, UK

Introduction

Despite their increasing importance in the pharmaceutical and healthcare industries, chitosans [cationic polysaccharides consisting of *N*-acetyl-D-glucosamine units and D-glucosamine units in varying proportions (see Fig. 1)] have proved difficult to characterize with regard to molecular weight owing to their polycationic nature. This is primarily because of the failure of results from SEC-MALLS (size-exclusion chromatography coupled on-line to a multi-angle laser light-scattering detector) to agree or show compatibility with other techniques, such as sedimentation equilibrium in the ultracentrifuge, or measurements from viscometry. These difficulties have largely been attributed to anomalous behaviour on the size-exclusion columns that have been available, and discrepancies of over an order of magnitude in the weight average molecular weight have been observed.

When dissolved in aqueous acidic medium, chitosan becomes a cationic polyelectrolyte, making it a potential excipient for many applications in the food and pharmaceutical industries. These include, for example, controlled drug and flavour release from tablets or using microencapsulation techniques, film formation or as fillers in dietary foods, etc. (Illum 1998; Skaugrud et al. 1999). Chitosan is of particular interest to the pharmaceutical industry since it possesses mucoadhesive properties (see, for example, Harding et al. 1999), which result in increased contact time with a mucosal surface leading to enhanced drug absorption, and has also been demonstrated to enhance the delivery of proteins and peptides across mucosal membranes (Artursson et al. 1994; Illum et al. 1994, 2001; Natsume et al. 1999; Tengamnuay et al. 2000; Davis 2001). The mucoadhesive properties have been attributed to interactions between the $-NH_3^+$ groups left after deacetylation of the chitin and the terminal $-COO^-$ (sialic acid) on mucosal surfaces, reinforced through hydrophobic interaction between groups of un-deacetylated residues on chitosan with fucose on mucins (Deacon et al. 1999).

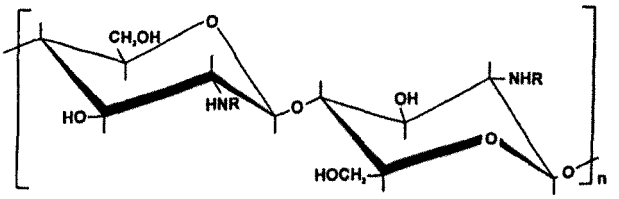

Fig. 1 Schematic representation of chitosan; R = acetyl or H, depending on the degree of acetylation

Chitosan has also been shown to cause a transient widening of the tight junctions of the epithelial cells in vitro, which is thought to contribute to enhanced drug permeability (Illum and Davis 2001; Illum et al. 2001).

For many applications of chitosan, and especially in the pharmaceutical industry, the molecular weight and degree of acetylation dictate the properties and thereby the effectiveness of the chitosan for a particular application. For example, Schipper et al. (1996) have reported that both these properties are very important for its absorption enhancement of hydrophilic drugs across mucosal surfaces. They found that a low degree of acetylation and/or high molecular weight appeared to be necessary for chitosans to increase epithelial permeability.

It is clear that the pharmaceutically important properties of chitosan (including solubility) are not only dependent on their chemical nature (dictated by the degree of acetylation), but also their physical properties (molecular weight and conformation). Although the degree of acetylation can be measured with considerable confidence [e.g. by NMR (Vårum et al. 1991)], it is also important to be able to attach some degree of confidence to the SEC/MALLS determination method for molecular weight. Successful molecular weight determinations of chitosan by SEC/MALLS have been reported by Beri et al. (1993). However, these authors did not compare their results with those from other independent techniques. Attempts at molecular weight determinations by SEC/MALLS in our own laboratories have previously proved difficult due to the anomalous behaviour of chitosan on our SEC columns, and results were generally incompatible with those obtained by sedimentation equilibrium in the analytical ultracentrifuge. The cationic nature of chitosan is responsible for its wide range of desirable interactions; however, it may also cause interactions with the SEC column packing material and/or residues from other previously run samples. A dedicated column system for chitosan was therefore used for the re-examination of the use of SEC/MALLS which was considered important due to:

1. The ease of obtaining absolute molecular weight data from SEC-MALLS compared with the use of other methods. Since 1991 (Horton et al. 1991; Rollings 1991, 1992), this method has become the most popular for characterizing polysaccharide molecular weights in solution, and, since 1996, also glycoconjugates such as mucus glycoproteins (Jumel et al. 1996, 1997).
2. The belief that there is a clear link between the functional properties of chitosans and their mucoadhesive and epithelial absorption enhancement capabilities for drug delivery and film forming potential for healthcare products (e.g. shampoos).

This paper explores the use of SEC/MALLS for four polysaccharides of pharmaceutical grade covering a range of degree of acetylation, DA (4–30%), and molecular weight. Comparative molecular weight data were obtained by sedimentation equilibrium in the analytical ultracentrifuge. A correlation of the Mark–Houwink–Kuhn–Sakurada (MHKS) power-law type is also attempted between weight average molecular weight, M_w, and both the intrinsic viscosity or the sedimentation coefficient to check for consistency between the data and to see if these particular chitosans of different DA and M_w approximate a homologous series.

Materials and methods

Materials

Four chitosans were provided by Pronova Biomedical, Oslo, Norway (G112, G114, G213 and G214). These were glutamate salts with DA values ranging from 4 to 30% and of reputedly different molecular weight, as indicated by the dynamic viscosity values (of 1% solutions) provided by Pronova (Table 1). A separate batch of G213 was also supplied.

For all experiments, the chitosan samples were dissolved in a 0.2 M acetate buffer (pH 4.3). For sedimentation equilibrium experiments, samples were dialysed against the buffer solution overnight so that the chemical potential of the solvent was equal in both the sample solution and the reference solvent (dialysate).

Methods

Molecular weight: sedimentation equilibrium

Low-speed sedimentation equilibrium was used to determine the molecular weights (weight averages) of the various chitosans. Two analytical ultracentrifuges (AUCs) were employed. Firstly, a Beckman XL-I Analytical Ultracentrifuge was used for chitosan solutions in the range of concentrations 0.5–1.0 mg/mL, at a rotor speed of 14,000 rpm (sample G112) or 8000 rpm (the other samples) and a temperature of 20.0 °C. The data collected from the Rayleigh interference optical system were analysed using the MSTARI algorithm (Cölfen and Harding 1997) to give an apparent weight average molecular weight, $M_{w,app}$. A low concentration sample (0.3 mg/mL) was also analysed using a Beckman Model E

Table 1 Commercial manufacturer's data (courtesy of Pronova, Drammen, Norway)

Chitosan*	G112	G114	G213[(a)]	G213[(b)]	G214
Degree of acetylation (%)	30	7	17	20	4
Viscosity of 1% solution (mPa s)	5	18	79	153	59

*G213[(a)], batch no. 610-583-09; G213[(b)], batch no. FP1-A-708-01

Analytical Ultracentrifuge (at rotor speeds between 10,000 and 20,000 rpm and a temperature of 20.0 °C) equipped with Schlieren optics, adapted with a CCD camera system (Clewlow et al. 1997) for automatic capture of the optical data. Use was made of the long optical path cells (30 mm), impossible to use in the XL-I. The data were analysed by fitting to the Lamm equation (see, for example, Clewlow et al. 1997):

$$\mathrm{d}\ln\left(\frac{1}{r}\frac{\mathrm{d}n}{\mathrm{d}r}\right)/\mathrm{d}(r^2) = M_{z,\mathrm{app}}(1-\bar{v}\rho)\omega^2/2RT \qquad (1)$$

where $\bar{v}$ is the partial specific volume (mL/g) determined by precision densimetry for each chitosan (Kratky et al. 1973), ρ the solvent density (ml/g) R is the gas constant and T the temperature (K). A plot of $\ln(\frac{1}{r}\frac{\mathrm{d}n}{\mathrm{d}r})$ versus r^2 has a slope proportional to the apparent z-average molecular weight ($M_{z,\mathrm{app}}$). The data set was then transformed by integrating with respect to r (distance from the centre of rotation in cm) and analysed using MSTARI (Cölfen and Harding 1997) to obtain $M_{w,\mathrm{app}}$.

To account for non-ideality, the reciprocal of the apparent weight average molecular weights $M_{w,\mathrm{app}}$ determined over a range of concentrations, c, were extrapolated to zero concentration. The thermodynamic or "osmotic pressure" second virial coefficient, B, and the "ideal" or "true" weight average molecular weight, M_w, were estimated from plots of $1/M_{w,\mathrm{app}}$ versus concentration according to (see, for example, Harding 1995a):

$$1/M_{w,\mathrm{app}} = (1/M_w)(1+2BM_wc) \qquad (2)$$

Molecular weight: SEC-MALLS

The molecular weights (weight averages) of the chitosan samples were then also determined by using SEC-MALLS. Acetate buffer, pH 4.3, was pumped at a flow rate of 0.8 mL/min through a column system consisting of TSK-G5000PW, TSK-G4000PW and TSK-G3000PW analytical columns protected by a guard column. Solutions of each chitosan sample were prepared in acetate buffer, pH 4.3, at a concentration of 5 mg/mL and 100 µL was injected onto the columns at ambient temperature (sample filtered through 0.45 µm filter to remove any insoluble material or dust prior to injection). The eluting fractions were monitored using a Dawn DSP multi-angle light-scattering photometer (Wyatt Technology, Santa Barbara, USA) fitted with a 5 mW He-Ne laser and a differential interferometric refractometer (Optilab 903, Wyatt Technology, Santa Barbara, USA). Apparent weight average molecular weights, $M_{w,\mathrm{app}}$, were obtained using the so-called Debye plot method (see, e.g. Wyatt 1992, 1993), where a plot of $R(\theta)/Kc$ versus $\sin^2\theta/2$ yields $M_{w,\mathrm{app}}$ from the intercept, θ being the scattering angle, $R(\theta)$ the Rayleigh excess scattering ratio and K, the optical constant, is $4\pi^2n^2(\mathrm{d}n/\mathrm{d}c)^2/(\lambda_0{}^4N_A)$; n is the solvent refractive index, $\mathrm{d}n/\mathrm{d}c$ is the specific refractive index increment (mL/g), N_A is Avogadro's number and λ_0 is the wavelength of the scattered light in vacuo (cm). The specific refractive index increment was calculated from the DA using the equation of Anthonsen et al. (1994):

$$\mathrm{d}n/\mathrm{d}c = 0.201 - 0.056(\mathrm{DA}) \qquad (3)$$

Because of the low concentrations after dilution from the column, the contribution from the $2BM_wc$ term in Eq. (2) can be reasonably assumed to be ~0, so to a good approximation $M_w \approx M_{w,\mathrm{app}}$.

Sedimentation coefficient measurements

A Beckman XLI Analytical Ultracentrifuge was used for the determination of the sedimentation coefficients at 20.0 °C and a rotor speed of 45,000 rpm. Sedimentation coefficients (s_{obs}) were obtained by analysing 10 consecutive scans using the "time derivative" algorithm DCDT+ (Philo 2000). These were corrected to standard solvent conditions (the density and viscosity of water at 20.0 °C) using the equation (see Schachman 1959):

$$s_{20,w} = \{(1-\bar{v}\rho_{20,w})/(1-\bar{v}\rho_{T,b})\}\{\eta_{T,b}/\eta_{20,w}\}s_{\mathrm{obs}} \qquad (4)$$

where $s_{20,w}$ is the sedimentation coefficient in terms of the standard solvent water at 20 °C; s_{obs} is the measured sedimentation coefficient in the experimental solvent/buffer at temperature T; $\rho_{20,w}$ and $\eta_{20,w}$ are the density and viscosity of water at 20 °C and $\rho_{T,b}$ is the density and viscosity of the buffer used for the experiments at temperature T. Measurements were made at a series of low concentrations (0.3–1.0 mg/mL) to minimize non-ideality; nonetheless, $s_{20,w}$ values (or reciprocals thereof) were then extrapolated to infinite dilution to yield $s^\circ_{20,w}$.

Determination of intrinsic viscosity

Intrinsic viscosities were determined using an Ostwald-type viscometer of 2 mL capacity over a concentration range of 0.2–2.0 mg/mL. The flow times were recorded at 20.00 ± 0.01 °C. From the solution/solvent flow-time ratio the kinematic relative viscosity was obtained. Because of the low concentrations used (< 1 mg/mL), the density corrections were assumed to be negligible and the kinematic viscosities were assumed to be approximately equal to the dynamic viscosities (Tanford 1955). The intrinsic viscosity was found by extrapolation to infinite dilution of the reduced viscosities using the Huggins equation (see, for example, Harding 1997).

Results and discussion

Molecular weight

For four of the chitosans, much better agreement than previous is seen between the two totally independent

Table 2 Thermodynamic and hydrodynamic data

Property*	Units	Fraction				
		G112	G114	G213[(a)]	G213[(b)]	G214
M_w (sed. eqm.)	g mol^{-1}	57,000 ± 800	82,000 ± 9000	161,000 ± 18000	–	132,000 ± 15000
M_w (SEC-MALLS)	g mol^{-1}	42,400 ± 3000	129,000 ± 6000	203,000 ± 8000	207,500 ± 8000	172,000 ± 6000
M_z (sed. eqm.)	g mol^{-1}	90,000 ± 11,000	386,000 ± 30,000	442,000 ± 30,000	417,000 ± 41,000	246,500 ± 18,000
$M_w/M_n = M_z/M_n$	–	2.2	3.4	2.5	2.9	1.5
$2BM$ (sed. eqm.)	mL g^{-1}	–	2200	4600	–	4100
$s^\circ_{20,w}$	S	1.76 ± 0.04	1.99 ± 0.05	2.71 ± 0.22	2.69 ± 0.07	2.74 ± 0.12
$[\eta]$	mL g^{-1}	100 ± 8	310 ± 15	420 ± 20	610 ± 30	550 ± 20

*M_w (sed. eqm.): weight average molecular weight obtained from sedimentation equilibrium. M_w (SEC-MALLS): weight average molecular weight obtained from SEC-MALLS. M_z (sed. eqm.): z-average molecular weight obtained from sedimentation equilibrium. $M_w/M_n = M_z/M_w$: identity holds for a log-normal distribution (Fujita 1962). BM: product of second virial coefficient (B) and molecular weight

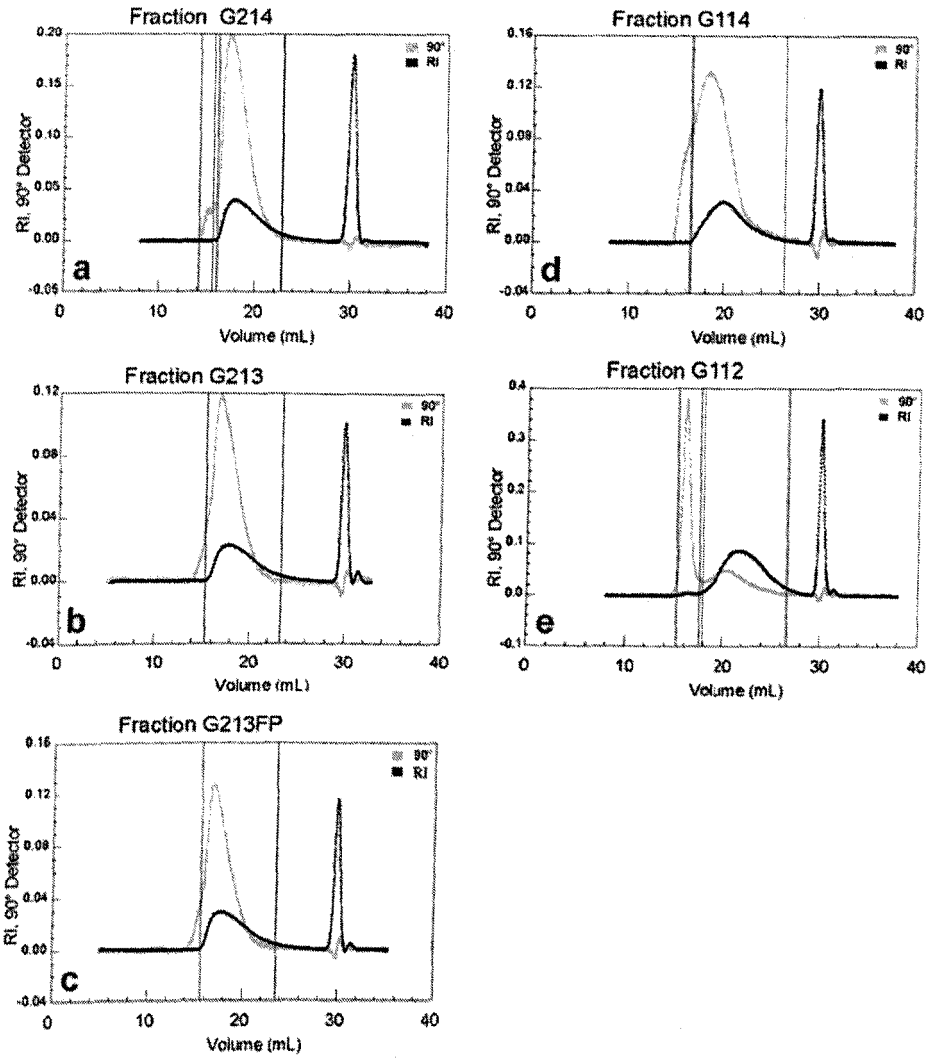

Fig. 2a–e SEC-MALLs elution volume for each chitosan fraction. Signals from the refractive index or RI (concentration) and 90° angle light-scattering detectors are shown in each case. The *vertical lines* indicate the regions of the two traces chosen to calculate the weight average molecular weight corresponding to Table 2. The *additional pair of vertical lines* on the *left* for chitosans G214 and G112 at low elution volume correspond to the peaks for the trace amounts of supramolecular aggregate. The RI peaks at high elution volume correspond to salt elution

techniques of sedimentation equilibrium and SEC-MALLS (Table 2) for the weight average molecular weights, M_w, although, with the exception of G112, sedimentation equilibrium molecular weights still come out somewhat lower.

Figure 2 shows the light-scattering and refractive index (RI, measurement of concentration) traces obtained from SEC-MALLS for each chitosan sample. From the light-scattering traces it can be seen that in each case the peaks from the macromolecular component are skewed and not symmetrical. There was also evidence of persistently occurring trace amounts of high molecular weight aggregate from the 90° angle light-scattering traces, as indicated by the shoulders on the low elution volume or high molecular weight side of the light-scattering peaks. However, except for sample G112, these light-scattering signals are not accompanied by corresponding RI (concentration) signals, indicating that only negligible amounts (<1%) are present in the samples. No such supramolecular particles were observed from the sedimentation velocity $g^*(s)$ distributions obtained using time-derivative DCDT+ analysis, which showed only a single, approximately symmetrical, peak for in each case, including G112 (Fig. 3), and no fast moving supramolecular boundary was observed.

Significance of non-ideality: advantage of SEC-MALLS

Both the SEC-MALLS and the sedimentation equilibrium methods allow direct evaluation of the absolute molecular weight of the macromolecule. However, the time scale for each method varies greatly, with the SEC-MALLS measurement taking approximately 60 minutes (after appropriate equilibration of the SEC columns). The sedimentation equilibrium method, on the other hand, can require up to 3 days for equilibrium to be reached per sample. Further, since higher concentrations are required (absolute minimum is 0.2 mg/mL),

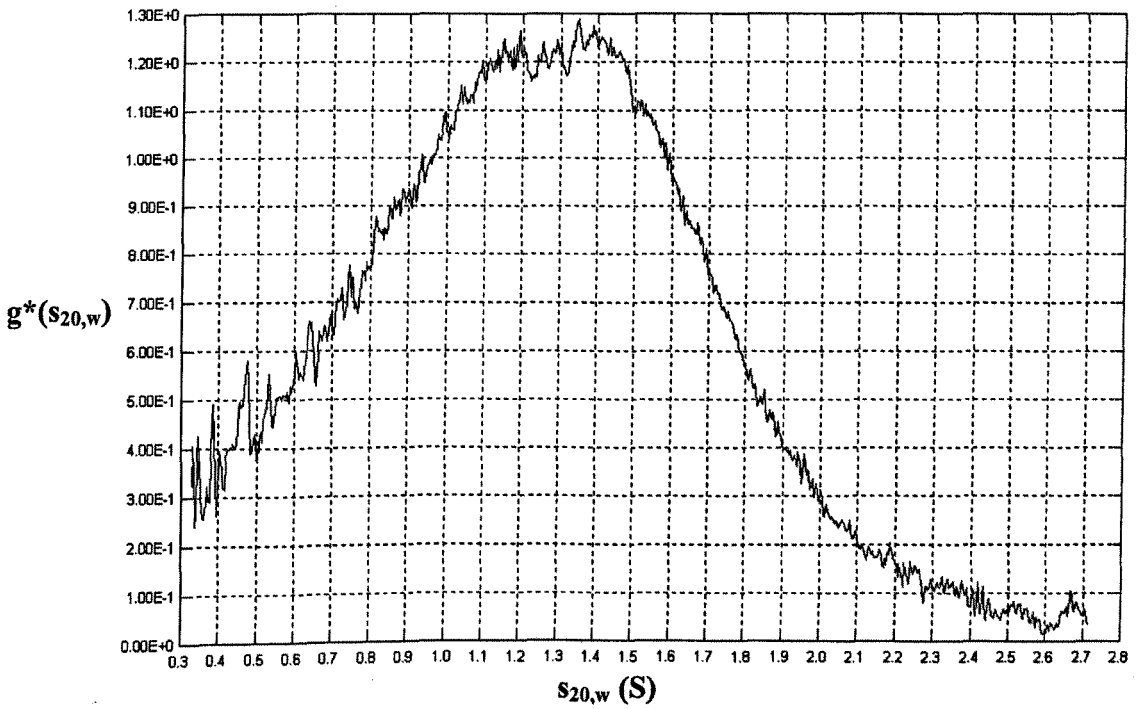

Fig. 3 $g^*(s_{20,w})$ versus $s_{20,w}$ plot for chitosan G112 from a sedimentation velocity experiment (45,000 rpm, 20.0 °C) and DCDT+ analysis

thermodynamic non-ideality effects cannot be neglected and measurements at several concentrations (and extrapolation to infinite dilution) are normally required. The problem is particularly acute for chitosans because suppression of one of the two main causes of solution non-ideality – polyelectrolyte behaviour – by increasing ionic strength is only partially possible because of solubility problems.

We explain further: non-ideality causes the molecular weight for chitosan calculated from AUC data to be lower than the true molecular weight. There are two major contributing factors to this phenomenon: the excluded volume and the polyelectrolye effect. The excluded volume arises from one molecule excluding another from the space occupied by it. For a sphere the excluded volume is eight times the molecular volume: the more extended the molecule (e.g. through intramolecular charge repulsion effects if the molecule is charged), the greater the excluded volume. Another contribution to exclusion volume comes from the swelling of the molecule through "hydration" or time-averaged association with water molecules. For a polysaccharide molecule in solution, the swollen volume can be 100 times its volume in the dry state (see, for example, Harding 1995b). The second contribution to solution thermodynamic non-ideality comes from polyelectrolyte phenomena through intermolecular repulsions. Such effects will be large for chitosan owing to the high charge density on the molecule (e.g. for a molecule of ~10% DA, there will be ~90 charges per 100 monomer residues) when in aqueous acidic solution. Such effects can normally be suppressed by charge shielding simply by increasing the ionic strength of the solution medium. Unfortunately for chitosans, large increases in ionic strength lead to reduced solubility and salting out can occur.

To illustrate the significance of the non-ideality, we have included in Table 2 values for the term $2BM_w$ (2×second virial coefficient×weight average molecular weight) in Eq. (2). For a spherical, uncharged molecule this would have a value of approximately 5–10 mL/g, and the value increases as the system deviates from ideality. From Table 2 it can be seen that values calculated for this term are in the range 1000–2000 mL/g, indicating that chitosan is a highly non-ideal macromolecule [a comparative table for polysaccharides is given in Harding (1995b)].

At very low solute concentrations, ideal behaviour is approached (Van Holde 1998) and the effects of non-ideality should be small. For many systems of biological macromolecules, particularly globular proteins, measurement at a single finite, but low (0.2–0.5 mg/mL) concentration can give an estimate of the apparent molecular weight within a few percent of the true molecular weight. However, even with loading concentrations as low as 0.2 mg/mL there can be non-negligible underestimates of the true molecular weight (Harding 1992) for those polysaccharides yielding solutions of high $2BM_w$ values; chitosan appears to be in that category (Harding 1995b). The problem is compounded since the modern commercial instrument (XL-I) permits a minimum concentration of not 0.2 but 0.5 mg/mL.

With SEC-MALLS, however, there is normally no need to correct for non-ideality in the system so long as the sample is diluted in the columns to such an extent that the concentrations of the volume "slices" passing through the light-scattering detector are much lower than the initial loading concentration. These concentrations are usually 0.1 mg/mL or less (depending on the molecular weight of the scatterer), and corrections arising from thermodynamic non-ideality are not significant (Wyatt 1993).

Inertness of the SEC column

Although the SEC-MALLS method of determining the molecular weight of chitosan is very quick and simple, there may still remain some uncertainties in terms of the "inertness" of the column packing materials and in the extrapolation of the angular intensity functions to zero angle, as highlighted by Harding (1995b). The former appears to be particularly important in the case of cationic polyelectrolytes; however, it seems that the use of a dedicated column system can eliminate most of these uncertainties. Nevertheless, it is still advisable to determine the molecular weight using the AUC to obtain a reliable and independent verification of the results.

Conformation

The conformation of chitosans has been the subject of considerable interest over the last decade, particularly with the regard to the effect of the degree of acetylation of the molecule, the molecular weight and the solvent conditions in which it is studied (see, e.g. Wang et al. 1991; Anthonsen et al. 1993; Errington et al. 1993; Ottøy et al. 1996; Berth et al. 1998; Cölfen et al. 2001; Berth and Dautzenberg 2002).

Many methods for assaying the conformation of chitosan and other polysaccharides in solution appear to be based on the dependence of a solution parameter (such as intrinsic viscosity, radius of gyration or sedimentation coefficient) with molecular weight. The simplest are the Mark–Houwink–Kuhn–Sakurada type of scaling or power-law plots of log(parameter) versus log(M_w) (see, e.g. Smidsrød and Andresen 1979; Tombs and Harding 1997). Figures 4 and 5 shows such plots for the four chitosans of this study in terms of log$s^\circ_{20,w}$ versus logM_w and log[η] versus logM_w, respectively. The SEC-MALLs values for M_w have been included, and an additional data point has been included corresponding to a separate batch of G213, called G213[(b)]. A linear fit to the log$s^\circ_{20,w}$ versus logM_w data yielded an MHKS exponent $b = 0.25 \pm 0.04$, i.e. between the limits of rod (0.15) and coil (0.4–0.5). Similarly, a linear fit to the log[η] versus logM_w scaling data yielded an MHKS exponent $a = 0.96 \pm 0.10$, again between the coil (0.5–0.6) and rod

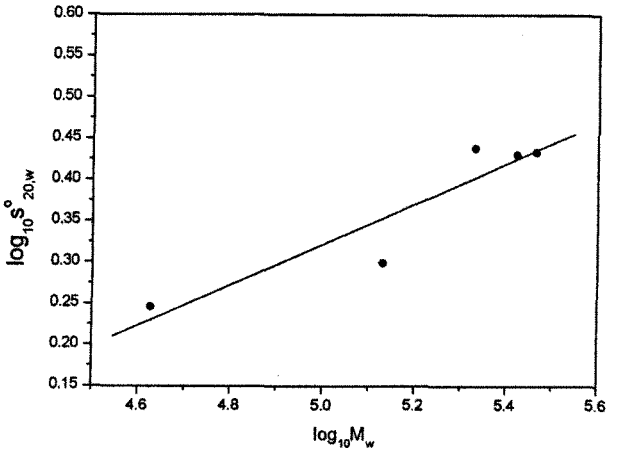

Fig. 4 Double logarithmic plot of sedimentation coefficient versus weight average molecular weight (SEC-MALLs values)

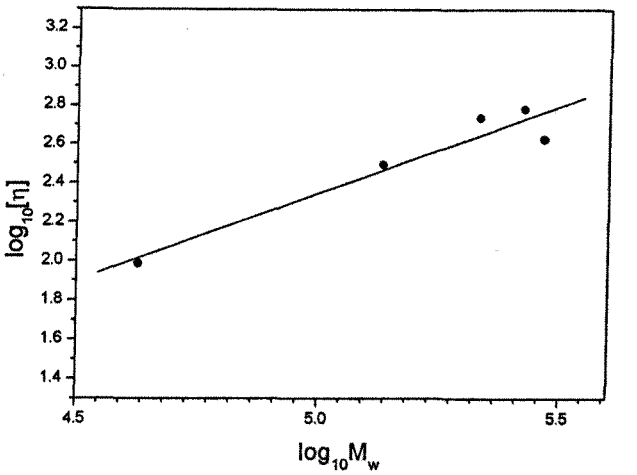

Fig. 5 Double logarithmic plot of intrinsic viscosity versus weight average molecular weight (SEC-MALLs values)

(1.8) limits. However, interpretation of such data should be done with caution because of claims by others of a dependence of conformation on the degree of acetylation (see, e.g. Anthonsen et al. 1993). Despite this reservation, the values obtained appear similar to those for three chitosans of DA in the range 22–31% (Cölfen et al. 2001): $a \approx 1$ and $b \approx 0.24$. Furthermore, the data reassuringly show consistency between the sedimentation coefficient and viscosity data. More advanced analyses, such as involving normalized scaling relations (Pavlov et al. 1997, 1999), can be used to take into account the differences in DA, but these await knowledge of the mass per unit length of chitosans as a function of DA. It should also be pointed out that if the sedimentation equilibrium values for M_w are used instead, different values of a and b are returned (~1.5 and 0.5, respectively), although these values are based on only four data points.

Conclusions

Confidence in our ability to measure molecular weight and conformation accurately is of particular relevance to the use of chitosans for the delivery of substances across the mucosal membrane through bioadhesion and absorption enhancement through transient widening of tight junctions (Kotzé et al. 1997). Larger molecular weights and more extended conformations would appear to offer more opportunities for interaction.

In conclusion, however, although much better agreement is now possible between SEC-MALLs and sedimentation equilibrium, some caution still needs to be exercised when interpreting molecular weight data for these materials, particularly with regards to the trace amounts of high molecular weight material appearing in the SEC-MALLs profiles. The use of two independent methods for determining the molecular weights for these substances is still highly recommended.

Acknowledgements We thank Professor Arthur Rowe for helpful comments and advice.

References

Anthonsen MW, Vårum KM, Smidsrød O (1993) Solution properties of chitosans: conformation and chain stiffness of chitosans with different degrees of N-acetylation. Carbohydr Polym 22:193–201

Anthonsen MW, Vårum KM, Hermansson AM, Smidsrød O, Brant DA (1994) Aggregates in acidic solutions of chitosans detected by static laser light scattering. Carbohydr Polym 25:13–23

Artursson P, Lindmark T, Davis SS, Illum L (1994) Effect of chitosan on the permeability of monolayers of intestinal epithelial cells (caco-2). Pharm Res 11:1358–1361

Beri RG, Walker J, Reese ET, Rollings JE (1993) Characterization of chitosans via coupled size-exclusion chromatography and multiple-angle laser light-scattering technique. Carbohydr Res 238:11–26

Berth G, Dautzenberg H (2002) The degree of acetylation of chitosans and its effect on the chain conformation in aqueous solution. Carbohydr Polym 47:39–51

Berth G, Dautzenberg H, Peter MG (1998) Physico-chemical characterization of chitosans varying in degree of acetylation. Carbohydr Polym 36:205–216

Clewlow AC, Errington N, Rowe AJ (1997) Analysis of data captured by an on-line image capture system from an analytical ultracentrifuge using Schlieren optics. Eur J Biophys 25:311–317

Cölfen H, Harding SE (1997) MSTARA and MSTARI: interactive PC algorithms for simple, model independent evaluation of sedimentation equilibrium data. Eur J Biophys 25:333–346

Cölfen H, Berth G, Dautzenberg H (2001) Hydrodynamic studies on chitosans in aqueous solution. Carbohydr Polym 45:373–383

Davis SS (2001) Nasal vaccines. Adv Drug Delivery Rev 51:21–42

Deacon MP, Davis SS, White RJ, Nordman H, Carlstedt I, Errington N, Rowe AJ, Harding SE (1999) Are chitosan-mucin interactions specific to different regions of the stomach? Velocity ultracentrifugation offers a clue. Carbohydr Polym 38:235–238

Errington N, Harding SE, Vårum KM, Illum L (1993) Hydrodynamic characterisation of chitosans varying in degree of acetylation. Int J Biol Macromol 15:113–117

Fujita H (1962) Mathematical theory of sedimentation analysis. Academic Press, New York, p 297

Harding SE (1992) Sedimentation analysis of polysaccharides. In: Harding SE, Rowe AJ, Horton JC (eds) Analytical ultracentrifugation in biochemistry and polymer science. Royal Society of Chemistry, Cambridge, UK

Harding SE (1995a) On the hydrodynamic analysis of macromolecular conformation. Biophys Chem 55:69–93

Harding SE (1995b) Some recent developments in the size and shape analysis of industrial polysaccharides in solution using sedimentation analysis in the analytical ultracentrifuge. Carbohydr Polym 28:227–237

Harding SE (1997) The intrinsic viscosity of biological macromolecules. Progress in measurement, interpretation and application to structure in dilute solution. Prog Biophys Mol Biol 68:207–262

Harding SE, Davis SS, Deacon MP, Fiebrig I (1999) Biopolymer mucoadhesives. Biotechnol Genet Eng Rev 16:41–85

Horton JC, Harding SE, Mitchell JR (1991) Gel permeation chromatography-multi angle laser light scattering characterisation of the molecular mass distribution of "Pro-nova" sodium alginate. Biochem Soc Trans 19: 510–511

Illum L (1998) Chitosan and its use as a pharmaceutical excipient. Pharm Res 15:1326–1331

Illum L, Davis SS (2001) Nasal vaccination: a non-invasive vaccine delivery method that holds great promise for the future. Adv Drug Delivery Rev 51:1–3

Illum L, Farraj NF, Davis SS (1994) Chitosans as a novel nasal delivery system for peptide drugs. Pharm Res 11:1186–1189

Illum L, Jabbal-Gill I, Hinchcliffe M, Fisher AN, Davis SS (2001) Chitosan as a novel nasal delivery system for vaccines. Adv Drug Delivery Rev 51:81–96

Jumel K, Fiebrig I, Harding SE (1996) Rapid size distribution and purity analysis of gastric mucus glycoproteins by size exclusion chromatography/multi angle laser light scattering. Int J Biol Macromol 18:133–139

Jumel K, Fogg FJJ, Hutton DA, Pearson JP, Allen A, Harding SE (1997) A polydisperse linear random coil model for the quaternary structure of pig colonic mucin. Eur Biophys J 25:477–480

Kotze AF, de Leeuw BJ, Luessen HL, de Boer AG, Verhoef JC, Junginger HE (1997) Chitosans for enhanced delivery of therapeutic peptides across intestinal epithelia: in vitro evaluation in Caco-2 cell monolayers. Int J Pharm 159:243–253

Kratky D, Leopold A, Stabinger H (1973) The determination of the partial specific volume of proteins by the mechanical oscillator technique. Methods Enzymol 27D:98–110

Natsume H, Iwata S, Ohtake K, Miyamoto M, Yamaguchi M, Hosoya K, Kobayashi D, Sugibayashi K, Morimoto Y (1999) Screening of cationic compounds as an absorption enhancer for nasal drug delivery. Int J Pharm 185:1–12

Ottøy MH, Vårum KM, Smidsrød O (1996) Compositional heterogeneity of heterogeneously deacetylated chitosans. Carbohydr Polym 29:17–24

Pavlov GM, Rowe AJ, Harding SE (1997) Conformation zoning of large molecules using the analytical ultracentrifuge. Trends Anal Chem 16:401–405

Pavlov GM, Harding SE, Rowe AJ (1999) Normalized scaling relations as a natural classification of linear macromolecules according to size. Prog Colloid Polym Sci 113:76–80

Philo JS (2000) A method for directly fitting the time derivative of sedimentation velocity data and an alternative algorithm for calculating sedimentation coefficient distribution functions. Anal Biochem 279:151–163

Rollings JE (1991) Use of online laser light-scattering photometry coupled to chromatographic separations for determination of biopolymer molecular mass, branching, size and shape distributions. Biochem Soc Trans 19:493–494

Rollings JE (1992) Use of on-line laser light scattering coupled to chromatographic separations for the determination of molecular weight, branching, size and shape distributions of polysaccharides. In: Harding SE, Sattelle DB, Bloomfield VA (eds) Laser light scattering in biochemistry. Royal Society of Chemistry, Cambridge, UK

Schachman HK (1959) Ultracentrifugation in biochemistry. Academic Press, New York

Schipper NGM, Vårum KM, Artursson P (1996) Chitosans as absorption enhancers for poorly absorbable drugs. 1. Influence of molecular weight and degree of acetylation on drug transport across human intestinal epithelium (Caco-2) cells. Pharm Res 13:1686–1692

Skaugrud Ø, Hagen A, Borgersen B, Dornish M (1999) Biomedical and pharmaceutical applications of alginate and chitosan. Biotechnol Genet Eng Rev 16:23–40

Smidsrød O, Andresen L (1979) Biopolymerkjemi. Tapir, Trondheim, Norway

Tanford C (1955) Intrinsic viscosity and kinematic viscosity. J Phys Chem 59:798–799

Tengamnuay P, Sahamethapat A, Sailasuta A, Mitra AK (2000) Chitosans as nasal absorption enhancers of peptides: comparison between free amine chitosans and soluble salts. Int J Pharm 197:53–67

Tombs MP, Harding SE (1998) An introduction to polysaccharide biotechnology. Taylor and Francis, London, p 15

Van Holde KE (1998) Principles of physical biochemistry. Prentice-Hall, Englewood Cliffs, NJ, USA

Vårum KM, Anthonsen MW, Grasdalen H, Smidsrød O (1991) High-field NMR spectroscopy of partially N-deacetylated chitins (chitosans). 1. Determination of the degree of N-acetylation and the distribution of N-acetyl groups in partially N-deacetylated chitins. Carbohydr Res 211:17–23

Wang W, Bo S, Li S, Qin W (1991) Determination of the Mark-Houwink equation for chitosan with different degrees of deacetylation. Int J Biol Macromol 13:281–285

Wyatt PJ (1992) Combined differential light scattering with various liquid chromatography separation techniques. In: Harding SE, Sattelle DB, Bloomfield VA (eds) Laser light scattering in biochemistry. Royal Society of Chemistry, Cambridge, UK, pp 35–58

Wyatt PJ (1993) Light scattering and the absolute characterization of macromolecules. Anal Chim Acta 272:1–40